CHEMICAL REACTIONS OF METHANE AND OF n-HEXANE IN BALLISTIC PISTON APPARATUS

Thesis by

Paul Alan Longwell

In Partial Fulfillment of the Requiremen

for the Degree of

Doctor of Philosophy

California Institute of Technology
Pasadena, California

1957

ACKNOWLEDGMENTS

Professor B. H. Sage directed the work reported herein and his interest and guidance were very helpful in its accomplishment. The laboratory measurements required several people, and the assistance of P. F. Helfrey, N. P. Wilburn, H. Smith and H. H. Reamer is appreciated. Special credit is given to N. P. Wilburn who was responsible for the timing instrumentation used. The Montebello Laboratory of The Texas Company analyzed the gas samples.

Financial support for the ballistic piston project was provided by The Texas Company and Hercules Powder Company. The writer was a Dow Chemical Company Fellow for 1954-1955.

Evelyn Anderson typed the manuscript and Virginia Berry prepared the figures.

ABSTRACT

The results of ballistic piston tests on methane and on n-hexane are described. In the case of methane the calculated reaction temperatures are 2500 to 3500° R. and maximum pressures range up to 100,000 pounds per square inch. The distribution of reaction products and the amount of reaction are correlated with the reaction conditions. For n-hexane the products are correlated with reaction conditions and in addition reaction rate coefficients were obtained. The decomposition reaction was found to be of apparent one half order with a low apparent activation energy. The range of reaction temperatures investigated for n-hexane was 1600-2800° R. with maximum pressures up to 115,000 pounds per square inch.

In addition to the experimental results there are included derivations of the differential equations describing the behavior of the ballistic piston apparatus and solutions of these equations for various conditions and assumptions. In order to obtain numerical solutions it was necessary to estimate the thermodynamic properties of gases at high pressures and temperatures. These are tabulated for 1500-20,000° R. for hydrogen, helium and nitrogen; for 1500-5000° R. for methane, and 1500-4000° R. for n-hexane. The range of pressures is 0-200,000 pounds per square inch in each case.

CONTENTS

NOMENCLATURE

A	cross-sectional area of cylinder, (sq.ft.)
A'	Arrhenius frequency factor $(sec.^{-1})$
a	acceleration of piston (ft.)/$sec.^2$)
a_1	constant
$(a^*)^3$	$(2\sqrt{2}\,\pi\,\underline{V}_o)/(3\,b_o)$
$B(T)$	second virial coefficient (cu.ft.)/(lb.mole)
$B^*(T)$	$(B(T))/(b_o)$
B_1	$RT_1(V_2^* - \alpha)C_3$ (cu.ft.)(atm.)(sec.)/(lb.mole)
B_4	$(\underline{V}_{B_o})^{3/2} \times (V_2^* - \alpha)^{3/2} \times (m_p)^{\frac{1}{2}}/(AN_{av})(2g)^{\frac{1}{2}}$ (cu.ft.)$(atm.^{\frac{1}{2}})$(sec.)/(lb.mole)
b	molal covolume (cu.ft.)/(lb.mole)
$\bar{b}$	$\left(\int_o^P bdP\right)/(P)$ (cu.ft.)/(lb.mole)
b_o	force constant (cu.ft.)/(lb.mole)
b'	constant
$C(T)$	third virial coefficient $(cu.ft.)^2/(lb.mole)^2$
$C^*(T)$	$(C(T))/(b_o^2)$
C_3	$(m_p\underline{V}_{B_o}N_o)^{\frac{1}{2}}/(2gP_{B_o}T_1^*\,N_{av})^{\frac{1}{2}}(A)$ (sec.)
C_v	specific heat at constant volume (B.t.u.)/(lb.)($^oR.$)
$\underset{o}{C}_v$	molal specific heat at constant volume (B.t.u.)/(lb.mole)($^oR.$)
c, c_1, c_2, c_3	constants
d	differential operator
E	specific internal energy (B.t.u.)/(lb.)
$\underset{o}{E}$	molal internal energy (B.t.u.)/(lb.mole)

$\underline{E}$	total internal energy (B.t.u.)
$\bar{E}$	partial specific internal energy (B.t.u.)/(lb.)
$\underline{E}_o^o$	molal internal energy at infinite attentuation (B.t.u.)/(lb.mole)
E'	activation energy (B.t.u.)/(lb.mole)
$\Delta \underline{E}_R$	change in total internal energy due to reaction of amounts in stoichiometric equation (B.t.u.)
ΔE_{oR}	change in molal internal energy due to reaction (B.t.u.)/(lb.mole)
e	base of natural logarithms 2.71828---
erf ( )	error function
exp ( )	exponential function
F	effective frictional force on piston (lb.)
f ( )	function of ( )
f_R	fugacity of reactant (atm.)
f^o	fugacity in pure state (atm.)
f_R^o	fugacity of reactant in pure state (atm.)
G	an intensive property of a unit weight system
$\underline{G}$	an extensive property of a system
G^*	normalized property $(G)/(G_o) = (\underline{G})/(\underline{G}_o)$
g	acceleration due to gravity (ft.)/(sec.^{2})
h_i	height of contact "i" (in.)
i	index of summation
k	polytropic path exponent
k	index of summation
k_c	reaction rate coefficient, concentrations (sec.$^{-1}$)

k_R reaction rate coefficient, (lb.moles)/(cu.ft.)(sec.)(atm.)^{1} or (lb.moles)/(cu.ft.)(sec.)(atm.)$^{\frac{1}{2}}$

k_1, k_2, k_3, k_4 reaction rate coefficients

ln ( ) natural logarithm

log( ) logarithm to base 10

M, M', M'' molecules in a reaction

M molecular weight (lb.)/(lb.mole.)

m weight (lb.)

m_p weight of piston (lb.)

$\underline{\overset{o}{m}}$ time rate of change of weight due to leakage (lb.)/(sec.)

N number of moles (lb.mole)

N_k number of moles of component "k" appearing in equation for reaction

n weight fraction

$\underline{\beta}$ mole fraction

P pressure (lb.)/(sq.in.) or (atm.)

P^* normalized pressure $(P)/(P_o)$

Q heat absorbed by unit weight system (B.t.u./(lb.)

$\underline{Q}$ heat absorbed by one mole of system (B.t.u.)/(lb.mole)

$\underline{Q}$ heat absorbed by system (B.t.u.)

$\underline{q}$ heat absorbed by system for infinitesimal change (B.t.u.)

R molal gas constant (B.t.u.)/(lb.mole)(^oR.)

^oR degrees Rankine

R_1, R_1', R_2 free radicals in reaction

r_1 reaction rate, component 1 (lb.moles)/(cu.ft.)(sec.)

S	specific entropy	(B.t.u.)/(lb.)(^{o}R.)
s	amount of reactant decomposed	(lb.mole)/(lb.mole original sample)
T	temperature ^{o} Rankine	
T^*	normalized temperature $(T)/(T_o)$	
T'	$(T^*)(T_r)$ ^{o} Rankine	
T_r	reference temperature, 536.7^{o} R. (77^{o} F., 25^{o} C.)	
t^*	$(T)/(\epsilon/k)$	
$\tan^{-1}(\ )$	arctangent	
u	velocity of piston	(ft.)/(sec.)
V	specific volume	(cu.ft.)/(lb.)
$\underset{o}{V}$	molal volume	(cu.ft.)/(lb.mole)
$\underline{V}$	total volume	(cu.ft.)
V^*	normalized volume $(V)/(V_o)$	
$\underset{o}{\underset{\sim}{V}}$	molal residual volume	
W	work done by unit weight system	(B.t.u.)/(lb.)
$\underset{o}{W}$	work done by one mole of system	(B.t.u.)/(lb.mole)
$\underline{W}$	work done by system	(B.t.u.)
x	distance measured upward	(ft.)
y	$\left[\ln (V^* - \alpha) - \ln (V_2^* - \alpha)\right]^{\frac{1}{2}}$	
Z	compressibility factor $(PV)_o/(RT)$	
α	normalized covolume $(b)/(V_o)$	
β	$(\underline{V}_{Ao})/(\underline{V}_{Bo})$	
γ	stoichiometric (final moles gas)/(initial moles)	

Δ	difference in
ϵ/k	force constant, ° Rankine
η	specific covolume (Noble-Able) (cu.ft.)/(lb.)
θ	time (sec.) or (millisec.) or (microsec.)
$\theta_1, \theta_2, \theta_3, \theta_4$	time at bottom contacts, (microsecs.)
μ	Joule-Thomson coefficient (°R.)/(lb./sq.in.)
π	3.14159---
$\sum_{K=1}^{n}$	summation of n terms
∇_o	reciprocal molal volume (lb.moles)/(cu.ft.)
$\Phi_1(y)$	first derivative of erf(y) = $\left[2 \exp(-y^2) \right] / (\sqrt{\pi})$
ϕ	$\left[\int_0^{\ln T^*} C_{ov} d(\ln T^*) \right] / (\ln T^*)$ (B.t.u.)/(lb.mole)(°R.)
ϕ'	value of ϕ for T' (B.t.u.)/(lb.mole)(°R.)
ψ	$\int_1^{T^*} C_{ov} dT^*$ (B.t.u.)/(lb.mole)(°R.)
ψ'	value of ψ for T' (B.t.u.)/(lb.mole)(°R.)
∂	partial differential operator
$\int$	integration operator
$\lvert ( ) \rvert$	absolute value of ( )
$\simeq$	approximately equal to

Subscripts

o	initial value of
1	value at state 1, start of isothermal path
2	value at state 2, maximum compression
A	pertaining to driving gas

av	average
B	pertaining to sample gas
i	component i
k	component k
R	pertaining to reactant or reaction
r	at reference temperature T_r (536.7° R.)
T	value at temperature T

I. INTRODUCTION

During the last ten years interest has been aroused in the use of extremely rapid compressional processes to investigate the physical properties and chemical reactions of gases. It is possible in this manner to subject samples to conditions of pressure and temperature which cannot be tolerated by more conventional equipment of steady state type. In general it has been desired either to determine the pressure-volume-temperature relationships for gases under conditions of high temperature and pressure, or to investigate the chemical reactions which samples undergo when subjected to extreme conditions for short periods of time.

Ryabinin (1) described an apparatus which uses a free piston propelled by high pressure air to compress samples rapidly and made measurements of the ionization of argon at these conditions. He stated that this apparatus was suitable for measurements of PVT relationships. The U. S. Naval Ordnance Laboratory developed an "adiabatic compressor" (2,3) of the free piston type for investigation of PVT properties of gases and Price et al. (4) reported preliminary tests made with this apparatus on carbon dioxide and nitrogen.

Apparatus using the rapid expansion of a gas behind a free piston for the measurement of the pressure-volume-temperature relationships of gases below ambient temperature was described by Seigel (5,6) and Jacobs (7). Jacobs (7) gave a limited amount of data for nitrogen while Seigel (8) investigated the thermodynamic properties of argon.

Several investigators have reported chemical reactions obtained in compressional apparatus of the free piston type. Tsiklis (9) reported the formation of ammonia from adiabatically compressed mixtures of nitrogen and hydrogen but did not report the extent of conversion. He used apparatus similar to that described by Ryabinin (1). Ryabinin, Markevich and Tamm (10) made up to 1.6 per cent nitric oxide by compression of mixtures of nitrogen, oxygen and argon. Furman and Tsiklis (11) investigated the oxidation of methane under conditions of adiabatic compression with the objective of determining the effect of a cold wall on a chain reaction.

Hanson (12) reported work done by E. I. du Pont de Nemours and Company with a compression reactor of the free piston type. They made exploratory measurements on many mixtures of gases with the primary objective of commercial application. Mixtures investigated included nitrogen and oxygen, nitrogen and hydrogen, methane and carbon monoxide, carbon monoxide and hydrogen, carbon monoxide and methanol, hydrogen and oxygen, carbon monoxide and ammonia, methane and oxygen, and hydrocarbons and nitrogen. Up to 30 per cent of the ammonia in the mixture with carbon monoxide was converted to hydrogen cyanide, and 2 mole per cent nitric oxide was formed from the nitrogen-oxygen mixture, while the results from other mixtures were judged to be of little commercial interest.

Kouzmine has patented (13,14) adiabatic compressional processes and also (15) such a process for the manufacture of hydrazine from the

elements. He cites the dilution of the mixture with argon or other monatomic gas in the latter patent. It is not known whether Kouzmine has demonstrated these processes.

The authors cited have not reported attempts to determine reaction rates or mechanisms. The Russians (9,10,11) reported products and maximum pressures, the latter apparently measured by crusher gage. du Pont (12) measured pressure as a function of time and maximum temperature, and reported products obtained. It is believed that reaction rates and apparent order can be determined, and that some information regarding reaction mechanisms can also be obtained with equipment of the free piston type.

It is believed likely that rapid compressional processes may have commercial applications in addition to their utility for research purposes. The requirement for successful commercial use is of course that the process make possible the manufacture of marketable chemicals at lower cost than competitive processes. No current commercial application is known, but actually the field is new and the amount of effort expended in it has been small.

This thesis treats experimental work on the chemical reactions of methane and of n-hexane performed with the ballistic piston apparatus described by Longwell and Sage (16). This apparatus is a free piston device capable of subjecting gas samples to transient high pressures and temperatures. This ballistic piston apparatus has not been fully instrumented as yet and consequently pressures and temperatures were

not measured. Nevertheless it was possible to calculate temperatures and pressures which are believed sufficiently accurate to be useful. In the case of n-hexane, reaction rate coefficients for the decomposition reaction were obtained. The final products of reaction were determined for both methane and n-hexane.

In addition to the experimental work which is described in Parts IV and V, a sizable proportion of this thesis is devoted to the derivation of the equations describing the behavior of the sample gas in the ballistic piston apparatus and to solutions of these equations for various conditions and assumptions. The thermodynamic properties of the gases must be used in the solution of these equations. Since the pressure-volume-temperature relationships for the gases employed are not known experimentally in the range of temperatures and pressures encountered it was necessary to estimate them. Information based on statistical mechanical considerations and presented by Hirschfelder, Curtiss and Bird (17) was used for these estimates, which are described in Appendix I.

This thesis, and one currently being prepared by Paul F. Helfrey describing investigations of the nitrogen-oxygen system, are concerned with the first work done on the ballistic piston apparatus.

II. DESCRIPTION OF APPARATUS

Basic Apparatus

The ballistic piston apparatus has been described (16) in some detail and accordingly only an abbreviated description of it will be included here. The only major changes from reference (16) in the ballistic piston apparatus as used for the later of these investigations were those necessary for making time-position measurements during the downstroke of the piston.

Figure II-1 shows a schematic diagram of the apparatus without the modifications for making time-position measurements. The apparatus consists of a 3 inch internal diameter cylinder A having 1.5 inch wall thickness for most of its length, and a piston B which is free during actual operation of the apparatus. The cylinder is closed at each end by suitable closures having unsupported area seals. The piston is initially supported close to the upper end by means of a shear pin arrangement and is released at the desired time by manual operation of the handle M which actuates a jack screw. The piston is accelerated by compressed air which has been previously introduced into the upper volume H through the valve C. The calibrated pressure gauge E' was used to measure the pressure of the compressed air in these investigations although provision has been made for installation of a trap D to allow use of a pressure balance E for this measurement. The sample undergoing investigation is introduced into the lower volume G through valves K or U. The vacuum pump F maintains a vacuum in the annular

space around the piston B between the O-ring seals J and J' during loading operations, while the valve L is closed just before firing to avoid loss of compressed air through the vacuum pump.

When the piston is released it is accelerated downward and travels down the barrel almost to the bottom N of the recess in the lower closure Q, coming as close as 0.015 inch on occasion. This distance corresponds to a compression ratio of about 7000 to 1, since the initial length of the lower volume is about 100 inches. The sample gas, which initially was at a low pressure of the order of 2 pounds per square inch absolute, is raised to high pressure and temperature by this compression. Since the piston used in these investigations, weighing about 31 pounds, travels at about 70 feet per second, compression takes about 0.15 second, however most of the kinetic energy of the piston is transferred to the sample during the last few inches of travel. The piston is accelerated back up the barrel by the pressure developed in the sample gas which therefore cools at a rate comparable to that at which it was heated. The piston comes to rest after some oscillation. Mechanical friction of the piston in the barrel and other causes of degradation made the oscillation be highly damped in the cases investigated for this thesis.

Figure II-2 shows diagramatically the equipment used for the addition of samples and measurement of their pressures, the addition of compressed air to the upper volume, and the taking of samples of products after a run. The latter is done by evacuating the sample bulbs and the lines to the apparatus, then opening the bottom valve U.

A photograph of the lower portion of the apparatus is shown in Figure II-3. The apparatus is mounted on the platform seen in Figure II-3, and is stabilized at its upper end, above the grating seen in the photograph. The pressure gages and sample addition system are mounted on the wall in back and to the left of the apparatus, with access afforded by the platform.

Current Instrumentation and Measurements

The more important measurements made in the course of a run for the most recent tests reported herein are tabulated below. Earlier runs differed principally by involving less timing data.

Before firing:

1. Heights of contact wires placed in the bottom closure.
2. Pressure and temperature of the gas in the lower volume after addition of each component.
3. Pressure and temperature of the sample in the lower volume before firing.
4. Pressure and temperature of the compressed air in the upper volume.

During firing:

1. Time intervals between passage of the piston by three fixed points along the length of the barrel (four contacts are actually available).
2. Time intervals between the piston hitting four vertical wires of selected heights in the bottom closure.

3. Closest approach of the piston to the bottom of chamber.

After firing:

1. Volume and pressure of the sample gas.

2. Sampling and analysis of the product gas.

The pressures of gas in the lower volume before and after firing were measured with a mercury in glass manometer read by a cathetometer with an uncertainty of 0.01 inch. The temperature of the gas in the lower volume was estimated by reading the temperature of the top part of the lower collar of the apparatus by means of a mercury in glass thermometer placed in a well. Since there are temperature gradients along the apparatus which occasionally amount to as much as 15° F., although 5° F. is more normal, the error in the sample temperatures can amount to as much as 3 or 4° F. This error has not been considered sufficiently great as to require corrections on the exploratory type tests made to date, but when more instrumentation for recording transient behavior becomes available it will be necessary to measure the initial temperature with better accuracy.

The pressure of the compressed air was measured with a calibrated bourdon tube gage and is known to within 1%. The temperature was measured by means of a mercury in glass thermometer placed in a well in the top closure and in this case the gas temperature is believed known within 2° F. Both these measurements were considered of adequate accuracy for their purposes.

A lead crusher gage of suitable height was used to record the

distance of closest approach of the piston to the bottom closure. When this distance was expected to be less than 0.075 inch a slightly flattened lead shot was used, while for larger distances specially formed conical gages were used. Heights of the gages were measured with a micrometer caliper to 0.0002 inch before and after the run. When more than one gage was used on a run their heights after the run agreed within the flatness tolerances of the end of the piston and the end of the cylinder. Consequently it is considered that this measurement gives the actual closest approach of the piston within 0.001 inch.

N. P. Wilburn has had responsibility for timing instrumentation and he will report it in detail. The passage of the piston is timed by obtaining pulses from the grounding of contact wires having small DC potentials impressed on them, and using the pulses so obtained to start or stop digital time interval meters. A bottom closure was constructed which has four insulated contact wire holders in it. These holders allow vertical wires of heights as desired to be placed in the bottom of the chamber, so that time intervals over small distances can be measured in this region. Pulses from these contacts have been used in conjunction with three Berkeley Instrument Company Model 5120 Time Interval Meters which count in microseconds.

Later, four insulated contact wire holders were mounted in holes bored through the side of the main cylindrical portion of the apparatus at selected locations. These are used to time the passage of the piston over approximately 20 inch segments of its travel down the tube.

The pulses from these side contacts are fed into electronic circuitry of local design which controls Berkeley Instrument Company Model 5424 and 424-S Preset Counters and causes them to act as time interval meters counting in units of 100 microseconds.

Future Instrumentation and Measurements

The instrumentation described above does not measure some of variables of most interest. However in the near future it is intended to measure the pressure of the sample as a function of time, and to measure the integrated thermal flux to the walls of the chamber. Attempts may also be made to estimate the temperature of the sample by spectroscopic means.

In the event the pressure measurements show that oscillation of the piston can cause interference in measurements involving chemical reactions by allowing reaction on the second stroke, it will be necessary to add equipment to rectify this. A valve of appropriate size which vents the upper chamber to the atmosphere may accomplish this if its opening can be carefully timed in relation to the piston motion.

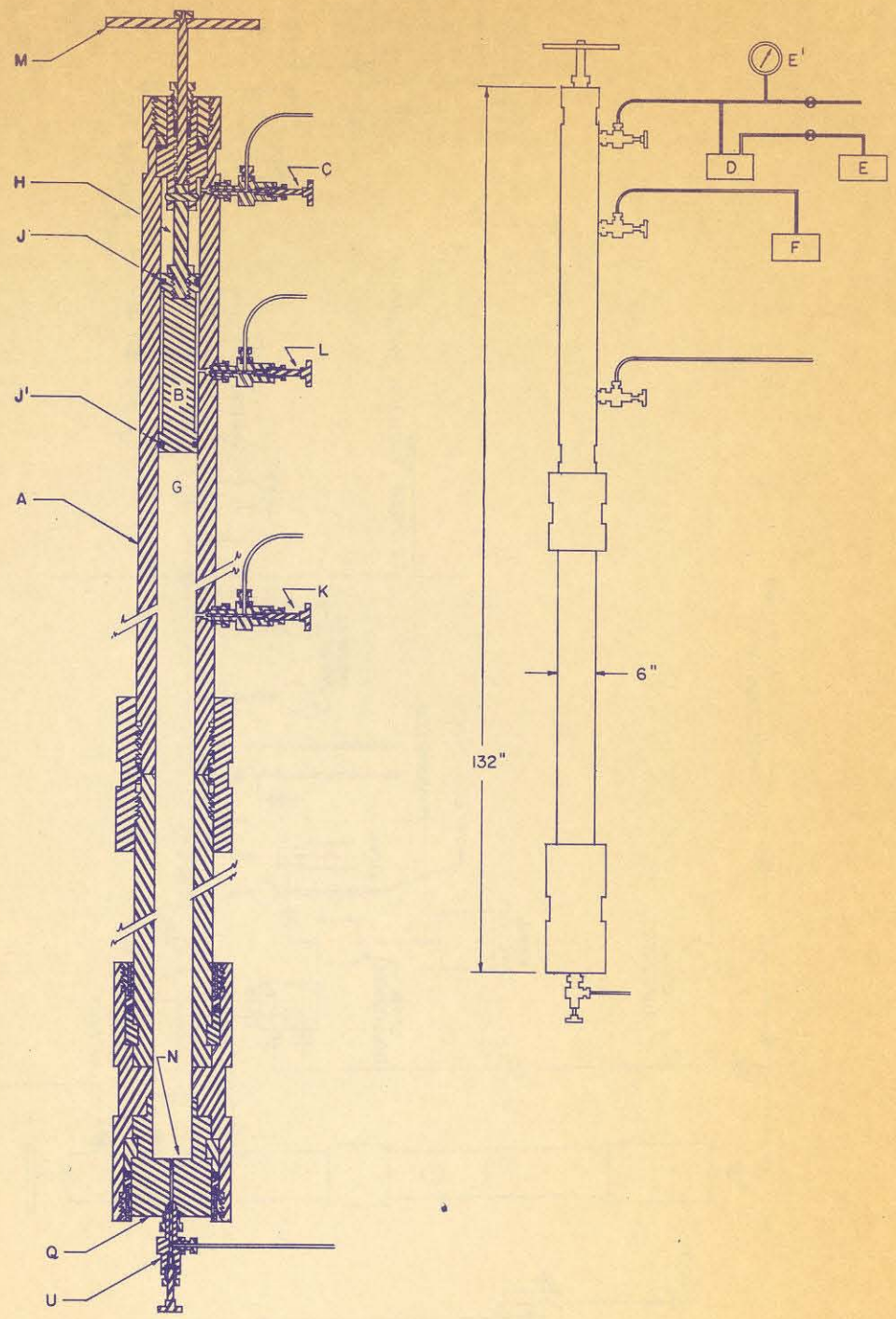

Fig.II-1.Schematic Diagram of Apparatus

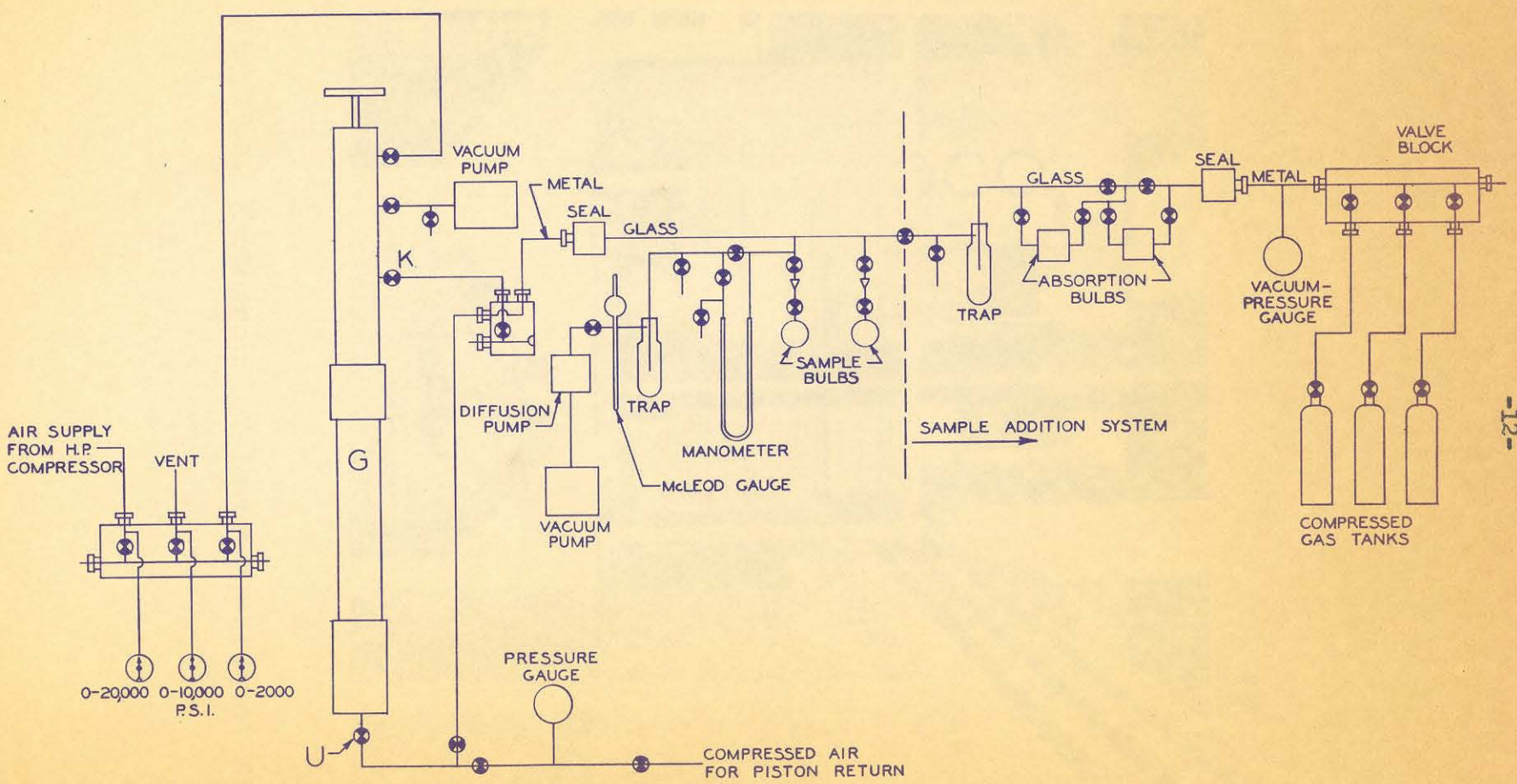

Fig.II-2. Schematic Diagram of Equipment Used in Adding and Withdrawing Samples

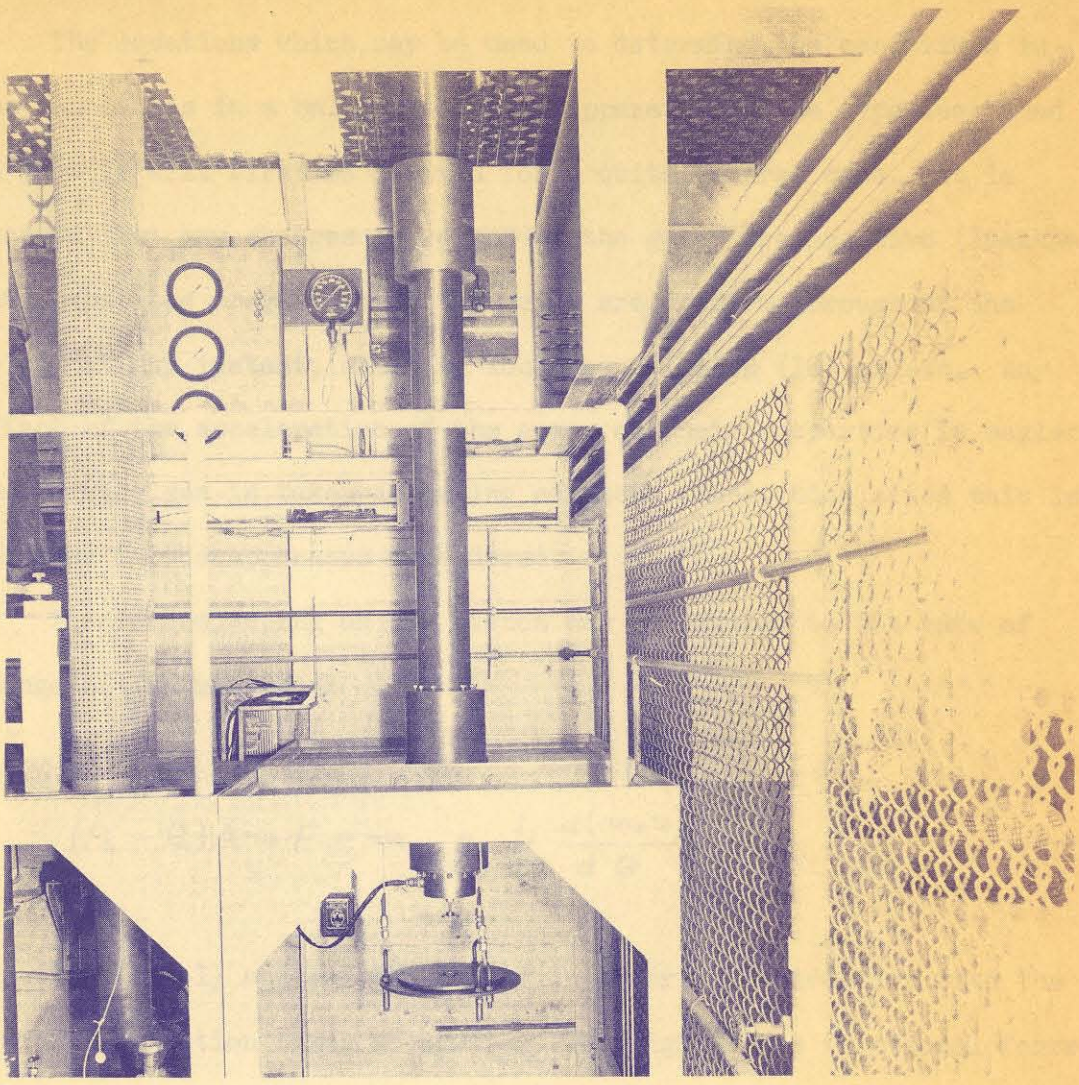

Fig. II-3. Photograph of Lower Portion of Apparatus

III. DERIVATION OF MATHEMATICAL RELATIONSHIPS

General Equations of Motion

The equations which may be used to determine the conditions in the sample gas in a ballistic piston apparatus of the type described in Part II will first be derived for a quite general case. It is assumed that any changes in weight of the gases are negative (leakage out), that the properties of the gases are uniform throughout the volume at any instant, and that local equilibrium (18) exists. Any effect of the acceleration of the gases on their properties is neglected. The driving gas is taken as having constant composition since this is the case in the apparatus considered.

The forces acting on the piston may be equated to the rate of change of its momentum:

$$(P_B - P_A)A + F - m_p = \frac{1}{g}\frac{d(m_p u)}{d\theta} \qquad \text{(III-1)}$$

Equation (III-1) applies for travel in a vertical direction with the positive direction taken as upward. The sign of the frictional force term is for a downstroke as written. If mechanical friction is considered as inherently positive, the sign of the frictional force term in the equation must be opposite to the direction of motion of the piston, and thus the sign must change when the direction of piston motion changes.

If these forces are applied through a distance dx, since

$$d\,\underline{V}_A = -A\,dx = -d\,\underline{V}_B \tag{III-2}$$

there is obtained

$$\frac{m_p}{g}\,u\,du = (F - m_p)dx + P_A\,d\,\underline{V}_A + P_B\,d\,\underline{V}_B \tag{III-3}$$

Now, since

$$d\,\underline{V}_A = d(m_A V_A) = m_A\,dV_A + V_A\,dm_A \tag{III-4}$$

and similar relations hold for $\underline{V}_B$, equation (III-3) may be rewritten as

$$\frac{m_p}{g}\,u\,du = (F - m_p)dx + m_A P_A\,dV_A + P_A V_A\,dm_A + m_B P_B\,dV_B + P_B V_B\,dm_B \tag{III-5}$$

Since the process in the gas is considered frictionless, there is obtained from the first law of thermodynamics

$$m_A\,dE_A = \underline{q}_A - m_A P_A\,dV_A \tag{III-6}$$

or

$$m_A P_A dV_A = \underline{q}_A - m_A dE_A \qquad \text{(III-7)}$$

Substitution of equation (III-7) and a similar relationship for gas B in equation (III-5) gives

$$\frac{m_P}{g} u\, du = (F - m_P)dx + \underline{q}_A + \underline{q}_B - m_A dE_A - m_B dE_B + P_A V_A dm_A + P_B V_B dm_B \qquad \text{(III-8)}$$

If desired, the internal energy differentials can be expanded:

$$dE = \left(\frac{\partial E}{\partial T}\right)_{P,n} dT + \left(\frac{\partial E}{\partial P}\right)_{T,n} dP + \sum_{k=1}^{n} \bar{E}_k\, dn_k \qquad \text{(III-9)}$$

Substitution of equation (III-9) in equation (III-8) and division by $d\theta$ gives

$$\frac{m_P}{g} u \frac{du}{d\theta} = \left\{ \begin{array}{l} (F - m_P)u + \underline{\dot{q}}_A + \underline{\dot{q}}_B + P_A V_A \underline{\dot{m}}_A + P_B V_B \underline{\dot{m}}_B \\ -m_B\left[\left(\frac{\partial E_B}{\partial T}\right)_{P,n} \frac{dT_B}{d\theta} + \left(\frac{\partial E_B}{\partial P}\right)_{T,n} \frac{dP_B}{d\theta} + \sum_{k=1}^{n} \bar{E}_k \frac{dn_k}{d\theta}\right] \\ -m_A\left[\left(\frac{\partial E_A}{\partial T}\right)_P \frac{dT_A}{d\theta} + \left(\frac{\partial E_A}{\partial P}\right)_T \frac{dP_A}{d\theta}\right] \end{array} \right\} \qquad \text{(III-10)}$$

The partial internal energies $\bar{E}_k$ in equations (III-9) and (III-10) must include internal energies of formation. Equation (III-10) is subject to the restrictions mentioned earlier, namely that the $\underline{\overset{\circ}{m}}$'s must not be positive, the properties of each gas are uniform throughout the respective volumes, and local equilibrium exists so that the thermodynamic state is defined. The composition of the driving gas A is taken as constant.

The summation term in equation (III-10) is the one in which chemical reactions (including dissociation and ionization) specifically enter, although the partial derivatives of the internal energy with respect to temperature and pressure may be affected by such reactions.

The equation for a single chemical reaction can be written in general form as

$$N_1 + N_2 + \cdots + N_i \rightleftharpoons N_{i+1} + N_{i+2} + \cdots + N_n \qquad \text{(III-11)}$$

As an example, in the reaction

$$2\,CO + O_2 \rightleftharpoons 2\,CO_2 \qquad \text{(III-12)}$$

the numerical value of N_1 is two, that of N_2 is one, and that of N_3 is two.

The reaction rate can be expressed in terms of moles of component 1 disappearing per unit volume per unit time:

$$r_i = \frac{1}{V_B}\left[-\left(\frac{\partial(\text{mols } i)}{\partial \theta}\right)_{m_B}\right] = -\frac{1}{M_i V_B}\left(\frac{dn_i}{d\theta}\right) \qquad \text{(III-13)}$$

Since

$$\frac{dn_k}{d\theta} = \pm \frac{N_k M_k}{N_i M_i}\frac{dn_i}{d\theta} \qquad \begin{matrix} + \; k \leq i \\ - \; k > i \end{matrix} \qquad \text{(III-14)}$$

equations (III-13) and (III-14) may be combined to give

$$\frac{dn_k}{d\theta} = \mp \frac{N_k M_k V_B}{N_i} r_i \qquad \begin{matrix} - \; k \leq i \\ + \; k > i \end{matrix} \qquad \text{(III-15)}$$

Thus

$$\sum_{k=1}^{n} \bar{E}_k \frac{dn_k}{d\theta} = \frac{V_B}{N_i}\left[\sum_{k=i+1}^{n} N_k M_k \bar{E}_k - \sum_{k=1}^{i} N_k M_k \bar{E}_k\right] r_i \qquad \text{(III-16)}$$

The term in brackets in equation (III-16) represents the change in internal energy corresponding to the reaction of equation (III-11) carried out at constant temperature. If this is designated as $\Delta \underline{E}_R$, equation (III-16) becomes

$$\sum_{k=1}^{n} \bar{E}_k \frac{dn_k}{d\theta} = \left[\frac{\Delta E_R}{N_1}\right] V_B r_1 \qquad \text{(III-17)}$$

The relationship of equation (III-17) may be substituted in equation (III-10). In the event more than one reaction is occurring one must substitute a term of the form of the right side of equation (III-17) for each reaction. The reaction rates will in general be rather complicated functions of the instantaneous composition and conditions of the sample.

The difficulty of solution of equation (III-10) is of course markedly dependent upon the specific situation at hand and also upon what information is desired from the solution. There are at least two general classes of studies which can be carried out in this type of ballistic piston apparatus; the investigation of thermodynamic properties of gases under conditions of high temperature and pressure, and the investigation of chemical reactions under conditions of high temperature and pressure. It seems unlikely that both thermodynamic properties and chemical reactions can be successfully investigated simultaneously, certainly not with the instrumentation currently planned. Thus, for PVT measurements the reactions, if any, should preferably be of minor consequence and sufficiently well known that correction can be made for their effects. When chemical reactions are the subject of the investigation the thermodynamic properties of the gases concerned must be known in order that the reaction data can be extracted.

Unfortunately experimental determinations of the equations of state of gases in the region of interest in this investigation are not available and therefore the thermodynamic properties must be estimated. Appendix I contains a discussion of this problem and the methods used to develop the thermodynamic data necessary for this investigation. The data developed for several gases are also contained in Appendix I. The PVT data for pure materials are shown in the form of the molal covolume b as a function of temperature and pressure, where the equation of state is

$$P(V_o - b) = RT \qquad \text{(III-18)}$$

with

$$b = f(P, T) \qquad \text{(III-19)}$$

Internal energy information is found in Appendix I in terms of a state function ψ . The increase in internal energy at infinite attenuation from that at a datum temperature T_r is given by

$$(\Delta E_o)_{P=0} = T_r \psi \qquad \text{(III-20)}$$

A datum temperature of 536.7° R. (77° F.) is used.

Solution for Simplified Isentropic Case

A solution of the equation of motion for a very simple case is presented by Davis, Corcoran and Sage (19). For this solution it was assumed that both the driving gas and the sample gas were perfect gases having the same constant heat capacities, and that isentropic paths were followed. The effects of gravity and of the friction of the piston on the walls were neglected. As a consequence of the very restrictive assumptions the results obtained are not useful for present purposes and it is necessary to undertake solutions of the equations of motion with more descriptive assumptions.

It will be assumed for the sample gas that

a) an ideal solution (20) is formed
b) the composition is constant (no reactions)
c) there is no heat transfer
d) leakage is negligible
e) there are no friction or shock waves in the gas
f) the covolume is constant over the conditions encountered in compression.

It is shown in Appendix I equations (AI-33), (AI-34) and (AI-35) that when the covolume is constant

$$\left(\frac{\partial E_o}{\partial P}\right)_T = 0 \qquad \text{(III-21)}$$

$$\left(\frac{\partial C_{v}^{\circ}}{\partial P}\right)_{T} = 0 \qquad \text{(III-22)}$$

and

$$\left(\frac{\partial T}{\partial V^{\circ}}\right)_{S} = -\frac{P}{C_{v}^{\circ}} \qquad \text{(III-23)}$$

For an isentropic change in state, equation (III-23) gives

$$C_{v}^{\circ}\, dT = -P\, dV^{\circ} = -\frac{RT}{(V^{\circ}-b)}\, dV^{\circ} \qquad \text{(III-24)}$$

It is convenient to use dimensionless variables defined as

$$G^{*} = \frac{G}{G_{o}} = \frac{\underline{G}}{\underline{G}_{o}} \qquad \text{(III-25)}$$

where G represents any of several intensive properties of a system. With this normalized variable notation and rearrangement, equation (III-24) becomes

$$\frac{C_{v}^{\circ}}{R}\, d\left(\ln T^{*}\right) = -\, d\left[\ln\left(V^{*}-\alpha\right)\right] \qquad \text{(III-26)}$$

where

$$\alpha = \frac{b}{V_{o}^{\circ}} \qquad \text{(III-27)}$$

Equation (III-26) integrates to

$$\int_0^{\ln T^*} \frac{C_{v_o}}{R}\, d(\ln T^*) = -\ln\left[\frac{V^* - \alpha}{1-\alpha}\right] \simeq -\ln(V^* - \alpha) \qquad \text{(III-28)}$$

Since α is generally negligible with respect to unity the approximation in equation (III-28) which neglects it will be used. A new function ϕ is defined

$$\phi = \frac{1}{\ln T^*} \int_0^{\ln T^*} C_{v_o}\, d(\ln T^*) \qquad \text{(III-29)}$$

and the use of equation (III-29) in equation (III-28) gives

$$\ln T^* = -\frac{R}{\phi} \ln(V^* - \alpha) \qquad \text{(III-30)}$$

so

$$T^* = (V^* - \alpha)^{-\frac{R}{\phi}} \qquad \text{(III-31)}$$

for an isentropic path for a gas whose covolume is constant.

The equation of state, equation (III-18) when expressed in normalized variables, is

$$P^*(V^* - \alpha) = T^* \qquad \text{(III-32)}$$

The properties of the driving gas are of interest only in that it is necessary to determine the work which it does on the piston. Over the range used in the ballistic piston apparatus a polytropic expansion path may be employed. The exponent can be determined from the known thermodynamic properties of air if a path is assumed. This is discussed in Appendix I. Thus, for the driving gas

$$P_A^* V_A^{*k} = 1 \qquad \text{(III-33)}$$

It is assumed that leakage of the driving gas is negligible.

The physical situation is such that

$$\underline{V}_{Ao} + \underline{V}_{Bo} = \underline{V}_A + \underline{V}_B = m_A V_A + m_B V_B \qquad \text{(III-34)}$$

If the ratio of initial volumes

$$\frac{\underline{V}_{Ao}}{\underline{V}_{Bo}} = \beta \qquad \text{(III-35)}$$

is used, equation (III-34) may be rearranged and divided by $\underline{V}_{Ao}$ to give

$$V_A^* = \frac{1}{\beta}\left[1 + \beta - V_B^*\right] \tag{III-36}$$

Differentiation of equation (III-34) and introduction of dV_B^* leads to

$$d\,\underline{V}_A = -\,\underline{V}_{Bo}\,dV_B^* \tag{III-37}$$

Equation (III-2) becomes

$$dx = \frac{\underline{V}_{Bo}}{A}\,dV_B^* \tag{III-38}$$

and from equation (III-38) one can obtain

$$u\,du = \left[\frac{\underline{V}_{Bo}}{A}\right]^2 \left(\frac{dV_B^*}{d\theta}\right) d\left(\frac{dV_B^*}{d\theta}\right) \tag{III-39}$$

Equations (III-33) and (III-36) combine to give

$$P_A = P_{Ao}P_A^* = \frac{\beta^k P_{Ao}}{\left[1 + \beta - V_B^*\right]^k} \tag{III-40}$$

While the general equation of motion, equation (III-10), could be used, it is easier in this case to use a form which is obtained from equations (III-5) and (III-7) for constant weight systems

$$\frac{m_p}{g} u\, du = (F - m_p)dx + P_A d\underline{V}_A + \underline{q}_B - m_B dE_B \qquad \text{(III-41)}$$

also, for the case considered, $\underline{q}_B = 0$ and

$$dE_B = C_{v_B} dT_B = \frac{T_{Bo}}{M_B} \mathring{C}_{v_B} dT_B^* \qquad \text{(III-42)}$$

Substitution of equations (III-37), (III-38), (III-39), (III-40) and (III-42) into equation (III-41) gives

$$\frac{m_p}{g}\left[\frac{\underline{V}_{Bo}}{A}\right]^2 \left(\frac{dV_B^*}{d\theta}\right) d\left(\frac{dV_B^*}{d\theta}\right) = (F - m_p)\frac{\underline{V}_{Bo}}{A} dV_B^*$$

$$- \frac{\beta^K P_{Ao} \underline{V}_{Bo}}{\left[1 + \beta - V_B^*\right]^K} dV_B^* - \frac{m_B T_{Bo}}{M_B} \mathring{C}_{v_B} dT_B^* \qquad \text{(III-43)}$$

Since the subscripts "A" and "B" become bothersome, and attention is now centered on the sample gas "B", the subscript "B" for other than initial conditions will be omitted in all cases except when essential for clarity.

If the covolume is neglected with respect to the initial molal volume, equation (III-43) becomes

$$\frac{m_p}{g} \frac{\underline{V}_{Bo}}{A} \left(\frac{dV^*}{d\theta}\right) d\left(\frac{dV^*}{d\theta}\right) = (F - m_p) dV^*$$

$$- \frac{\beta^K A P_{Ao}}{\left[1 + \beta - V^*\right]^K} dV^* - \frac{A P_{Bo}}{R} \mathring{C}_v dT^* \qquad \text{(III-44)}$$

This can be integrated if the dependence of the piston frictional force on V^* is known. F will be assumed constant. For the first downstroke the initial conditions are

$$\frac{dV^*}{d\theta} = 0 \quad ; \quad V^* = 1 \quad ; \quad T^* = 1 \tag{III-45}$$

Using the initial conditions of equation (III-45), one integration of equation (III-44) gives

$$\frac{m_p \; V_{Bo}}{2g \quad A}\left[\frac{dV^*}{d\theta}\right]^2 = (m_p - F)(1 - V^*) + \frac{A\,P_{Ao}}{k-1}\left[\beta - \beta^k(1+\beta-V^*)^{1-k}\right] - \frac{A\,P_{Bo}}{R}\psi \tag{III-46}$$

where

$$\psi = \int_1^{T^*} C_v \, dT^* \tag{III-47}$$

Equation (III-46) is sufficiently complicated that further integration analytically has not been found possible, however numerical or graphical integration for specific cases is not too difficult. The conditions at the bottom of the stroke (if the assumptions remain valid) may be easily obtained from equation (III-46) since the velocity is zero there. Designating conditions at the bottom of the stroke by a subscript 2, equation (III-46) may be solved for the initial ratio of pressures:

$$\frac{P_{AO}}{P_{BO}} = [K-1] \frac{\frac{\psi_2}{R} + \left[\frac{F - m_p}{A P_{BO}}\right](1 - V_2^*)}{\left[\beta - \beta^K (1 + \beta - V_2^*)^{1-K}\right]} \qquad \text{(III-48)}$$

This equation is particularly useful in setting conditions for a run. Equation (III-48) must be used in conjunction with equation (III-31) since ψ is a temperature function, and if maximum sample pressure is of interest it is obtained from equation (III-32).

Since equations (III-29) and (III-47), which define the specific heat functions ϕ and ψ, are both linear in the specific heats, it follows from the assumption of an ideal solution that the values of these functions for mixtures are calculated by

$$\phi = \sum_{k=1}^{n} n_{ok} \phi_k \qquad \text{(III-49)}$$

and

$$\psi = \sum_{k=1}^{n} n_{ok} \psi_k \qquad \text{(III-50)}$$

Equation (III-46) is solved for positions other than the bottom of the stroke by first obtaining V^* and the reduced velocity

$$\frac{dV^*}{d\theta} = \left[\frac{2Ag}{m_p V_{Bo}}\right]^{\frac{1}{2}} \left\{ (m_p - F)(1 - V^*) + \frac{AP_{Ao}}{K-1}\left[\beta - \beta^K (1+\beta-V^*)^{1-K}\right] - \frac{AP_{Bo}}{R}\psi \right\}^{\frac{1}{2}} \quad \text{(III-51)}$$

as functions of T^*. Times are then calculated by either numerical or graphical integration of

$$\theta - \theta_o = \int_1^{V^*} \frac{dV^*}{\left(\frac{dV^*}{d\theta}\right)} \quad \text{(III-52)}$$

If it is desired to carry the solution past the bottom of the stroke one must change the sign of the frictional force term F in equation (III-44) and integrate from a new set of initial conditions

$$\frac{dV^*}{d\theta} = 0 \quad ; \quad V^* = V_2^* \quad ; \quad T^* = T_2^* \quad \text{(III-53)}$$

This integration yields for the first return stroke

$$\frac{m_p V_{Bo}}{2gA}\left[\frac{dV^*}{d\theta}\right]^2 = -(m_p + F)(V^* - V_2^*) + \frac{AP_{Bo}}{R}(\psi_2 - \psi) - \frac{\beta^K A P_{Ao}}{K-1}\left[(1+\beta-V^*)^{1-K} - (1+\beta-V_2^*)^{1-K}\right] \quad \text{(III-54)}$$

Equation (III-54) can be solved for $(dV^*/d\theta)$ and times calculated by continuing integration of equation (III-52) past the bottom of the stroke. The integrand of equation (III-52) exhibits a singularity when the velocity is zero, although the integral is bounded. This difficulty may be overcome by approximating over a small interval from the singularity with

$$\Delta\theta = \frac{\Delta\left(\frac{dV^*}{d\theta}\right)}{\left(\frac{d^2V^*}{d\theta^2}\right)_{AV.}} \qquad \text{(III-55)}$$

where

$$\frac{d^2V^*}{d\theta^2} = \frac{Ag}{m_p \underline{V}_{Bo}}\left[AP_{Bo}P^* - \frac{A\beta^K P_{Ao}}{[1+\beta-V^*]^K} - m_p \pm F\right] \qquad \text{(III-56)}$$

Equation (III-56) is obtained directly from equation (1) by use of equations (III-25), (III-38) and (III-40). The positive sign for the frictional force term refers to the downstroke; the negative sign to the upstroke. In practice there is always a dominant term in equation (III-56); the first term in the brackets for the bottom of the stroke, and the second term in the brackets for the conditions at the instant of piston release.

The rates of change of temperature and of pressure are sometimes themselves of interest. Differentiation of equations (III-29) and

(III-30) and use of equation (III-32) lead to

$$\frac{dT^*}{d\theta} = -\frac{RP^*}{C_{v_o}}\left(\frac{dV^*}{d\theta}\right) \tag{III-57}$$

and

$$\frac{dP^*}{d\theta} = -\frac{P^*}{(V^*-\alpha)}\left[1+\frac{R}{C_{v_o}}\right]\left(\frac{dV^*}{d\theta}\right) \tag{III-58}$$

A knowledge of the value of the frictional force F is necessary in the use of the equations derived. The effective frictional force may be determined from velocity data or from a knowledge of V_2^*. If the piston velocity is known at a point during the first downstroke, the frictional force may be calculated from

$$F = m_p + \frac{A}{(1-V^*)}\left[\frac{P_{A_o}}{K-1}\left[\beta-\beta^K(1+\beta-V^*)^{1-K}\right]-\frac{P_{B_o}\psi}{R}-\frac{m_p u^2}{2g\,V_{B_o}}\right] \tag{III-59}$$

with the values of V^*, ψ and u all pertaining to the same point. If the minimum volume V_2^* is used, the effective frictional force is given by

$$F = m_p + \frac{A}{(1-V_2^*)}\left[\frac{P_{A_o}}{K-1}\left[\beta-\beta^K(1+\beta-V_2^*)^{1-K}\right]-\frac{P_{B_o}\psi_2}{R}\right] \tag{III-60}$$

The numbers resulting from the use of the equations (III-59) and (III-60) are descriptive of the actual frictional forces only to the extent of the validity of the assumptions on which the derivations of these equations are based. For the driving gas the assumption is essentially that the polytropic expansion path of equation (III-33) be followed, while the sample gas is assumed to be an ideal solution of constant weight, composition and covolume which is undergoing isentropic compression. If the assumptions for the sample gas are satisfied for the compression to the position under consideration, the value of F determined will, when used in conjunction with the assumed value of the polytropic expansion coefficient, allow satisfactory estimation of the work done on the sample gas. The value of F so determined will correspond to a real frictional force only if the path of equation (III-33) and the chosen value of the exponent k are correct. For this reason the value of "F" so determined will be called an effective frictional force.

The physical nature of some of the foregoing expressions may be obscured by the nomenclature and it may be useful to consider them in a different way. Equation (III-41) integrates during the downstroke to give

$$\frac{m_p u^2}{2g} = (F - m_p)\Delta X + \underline{W}_A + \underline{Q}_B - \Delta \underline{E}_B$$

$$= (F - m_p)\Delta X + \underline{W}_A + \underline{W}_B \qquad \text{(III-61)}$$

The potential energy and friction term is

$$(F - m_p)\Delta X = \frac{V_{B0}}{A}(F - m_p)(V^* - 1) \qquad \text{(III-62)}$$

The work done by the driving gas on the piston is

$$\underline{W}_A = \frac{P_{A0}\underline{V}_{B0}}{k-1}\left[\beta - \beta^k(1 + \beta - V^*)^{1-k}\right] \qquad \text{(III-63)}$$

Since, from equations (III-42) and (III-47)

$$\Delta \underline{E}_0 = T_{B0}\psi \qquad \text{(III-64)}$$

neglect of the covolume at the initial state leads to

$$\Delta \underline{E} = \frac{P_{B0}\underline{V}_{B0}}{R}\psi \qquad \text{(III-65)}$$

In the derivations of this section it was assumed that $\underline{Q}_B$ was zero. This assumption is necessary in order to use equation (III-31) for determination of temperature. Substitution of equations (III-62), (III-63), and (III-65) in equation (III-61) and setting $\underline{Q}_B$ equal to zero of course yields equation (III-50).

The results of a series of calculations made in accordance with the procedure outlined with equations (III-49) through (III-56) were

presented by Longwell and Sage (16). Perfect gas relationships were assumed for these calculations, and piston position and sample gas pressure and temperature were determined as functions of time. A polytropic exponent "k" of 1.424 and a value of frictional force "F" of 50 pounds were used. In order to illustrate the marked effect that sample specific heat has on temperatures, pressures and times, and to show in a general way the type of behavior predicted by the foregoing analysis, three figures from reference (16) are presented here. Figure III-1 shows piston position as a function of time for helium, for carbon dioxide, and for an equimolal mixture of helium and carbon dioxide. Only the lower 0.16 feet of travel is displayed in order to show detail in this region which is the one of most interest. Figure III-2 shows temperature as a function of time for the same interval as Figure III-1. It is evident that decreasing the specific heat not only raises the temperature but greatly changes the shape of the temperature-time curve. Temperature is shown as a function of pressure in Figure III-3. It can be seen there that the maximum pressure for the carbon dioxide is approximately 20 times that for the helium for the same initial conditions.

Solution for Simplified Case with Heat Transfer or Endothermic Reaction

When heat transfer or chemical reaction takes place in the sample gas, the assumption of an isentropic path, employed in several of the derivations in the preceding sections, is not valid, and a more suitable assumption as to path must be made.

Consider first a very simple case of heat transfer by radiation. If energy is added at a constant rate c_1 to a material having a constant specific heat, energy is lost by radiation to surroundings at zero temperature, and the emissivity is constant, the differential equation is of the form

$$c_1 - c_2 T^4 = c_3 \frac{dT}{d\theta} \qquad \text{(III-66)}$$

Letting $c_1/c_2 = a_1^4$, and if $T = 0$ at $\theta = 0$, this integrates to

$$\theta = \frac{c_3}{2c_2 a_1^3}\left[\frac{1}{2}\ln\left|\frac{1+\frac{T}{a_1}}{1-\frac{T}{a_1}}\right| + \tan^{-1}\frac{T}{a_1}\right] \qquad \text{(III-67)}$$

This function is plotted in Figure III-4. As would be expected, the effect of radiation becomes significant only after the temperature has reached 80 per cent or so of its limiting value, and the process could be approximated without great error by one in which there is no energy loss followed by an isothermal process.

Consider qualitatively next an endothermic reaction with a reaction rate which increases markedly with temperature and neglect the variation of reaction rate with factors other than temperature. Then, if energy is added at a constant rate, the temperature-time curve will resemble that shown in Figure III-4 for radiation loss. The sharpness of the break between the linear temperature rise and the isothermal portion will depend on the rate of change of reaction rate with temperature.

While conditions in the ballistic piston do not quantitatively satisfy the assumptions made above for the heat transfer by radiation, or for endothermic reaction, it is nevertheless believed that a useful approximation to the actual path can be made in this way, and the relationships applying are derived below.

It will be assumed that

a) an ideal solution is formed

b) leakage is negligible

c) no friction or shock waves exist in the gas

d) the covolume is constant

A path as shown in Figure III-5 is assumed. The sample is compressed isentropically (no heat transfer and no reaction) until it reaches a temperature T_1. For the remainder of the compression the sample remains at T_1. After reaching maximum compression the re-expansion of the sample gas lowers the temperature abruptly. The latter part of this path is suitable when the mechanism absorbing energy to maintain the isothermal state is irreversible, or substantially so; and may also be suitable if the mechanism is reversible but markedly a function of temperature.

For the isentropic compression from the initial state to state 1, since there is no heat transfer,

$$W_{o(o-1)} = E_{o_o} - E_{o_1} = -T_{Bo}\,\psi_1 \qquad \text{(III-68)}$$

This follows from equation (III-64) and the first law of thermodynamics. For the isothermal compression from state 1 to state 2 without friction

$$W_{o(1-2)} = \frac{1}{N_o}\int_1^2 P\,d\underline{V} = \frac{RT_1}{N_{o1}}\int_1^2 \frac{d\underline{V}}{(\underline{V}_o - b)} \qquad \text{(III-69)}$$

where the work is expressed per original mole of sample gas. It is convenient and probably reasonable to assume, for the case in which the extent of reaction is not great, that the total covolume of the gas remains constant, ie

$$Nb = \text{constant} \qquad \text{(III-70)}$$

Use of equations (III-27) and (III-70) yields

$$\underline{V}_o - b = \frac{V_{BO}}{N}(V^* - \alpha) \qquad \text{(III-71)}$$

in which α is constant. Substitution of equation (III-71) in equation (III-69) gives

$$W_{o(1-2)} = \frac{RT_1}{N_o}\int_1^2 \frac{N dV^*}{V^* - \alpha} = \frac{RT_1 N_{av}}{N_o} \ln \frac{V_2^* - \alpha}{V_1^* - \alpha} \qquad \text{(III-72)}$$

in which the integration is made by taking an average number of moles N_{av} for the case where the change in number of moles is not large. If the change is large this approximation, and the one of equation III-70), may become unacceptable.

Division of equations (III-68) and (III-72) by RT_{BO} and addition gives the work per original mole of sample for the total compressional path:

$$\frac{W_o W_{(0-2)}}{RT_{BO}} = \frac{N_{av}}{N_o} T_1^* \ln(V_2^* - \alpha) - \frac{N_{av}}{N_o} T_1^* \ln(V_1^* - \alpha) - \frac{\psi_1}{R} \qquad \text{(III-73)}$$

It is assumed V_2^* is known, and that it is desired to determine T_1^*. Use of equation (III-30) leads to

$$\frac{W_o W_{(0-2)}}{RT_{BO}} = \left[\frac{N_{av}}{N_o} \ln(V_2^* - \alpha)\right] T_1^* + \left[\frac{N_{av}}{N_o}\right] \frac{\phi_1}{R} T_1^* \ln T_1^* - \frac{\psi_1}{R} \qquad \text{(III-74)}$$

An independent equation for this work can be obtained from equations (III-61), (III-62) and (III-63). Equation (III-61), for the whole downstroke, is

$$\underline{W}_B = -\underline{W}_A - (F - m_p)\Delta X \qquad \text{(III-75)}$$

Substitution of equations (III-62) and (III-63) gives

$$\underline{W}_B = -\frac{P_{AO}\underline{V}_{BO}}{K-1}\left[\beta-\beta^K\left(1+\beta-V_2^*\right)^{1-K}\right]+\frac{\underline{V}_{BO}}{A}\left(F-m_P\right)\left(1-V_2^*\right) \qquad \text{(III-76)}$$

which, by neglect of the covolume with respect to the initial molal volume, becomes

$$\frac{W_{o(1-2)}}{RT_{BO}} = \frac{1}{P_{BO}}\left\{\frac{F-m_P}{A}\left(1-V_2^*\right)-\frac{P_{AO}}{K-1}\left[\beta-\beta^K\left(1+\beta-V_2^*\right)^{1-K}\right]\right\} \qquad \text{(III-77)}$$

If an appropriate value of F is known, equation (III-77) may be used to calculate a numerical value for the work. This value may then be substituted in equation (III-74). Assumption of a suitable value for the mole ratio N_{av}/N_o in equation (III-74) leaves a transcendental equation in several functions of T_1^* which can be solved for T_1^* by iterative means. Since α is a function of temperature, double iteration is required.

Since the path between states 1 and 2 is isothermal, the total change in internal energy for this path and equation of state is that due to reaction. The first law thus gives for a frictionless path

$$\left(\Delta E_{oR}-Q_o\right) = -W_{o(1-2)} = -\frac{RT_1N_{av}}{N_o}\ln\frac{\left(V_2^*-\alpha\right)}{\left(V_1^*-\alpha\right)} \qquad \text{(III-78)}$$

$$= -RT_{BO}\left[\frac{W_{o(1-2)}}{RT_{BO}}+\frac{\psi_1}{R}\right]$$

Now the equations necessary to determine time as a function of position during the isothermal portion of the path will be developed. Times during the isentropic portion can of course be determined by use of equations (III-51) and (III-52). If the pressure of the driving gas, and frictional and gravitational forces are neglected for the isothermal path, equating work to change in kinetic energy and use of equation (III-72) gives

$$\underline{W}_B = \frac{m_p}{2g} \Delta(u^2) = RT_1 \int \frac{N\, dV^*}{V^* - \alpha} \qquad \text{(III-79)}$$

Using equation (III-38) and taking an average value for the number of moles, there is obtained

$$\Delta\left(\frac{dV^*}{d\theta}\right)^2 = \frac{2gRT_1A^2N_{av}}{m_p \underline{V}_{Bo}^2} \int \frac{dV^*}{V^* - \alpha} \qquad \text{(III-80)}$$

which, if the covolume is neglected under initial conditions, may be written as

$$\Delta\left(\frac{dV^*}{d\theta}\right)^2 = \frac{2gP_{Bo}T_1^*A^2N_{av}}{m_p \underline{V}_{Bo} N_o} \int \frac{dV^*}{V^* - \alpha} \qquad \text{(III-81)}$$

Define a constant, having the dimensions of time:

$$C_3 = \frac{1}{A}\left[\frac{m_p \underline{V}_{Bo} N_o}{2g P_{Bo} T_1^* N_{av}}\right]^{\frac{1}{2}} \qquad \text{(III-82)}$$

Use of equation (III-82) in (III-81) gives

$$\Delta\left(\frac{dV^*}{d\theta}\right)^2 = \frac{1}{C_3^2}\int \frac{dV^*}{V^* - \alpha} \qquad \text{(III-83)}$$

and integration to state 2 as an upper limit gives

$$\left(\frac{dV^*}{d\theta}\right)^2 = \frac{1}{C_3^2} \ln \frac{V^* - \alpha}{V_2^* - \alpha} \qquad \text{(III-84)}$$

since the velocity is zero at that state.

At this point a change in variable is helpful. Define a new variable y:

$$y = \left[\ln \frac{V^* - \alpha}{V_2^* - \alpha}\right]^{\frac{1}{2}} = -C_3 \frac{dV^*}{d\theta} \qquad \text{(III-85)}$$

Differentiation of equation (III-85) gives

$$dV^* = 2y(V^* - \alpha)\,dy \tag{III-86}$$

and also, from equation (III-85)

$$V^* - \alpha = (V_2^* - \alpha)\,e^{y^2} \tag{III-87}$$

Use of equations (III-86) and (III-87) in (III-85) gives

$$d\theta = -2C_3(V_2^* - \alpha)\,e^{y^2}\,dy \tag{III-88}$$

and since

$$y = 0 \quad at \quad \theta = \theta_2 \tag{III-89}$$

$$\theta_2 - \theta = 2C_3(V_2^* - \alpha)\int_0^y e^{y^2}\,dy \tag{III-90}$$

The time interval from the position corresponding to y to the bottom of the stroke is given by equation (III-90). The integral may be evaluated by use of infinite series or, more conveniently, by use of tabulated values such as those given by Jahnke and Emde (21).

It is possible to obtain numerical values of reaction rate constants for certain types of reactions on the basis of the path assumed

above and shown in Figure III-5. If the reaction under consideration is irreversible (or essentially so under the conditions existing) and it is assumed to proceed only during the time represented by the isothermal path, then the compositions at state 1 and at state 2 are known and solution for the reaction rate constant can be made.

First-Order Kinetics

Consider first a first order reaction (such as a decomposition) and let η_o be the mole fraction of the reactant and otherwise the subscript "R" refer to the reactant. Then

$$-\frac{dN_R}{d\theta} = k_R \underline{V}_B (f_R) = k_R \underline{V}_B \eta_o f_R^\circ \qquad \text{(III-91)}$$

This is essentially the defining equation for k_R.

It follows from equation (AI-29) of Appendix I that

$$f_R^\circ = P \exp\left[\frac{P\bar{b}_R}{RT_1}\right] \qquad \text{(III-92)}$$

where, by equation (AI-28)

$$\bar{b} = \frac{1}{P}\int_0^P b\, dP \qquad \text{(III-93)}$$

with the integral taken at constant temperature. If the assumption made previously concerning the use of an average number of moles remains

valid

$$dN_R \simeq N_{av}\, d\eta_o \tag{III-94}$$

The equation of state gives

$$P = \frac{N P_{Bo} T_1^*}{N_o (V^* - \alpha)} \simeq \frac{N_{av} P_{Bo} T_1^*}{N_o (V^* - \alpha)} \tag{III-95}$$

if equation (III-70) is valid.

Substitution of the relationships of equations (III-92), (III-94) and (III-95) into equation (III-91) and simplification give

$$-\frac{1}{\eta_o}\frac{d\eta_o}{d\theta} = k_R R T_1 \left[\frac{V^*}{V^* - \alpha}\right] \exp\left[\frac{\bar{b}_R N_{av}}{V_{Bo}(V^* - \alpha)}\right] \tag{III-96}$$

Use of the variable y defined by equation (III-85) results in simplification of equation (III-96). Substitution of equation (III-87) in equation (III-96) gives

$$-\frac{1}{\eta_o}\frac{d\eta_o}{d\theta} = k_R R T_1 \left[1 + \frac{\alpha}{V_2^* - \alpha} e^{-y^2}\right] \exp\left[\frac{\bar{b}_R N_{av}}{V_{Bo}(V_2^* - \alpha)} e^{-y^2}\right] \tag{III-97}$$

Multiplication of equation (III-97) by equation (III-88) gives

$$\frac{d\eta_o}{\eta_o} = 2k_R C_3 RT_1(V_2^* - \alpha)\left[\frac{\alpha}{V_2^* - \alpha} + e^{y^2}\right]\exp\left[\frac{\bar{b}_R N_{av}}{V_{Bo}(V_2^* - \alpha)} e^{-y^2}\right] dy \quad \text{(III-98)}$$

which is to be integrated to obtain the reaction rate coefficient k_R. Since $\bar{b}_R$ is a tabulated function of pressure (and temperature), and equation (III-98) must be integrated numerically even if $\bar{b}_R$ were constant, another form which exhibits more physical significance is in order. If, again, the change in number of moles is neglected,

$$\frac{P_2}{P} = \frac{V^* - \alpha}{V_2^* - \alpha} = e^{y^2} \quad \text{(III-99)}$$

Use of equation (III-92) and (III-99) in equation (III-98) leads to

$$\frac{d\eta_o}{\eta_o} = 2k_R B_1\left[\frac{\alpha}{V_2^* - \alpha} + \frac{P_2}{P}\right]\exp\left[\frac{\bar{b}_R P}{RT_1}\right] dy \quad \text{(III-100)}$$

where

$$B_1 = RT_1(V_2^* - \alpha)C_3 \quad \text{(III-101)}$$

In order to make use of the tabulated first derivative of the error function, take

$$\Phi_1(y) = \frac{d}{dy}(\text{erf } y) = \frac{2}{\sqrt{\pi}} e^{-y^2} \qquad \text{(III-102)}$$

This function is tabulated by Jahnke and Emde (21) as $\Phi_1(x)$ and by others. Equation (III-99) becomes

$$\frac{P_2}{P} = \frac{2/\sqrt{\pi}}{\Phi_1(y)} = \frac{1.12838}{\Phi_1(y)} \qquad \text{(III-103)}$$

and equation (III-100) integrates to

$$\ln \frac{\eta_{o1}}{\eta_{o2}} = 2 k_R B_1 \int_0^{y_1} \left[\frac{\alpha}{V_2^* - \alpha} + \frac{P_2}{P}\right] \frac{f_R^\circ}{P} \, dy \qquad \text{(III-104)}$$

Numerical integration of this expression, using equations (III-92) and (III-103) and tabulated functions, is relatively easy, and k_R is then obtained.

It may be desired to calculate the composition and $(\Delta E_{\delta R} - \frac{Q}{\delta})$ as functions of time in order to check the compatibility of assumptions. Times may be found by using equation (III-90). Compositions are given by

$$\ln \frac{\eta_o}{\eta_{o2}} = 2 k_R B_1 \int_0^{y} \left[\frac{\alpha}{V_2^* - \alpha} + \frac{P_2}{P}\right] \frac{f_R^\circ}{P} \, dy \qquad \text{(III-105)}$$

which comes from equation (III-104). By use of equations (III-78) and (III-85), $(\Delta E_{oR} - \frac{Q}{o})$ is given by

$$\left(\Delta E_{oR} - \frac{Q}{o}\right)_{(y-2)} = \frac{N_{av}}{N_o} RT_1 y^2 \qquad \text{(III-106)}$$

These equations work backwards in time from the time of minimum volume, but this is no particular disadvantage.

One-Half Order Kinetics

Another possible reaction rate expression is that for a fractional order such as one half. Then the defining equation is

$$-\frac{dN_R}{d\Theta} = k_R \underline{V}_B (f_R)^{\frac{1}{2}} = k_R \underline{V}_B \left(\eta_o f_R^o\right)^{\frac{1}{2}} \qquad \text{(III-107)}$$

Methods and assumptions analogous to those used in obtaining equation (III-104) from equation (III-91) will yield for this case

$$\frac{d\eta_o}{(\eta_o)^{\frac{1}{2}}} = 2k_R \left\{ \frac{\left[\underline{V}_{Bo}(V_2^* - \alpha)\right]^{\frac{3}{2}}}{A N_{av}} \left[\frac{m_P}{2g}\right]^{\frac{1}{2}} \right\} \left[\frac{\alpha}{V_2^* - \alpha} + \frac{P_2}{P}\right] \left[\frac{P_2}{P} \times \frac{f_R^o}{P}\right]^{\frac{1}{2}} dy \qquad \text{(III-108)}$$

which may be integrated to give

$$(\eta_{o1})^{\frac{1}{2}} - (\eta_{o2})^{\frac{1}{2}} = k_R B_4 \int_o^{y_1} \left[\frac{\alpha}{V_2^* - \alpha} + \frac{P_2}{P}\right] \left[\frac{P_2}{P} \times \frac{f_R^o}{P}\right]^{\frac{1}{2}} dy \qquad \text{(III-109)}$$

in which

$$B_4 = \frac{\left[V_{BO}(V_2^* - \alpha)\right]^{\frac{3}{2}}}{A N_{av}} \left[\frac{m_p}{2g}\right]^{\frac{1}{2}} \qquad \text{(III-110)}$$

The integral in equation (III-109) may be evaluated numerically by using equations (III-92) and (III-103) and tabulated functions, and k_R is then determined.

The composition and $(\Delta E_{\delta R} - \frac{Q}{\delta})$ may be determined during the course of the reaction by use of

$$(\eta_o)^{\frac{1}{2}} = (\eta_{o2})^{\frac{1}{2}} + k_R B_4 \int_o^y \left[\frac{\alpha}{V_2^* - \alpha} + \frac{P_2}{P}\right]\left[\frac{P_2}{P} \times \frac{f_R^o}{P}\right]^{\frac{1}{2}} dy \qquad \text{(III-111)}$$

and equation (III-106) respectively.

Solutions Using Additional Experimental Data

It is planned to start measuring pressure as a function of time shortly and to measure the integrated thermal flux to a portion of the walls of the apparatus. Position-time measurements are now being made, and it is hoped ultimately to estimate temperatures by means of experimental measurement. The availability of such measurements will be of considerable aid to the experimenter.

No attempt will be made here to describe in any detail the treatment of the data which will be derived from future measurements. A few remarks are probably in order, however.

The integrated thermal flux measurement will allow estimation of the total heat transfer from the sample gas. If sufficiently small, heat transfer can be neglected with confidence; if sizable it will be necessary to assume a form for the heat transfer rate such that when it is integrated over the entire path the resulting quantity will match that estimated from measurement.

When pressure measurements become available, the pressure-time relation will of course be given directly. With the time base correlated with the position-time measurements now made at discrete points, integration twice of the pressure with respect to time will give continuous position-time data to be fitted to those measured directly on the downstroke, and pressure and volume will be known as continuous functions of time. Likewise the internal energy of the sample will be known as a continuous function of time since the work can be calculated and the heat estimated by use of thermal flux meter data. If no reactions take place, the equation of state can be obtained from these data. If the equation of state is known, simple reactions can be followed by following the change in internal energy due to reaction, and it will be possible to stay much closer to reality than has been possible here.

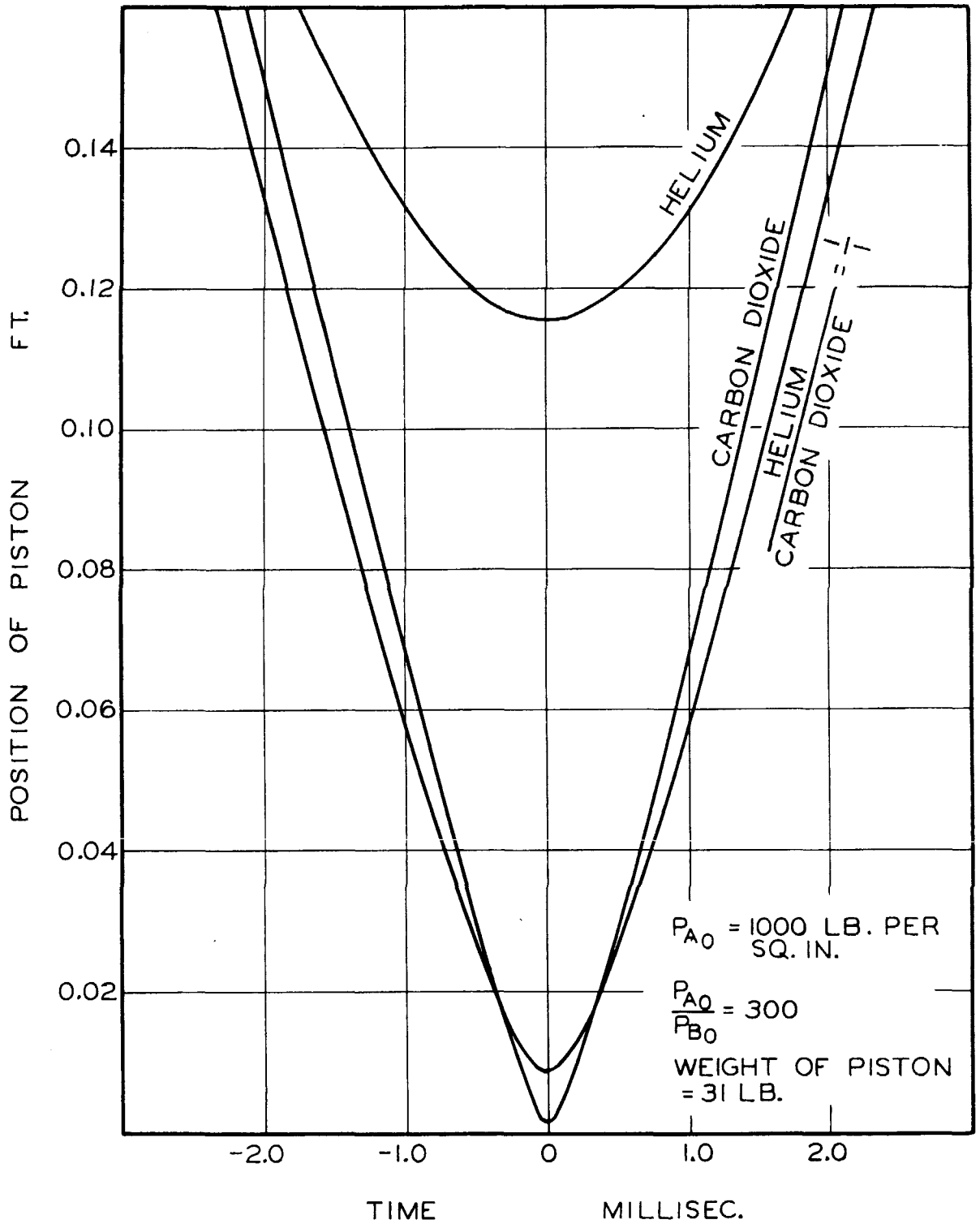

Fig. III-1. Effect of Sample Composition on Piston Position-Time Relationships

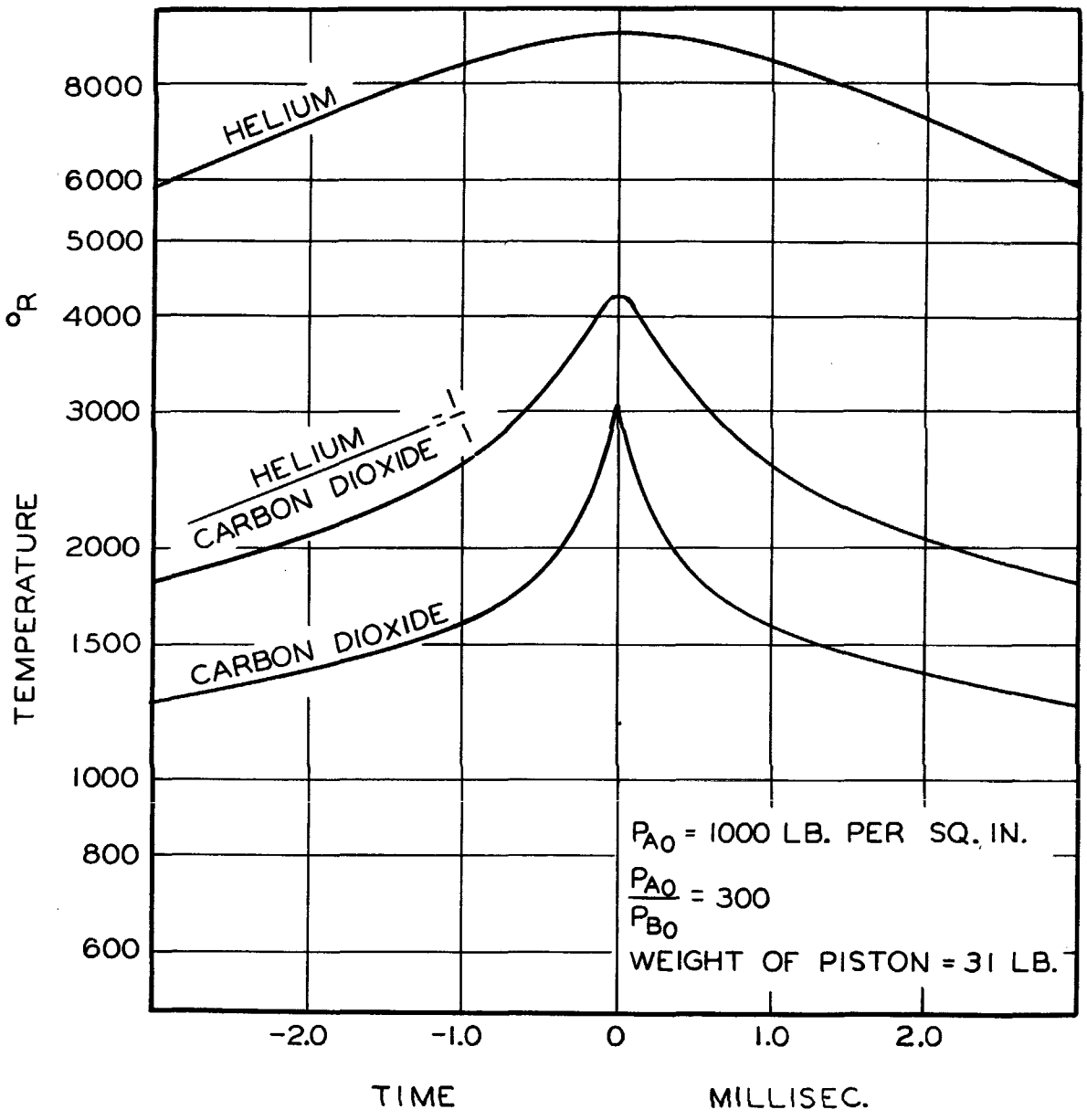

Fig. III-2. Effect of Sample Composition on Sample Temperature-Time Relationships

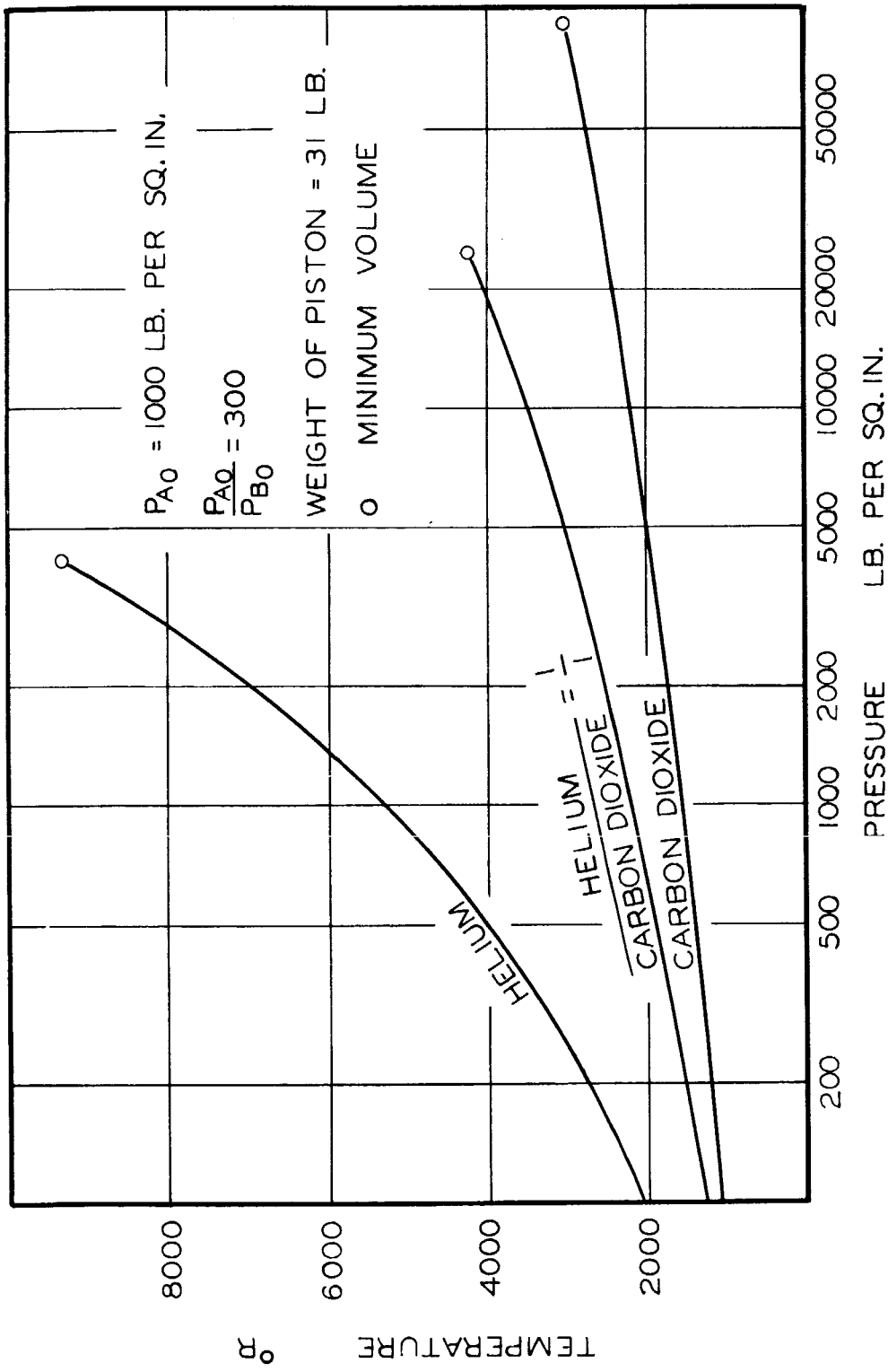

Fig. III-3. Effect of Sample Composition on Sample Temperature-Pressure Relationships

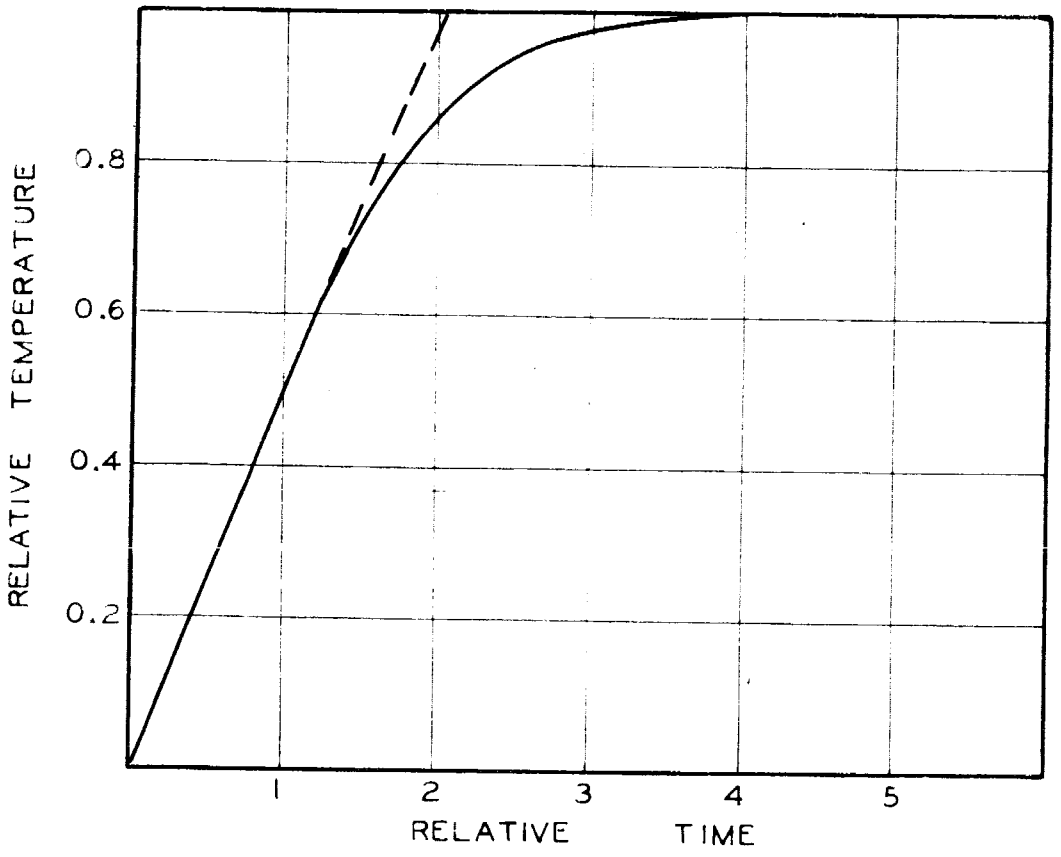

Fig. III-4. Limiting of Temperature by Radiation

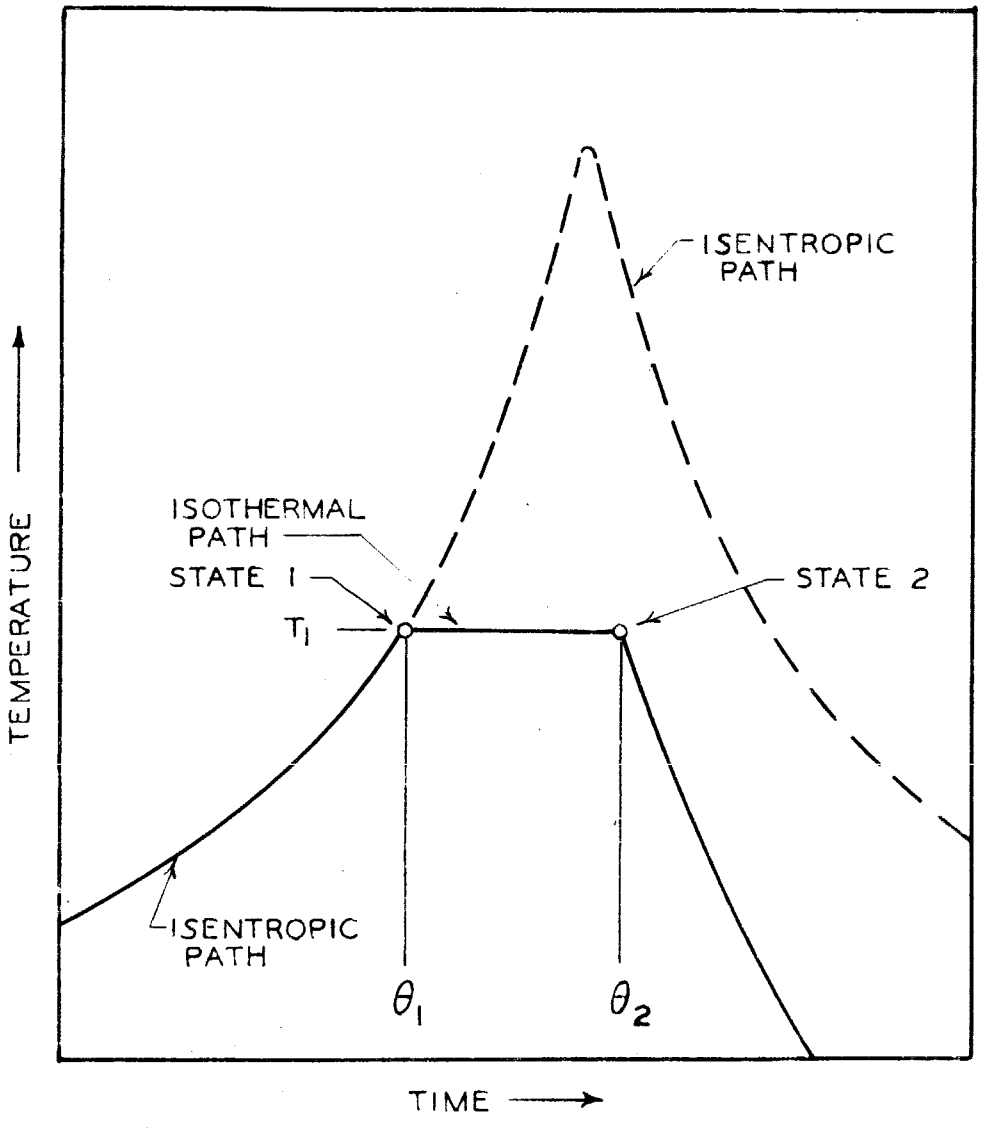

Fig. III-5. Assumed Path with Heat Transfer or Endothermic Reaction

IV. CARBON HYDROGEN SYSTEM: METHANE

Methane was selected as the first material to undergo investigation in the ballistic piston apparatus since it is a simple hydrocarbon which could be expected to react chemically under conditions of high temperature and pressure, and it was desired to determine in an exploratory manner what types of products might be formed in such reactions. Little is known experimentally concerning the behavior of methane under the extreme conditions obtainable with the ballistic piston apparatus. Hanson (12) described use of the du Pont compression reactor on methane, on methane and carbon monoxide, on methane and oxygen, and on methane and nitrogen, and reported that results were of no great interest, soot being formed with mixtures of methane and nitrogen. Furman and Tsiklis (11) reported ballistic piston tests on mixtures of methane with small amounts of oxygen having as the objective the determination of the effect of a cold wall upon the course of a chain reaction. These two references became available some time after the investigation described here was performed.

Most of the tests on methane were made during the period when the ballistic piston apparatus was first being placed in operation. There was essentially no instrumentation and experimental techniques were in a formative state. Two tests were made later when some timing equipment had been installed. As a result of the inadequacy of the data only a rather modest amount of effort on the analysis of the experimental results was considered warranted.

Experimental Procedure

The ballistic piston apparatus used for these tests was essentially as described briefly in Part II and in more detail by Longwell and Sage (16). The piston weighed approximately 31.0 pounds. The earliest tests were made on pure methane. During these tests the lead crusher gage technique for measurement of the distance of closest approach of the piston to the bottom of the chamber, as described in Part II, was developed. Also the original design of the bottom closure did not properly confine the high pressure gas and a revision of the closure was necessary. These first tests did not produce data pertinent to the reactions of methane and so are not included here.

The procedure for the series of tests without timing data (runs 23 - 35) was as follows:

The interior of the bottom closure was cleaned with carbon tetrachloride and dried. The barrel was lubricated with powdered molybdenum disulfide (Molylube). The piston, which was solid carbon steel, was assembled to the top closure with a 0.373 inch diameter brass shear pin, the O-rings lubricated with molybdenum disulfide, and the piston and closure inserted in the barrel. The unsupported area seal was then tightened. The lower closure, with a measured lead crusher gage in it, was inserted, the unsupported area seal tightened, and the vacuum line connected.

The apparatus was next evacuated to a pressure of 1 mm. or less, and purged with helium two or three times. The helium was passed

through a trap cooled with a dry ice-trichloroethylene mixture. After purging, the helium pressure was adjusted in accordance with the desired composition and measured with a mercury-in-glass manometer, then the chamber valves were closed and the lines evacuated. Methane from a tank was passed through a high pressure trap cooled with a dry ice-trichloroethylene mixture and into the lines. The chamber valve was opened, methane was added to give the desired composition at a pressure of about 80 cm., and the pressure measured. The chamber valves were closed and the lines evacuated. In the case of runs 23 and 24, in which helium was not used, the apparatus was evacuated until the pressure was less than about 0.1 mm. and the methane added. After standing for 30 minutes or more to allow mixing, a control sample was withdrawn into an evacuated bulb, then the chamber pressure reduced to that desired as an initial sample pressure. Compressed air was admitted to fill the upper chamber to the desired pressure, valves closed, and the piston released by means of the firing handle.

After firing, the driving air was vented. The measurements required for estimation of leakage were just being started and were not made on all runs. When made, the procedure was to remove the top closure and measure the distance to the piston using a weighted steel tape, and to measure the sample pressure by use of the mercury manometer. Two product samples were then taken in evacuated sample bulbs. When leakage measurements were not made, the two product samples were taken before the top closure was removed.

Finally, the piston and bottom closure were removed, the lead gage recovered, and its height measured.

The procedure followed for runs 86 and 87 differed in some details. One Berkeley Instrument Time Interval Meter was available, and the bottom closure used was fitted with two contact holders. Copper wires were placed in these holders and the heights of the wires above the bottom were measured to 0.0002 inch by use of a depth micrometer registering on the top of the bottom closure. Contact was detected by use of an electronic volt-ohmmeter.

The barrel and piston were lubricated with powdered graphite which had meanwhile been found more suitable than molybdenum disulfide for the service. After evacuation the chamber was purged with nitrogen rather than with helium, otherwise sample addition techniques were similar. Leakage measurements were made on both runs.

Materials

The methane used was supplied by The Texas Company. A mass spectrometer analysis of a sample of this methane was performed by the Montebello Laboratories of The Texas Company and the composition was determined as 99.58 mole per cent methane, 0.15 mole per cent hydrogen, 0.05 mole per cent propane, 0.07 mole per cent ethane, 0.11 mole per cent carbon dioxide and 0.04 mole per cent water.

The helium used was obtained from the Air Reduction Company. It was reported as being 99.97 per cent pure, however a mass spectrometer analysis by The Texas Company showed 0.14 mole per cent nitrogen as an impurity.

The nitrogen was purchased from Linde Air Products Company which reported it as 99.95 per cent pure. Analysis by mass spectrometer by The Texas Company showed 0.04 mole per cent oxygen, 0.02 mole per cent argon, and 0.07 mole per cent water as impurities.

Experimental Results

Ten ballistic piston runs were made with methane. Data for these runs are shown in Table IV-I. The first two, numbers 23 and 24, were made on methane without diluent, and no chemical reaction occurred. Following the precedent of Ryabinin (10) who used argon as a diluent to decrease the heat capacity, varying proportions of helium were used in the subsequent runs in order to obtain temperatures sufficiently high for chemical reactions to occur. The initial compositions are shown in Table IV-I, as are initial pressures of the driving air and of the sample. The measured distance of closest approach is shown; from this the normalized minimum volume V_2^* was calculated with corrections made for the volume of the lead gage and for the volume of any recesses in the bottom closure. The leakage calculated from the experimental measurements is shown for those runs for which measurements were made. It will be noted that the leakage was excessive on run 33.

The bottom contact timing data for the two runs made after timing equipment became available are shown in Table IV-II. Since only one time measurement was made for a run, the velocities shown are the average over the interval h_1 to h_3 and are assumed to apply at a point h_2 defined as the average of the heights h_1 and h_3.

The analyses of samples taken before and after the runs are shown in Table IV-III as reported by the Montebello Laboratories of The Texas Company, which performed the analyses using a mass spectrometer. No analysis was obtained for run 24. Since this run was a duplicate of run 23 and no reaction was obtained in the latter, it may be assumed that no reaction occurred in run 24. This is in accordance with experimental observations. It will be noted that most of the runs show appreciable amounts of air in the samples, both control and product. These do not correlate with CO_2 analyses, however if there were oxygen present it would tend to react to give CO rather than CO_2 (11) and CO is difficult to determine in the presence of nitrogen by mass spectrometer. It is believed that the air shown in the runs through number 35 is partially the result of using makeshift sample addition equipment, and partially the result of leakage by the O-rings on the piston. The sample addition equipment described in Part II and seen in Figure II-2 was placed in use in the interval between run 35 and run 86, and prior to the installation of this equipment it was difficult to avoid some contamination. Also the O-ring grooves on the piston were deepened prior to run 23 in an effort to reduce friction. This resulted in less friction but added leakage of air, and the bottoms of the grooves were built up with tin just before run 35. It will be noted that the air reported for runs 86 and 87 is small.

The product analysis for run 33 shows 73 per cent air, and an analysis of the second sample of the product showed 90 per cent air.

When this is considered in combination with the excessive leakage shown by this run, it appears that the data for this run are almost worthless, and they have been omitted in some subsequent presentations. No specific reason for this failure is known.

Analysis of the Composition Data

The analysis data in Table IV-III do not completely balance stoichiometrically, nor do the control analyses agree precisely with those computed from the measurements made during sample addition. These disagreements, amounting to as much as 5 per cent of the methane present, are within the error to be expected from the mass spectrometer. Since it was necessary to determine the amount of free carbon produced by difference from a set of data which did balance stoichiometrically, a set of adjusted analyses was computed and is shown in Table IV-IV.

These adjusted analyses were obtained by first eliminating the air, water, and carbon dioxide. The initial composition was then obtained from the measurements made during sample addition for the major components, while the mass spectrometer analyses were used for the minor components. Material balances were next written for each atomic species present and one additional equation for the sum of all components of the product was obtained. Unknowns equal in number to the equations were selected; these always included the free carbon, the ratio of final moles to initial moles, and the final diluent gases, and generally included the final methane. The amounts of the remaining components were taken from the mass spectrometer analysis as corrected

for air, water, and carbon dioxide. The equations were solved and the resulting compositions compared with those obtained from the mass spectrometer. In all cases they were within the error expected in mass spectrometer analyses, and the amounts of free carbon computed were in qualitative agreement with observation.

The stoichiometrically consistent adjusted analyses of Table IV-IV were used for the calculation of the distribution of the products from the conversion of methane. The distributions are shown in Table IV-V. The conversion to hydrogen is shown as the fraction of the reacted methane which appeared as hydrogen, based on a hydrogen balance, while the conversion to carbon and hydrocarbons is shown as the fraction of the reacted methane converted to the particular product, based on carbon content. The fraction of the total methane which reacted is also shown. It is apparent that as the amount reacted increases the fraction of reacted methane converted to carbon also increases, reaching as much as 80 per cent. The maximum conversion of reacted methane to benzene was 14 per cent and the maximum conversion to ethylene was 43 per cent, the latter with a very small fraction of the methane reacted however. The conversions will be discussed later in connection with the estimated temperatures and pressures to which the samples were subjected.

Analysis of Run Data

It is necessary to know the amount of energy transferred from the piston to the sample gas in order to estimate by the methods of Part III

the pressures and temperatures experienced by a sample undergoing chemical reaction. The energy involved can be calculated if a suitable value of the effective frictional force is known. Unfortunately timing data were obtained on only the last two of these tests so there are no measurements on the other runs in which reaction occurred that can be used to obtain values of the effective frictional force. It was possible to calculate effective frictional force for the two runs where no reaction occurred, however, and the average of these values was used for the runs which lacked timing data.

For runs 23 and 24 which had no chemical reaction it was assumed that the compression was isentropic and the pressure and temperature at maximum compression were calculated by means of equation (III-31) and (III-32), which are

$$T^* = (V^* - \alpha)^{-R/\phi} \tag{IV-1}$$

and

$$P^*(V^* - \alpha) = T^* \tag{IV-2}$$

in combination with equations (III-49) and (AI-10)

$$\phi = \sum_{K=1}^{n} \eta_K \phi_K \tag{IV-3}$$

and

$$b = \sum_{K=1}^{n} \eta_{oK} b_K \qquad \text{(IV-4)}$$

and the values of ϕ and b given in Appendix I. The compositions given in Table IV-I were used for these calculations which are iterative in nature. The temperatures and pressures calculated are shown in Table IV-VI. The effective frictional force was then found by use of equation (III-60)

$$F = m_P + \frac{A}{(1-V_2^*)}\left[\frac{P_{AO}}{K-1}\left[\beta - \beta^K\left(1+\beta-V_2^*\right)^{1-K}\right] - \frac{P_{BO}\,\psi_2}{R}\right] \qquad \text{(IV-5)}$$

and equation (III-50)

$$\psi = \sum_{K=1}^{n} \eta_{oK} \psi_K \qquad \text{(IV-6)}$$

A value of 1.424 for k was used for the methane runs, as is discussed in Appendix I. The values of effective frictional force calculated for the runs without reaction are shown in Table IV-VI. The agreement between runs 23 and 24, which had essentially identical initial conditions, is not particularly good. It is possible that excessive leakage occurred, however no leakage measurements were made.

Runs 86 and 87 had timing data and therefore velocities were known, as shown in Table IV-II. The conditions at h_2 were calculated as discussed above using equations (IV-1) through (IV-4) and are shown in Table IV-VII. The effective frictional force was calculated using equation (III-59)

$$F = m_p + \frac{A}{(1-V^*)}\left[\frac{P_{A0}}{K-1}\left[\beta - \beta^K(1+\beta-V^*)^{1-K}\right] - \frac{P_{B0}\Psi}{R} - \frac{m_p u^2}{2g\underline{V}_{B0}}\right] \qquad \text{(IV-7)}$$

with V^*, Ψ and u all for the point h_2, and equation (IV-6). The values of effective frictional force calculated are shown in Table IV-VII. The velocity was measured closer to the bottom than is desirable for this type of calculation and at least in the case of run 87 considerable reaction had probably taken place by the time the piston reached the point h_2, as shown by the high temperature calculated on the basis of an isentropic path. This tends to give an effective frictional force which is too low. The value of + 9.7 pounds for run 86 seems reasonable.

The average of the effective frictional forces for runs 23 and 24 is -28.0 pounds. As has been mentioned earlier the O-ring grooves on the piston were deeper for those runs than for runs 86 and 87 and the difference between the effective frictional forces for the two sets of runs is of the correct sign and approximately of the correct magnitude. The negative signs merely indicate that the driving air is not following the assumed polytropic path exactly.

The reaction temperature was estimated by assuming that the sample is compressed isentropically until it reaches this temperature and that the path is then isothermal until maximum compression is reached. This implies that an endothermic reaction takes place at a rate sufficient to stabilize the temperature. This path is discussed in Part III and shown diagramatically in Figure III-5.

The work done on the sample gas was calculated by use of equation (III-77)

$$\frac{W_B}{RT_{Bo}} = \frac{1}{P_{Bo}}\left\{\frac{F-m_p}{A}(1-V_2^*) - \frac{P_{Ao}}{k-1}\left[\beta-\beta^k(1+\beta-V_2^*)^{1-k}\right]\right\} \qquad \text{(IV-8)}$$

using values of effective frictional force shown in Table IV-VIII. The mean of the values of effective frictional forces for runs 23 and 24 was used for runs 25 through 35 since no other applicable data were available. A second relationship relating the work to the temperature of the isothermal path is given by equation (III-74):

$$\frac{W_B}{RT_{Bo}} = \left[\frac{N_{av}}{N_o}\ln(V_2^*-\alpha)\right]T_1^* + \left[\frac{N_{av}}{N_o}\right]\frac{\phi_1}{R}T_1^*\ln T_1^* - \frac{\psi_1}{R} \qquad \text{(IV-9)}$$

The values assumed for the ratio (N_{av}/N_o) are shown in Table IV-VIII and are equal to approximately one half the ratio of final moles to initial moles shown in Table IV-IV. The numerical value of the work

from equation (IV-8) was substituted in equation (IV-9) and the latter solved iteratively for the temperature using equations (IV-3), (IV-4) and (IV-6) and the values of b, ϕ/R and ψ/R tabulated in Appendix I. The maximum pressure was calculated by use of

$$P_2^*(V_2^* - \alpha) = \frac{N_2}{N_o} T_1^* \qquad \text{(IV-10)}$$

The reaction temperatures and the maximum pressures are shown in Table IV-VIII, as are also values of the term $(\Delta E_{oR} - Q_o)$ calculated by

$$\frac{(\Delta E_{oR} - Q_o)}{RT_{Bo}} = - \frac{W_B}{RT_{Bo}} - \frac{\psi_1}{R} \qquad \text{(IV-11)}$$

The positive nature of the $(\Delta E_{oR} - Q_o)$ terms indicates an endothermic reaction.

The time interval during which this assumed isothermal compression occurs is given by equation (III-90)

$$\Delta\theta = 2C_3(V_2^* - \alpha) \int_0^{y_1} e^{y^2} dy \qquad \text{(IV-12)}$$

where y is a variable defined by equation (III-85)

$$y = \left[\ln \frac{V^* - \alpha}{V_2^* - \alpha}\right]^{\frac{1}{2}} \qquad \text{(IV-13)}$$

and C_3 is, by equation (III-82)

$$C_3 = \frac{1}{A}\left[\frac{m_p \underline{V}_{Bo} N_o}{2g P_{Bo} T_1^* N_{av}}\right]^{\frac{1}{2}} \qquad \text{(IV-14)}$$

The time intervals are shown in Table IV-VIII. In order to show the deviation from perfect gas behavior predicted by the equation of state given in Appendix I, the values of the compressibility factor at the maximum compression are also shown. These were computed by use of

$$\frac{PV}{RT} = \frac{P_2^* V_2^* N_o}{T_1^* N_2} \qquad \text{(IV-15)}$$

Comparison of the temperatures T_1 for runs 86 and 87 with those shown in Table IV-VII as computed at the point h_2 shows in the case of run 87 a difference of about 1300° R. This gross departure from the assumption of isentropic compression to the position h_2 probably accounts for the low value of effective frictional force for run 87. This value was used however since no other data were available. It will also be noted that the reaction time $\Delta\theta$ for run 33 is shown as over twice

that for any of the others, and that the reaction temperature of 2452° R. is the lowest of those for runs showing chemical reaction. The amount of reaction and the distribution of products for run 33 however are similar to those for runs at about 2900° R. As mentioned earlier, run 33 showed large leakage and therefore it is considered that the computed temperature and time for this run are meaningless and this run is omitted from the graphical displays of the data.

The product distributions on the basis of carbon balances, from Table IV-V, are shown in Figure IV-1 in a cumulative fashion as functions of the calculated reaction temperatures. Similarly the fractions of the reacted methane which appeared as hydrogen, based on hydrogen balances, are shown in Figure IV-2 as functions of the reaction temperature. Quite definite trends are shown in Figures IV-1 and IV-2, the amounts of carbon and hydrogen increasing sharply with temperature, the amount of benzene being the largest in the middle range of temperatures, and the amounts of other hydrocarbons in general decreasing markedly with temperature increase. The trends are not smooth however, the points for runs 26 and 35 being noticeably odd. There is justification for believing that the temperature shown for run 35 is too high by an indeterminate amount since the O-ring grooves on the piston were changed before this run in a manner which increased the effective frictional force but this change was not taken into account in the calculations of the reaction temperature. Furthermore no account of possible effects of pressure or reaction time on product distribution

was taken in plotting Figures IV-1 and IV-2, and it is expected that these variables might influence product distributions.

The fraction of the total methane which reacted is shown in Figure IV-3 as a function of reaction temperature. The pattern of points is quite similar to those for free carbon in Figure IV-1 and for hydrogen in Figure IV-2. The line was calculated by regression with temperature as the independent variable. The deviations of the points from this line showed some correlation with the maximum pressure so a regression of the fraction of the total methane reacted with reaction temperature and maximum pressure was made. The relationship found was

$$(\text{Fract. } CH_4 \text{ react.}) = -1.076 + 3.986 \times 10^{-4} T_1 + 1.924 \times 10^{-6} P_2 \qquad \text{(IV-16)}$$

where the temperature is expressed in degrees Rankine and the pressure in pounds per square inch. The effectiveness of this correlation was determined by correcting the observed fractions reacted to a maximum pressure of 69,400 pounds per square inch, which was the average for the runs, and plotting the corrected fractions as functions of reaction temperature in Figure IV-4. The linearity of the relationship was markedly improved by taking account of the effect of pressure. This would be expected since the reaction rate would be a function of pressure, although this function is probably non-linear.

Since the patterns of points in Figures IV-1 and IV-2 do show

similarity to that in Figure IV-3, it can be concluded that at least a portion of the irregularity in the product distributions is due to the effect of pressure. However no attempt to further investigate this variable was deemed justified, since the data are rather unprecise.

The internal energy absorbed in reaction less the heat transferred to the sample is shown as a function of the amount of methane decomposed in Figure IV-5. The line is drawn through the origin since it was implicitly assumed that $(\Delta E_{oR} - Q_o)$ was zero for runs 23 and 24, which showed no reaction, in order to calculate values of effective frictional force. While the higher values of $(\Delta E_{oR} - Q_o)$ show a reasonably linear relationship with the amount of methane decomposed, the two lower points do not.

The change in internal energy due to reaction ΔE_{oR} was calculated for some of the runs using heat of formation data given by Rossini (22) and assuming that the reaction to give the observed products was completed at the reaction temperature T_1. These values of ΔE_{oR} are positive but are much smaller than the values of $(\Delta E_{oR} - Q_o)$ computed for the assumed isothermal path. Ratios found were 0.15 for runs 86 and 87, 0.13 for run 25 and 0.05 for run 29. These figures are interpreted as indicating that the composition of the sample at maximum compression is significantly different from that observed in the product samples. It is presumed that there are appreciable concentrations of free radicals remaining when the piston starts its return stroke and that these undergo further reactions thereafter. The physical behavior

of the apparatus in not showing noticeable oscillations of the type found in nitrogen-oxygen runs, for instance, leads to the conclusion that the reactions subsequent to maximum compression were sufficiently slow so that the energy liberated did not become available in time to be converted to kinetic energy of the piston. Thus subsequent oscillations of the piston were not bothersome.

The above observation concerning internal energies also leads to the conclusion that conditions of chemical equilibrium are not encountered. A trial calculation of compositions expected at equilibrium for one run verified this conclusion.

Errors

The values of reaction temperature, pressure, reaction time and $(\Delta E_{R} - Q)$ are subject to considerable error and must be regarded as fairly rough approximations. Not only are they affected by the assumed equation of state (see Appendix I) and all the assumptions made in the derivation of equations in Part III, but the amounts of work done on the samples were not known with any precision.

The compositions of the samples as determined by mass spectrometer are also subject to error but the errors introduced by this source and by the calculation of "adjusted" analyses are believed small in comparison with those caused by lack of knowledge of the work done on the sample and the uncertainties introduced by the assumptions.

Conclusions

This exploratory investigation of the reactions of methane under

conditions of high temperature and pressure was made essentially without instrumentation and the results cannot be considered quantitative. They were made over a range of conditions such that the reaction temperatures appeared to be between about 2500° R. and 3500° R., and maximum pressures up to 100,000 pounds per square inch were estimated. The estimated times during which the samples were subjected to the reaction temperatures ranged from 350 to 800 microseconds. In the lower range of temperatures ethylene, ethane, propylene and benzene, as well as free carbon and hydrogen, were found in significant amounts in the products of reaction, although only a small part of the methane reacted. In the range of higher temperatures, where a larger fraction of the methane reacted, free carbon and hydrogen were the major products.

The tests did demonstrate conclusively that the ballistic piston apparatus could be used to carry out chemical reactions.

TABLE IV-I. DATA FROM METHANE RUNS

Run No.	Initial Air Press. P_{Ao} (Lb./Sq.In.)	Initial Sample Conditions: Pressure P_{Bo} (Lb./Sq.In.)	Temperature (°R.)	Mole Fract Methane	Diluent	Closest Approach (In.)	V_2^* x 10^4	Leakage Fract.
23	1001.4	4.463	536.2	1.000	none	0.0731	7.616	-
24	1004.5	4.525	535.3	1.000	none	0.0692	7.224	-
25	1004.5	2.270	535.3	0.25165	He	0.0214	2.420	-
26	1004.5	2.706	533.5	0.35128	He	0.0292	3.203	0.117
29	1004.6	3.707	535.1	0.55123	He	0.0581	6.108	-
31	1006.5	2.952	533.0	0.38715	He	0.0368	3.967	0.023
33	582.0	1.694	533.6	0.35170	He	0.0163	1.906	0.556
35	1004.7	3.464	534.1	0.30199	He	0.1071	10.950	0.023
86	697.8	1.920	530.6	0.33288	N_2	0.0262	2.906	0.148
87	807.2	1.975	536.2	0.20077	(a)	0.0319	3.479	0.130

[a] 0.39934 He; 0.39989 N_2

TABLE IV-II. BOTTOM CONTACT TIMING DATA

Run No.	Heights of Contacts h_1 (In.)	h_3 (In.)	Time From h_1 θ_3 (Microsec.)	Velocity at h_2 (Ft./Sec.)	Av. Height h_2[a] (In.)
86	0.2023	0.1036	148	55.57	0.1530
87	0.1438	0.0760	113	50.00	0.1099

[a] $h_2 = \frac{1}{2}(h_1 + h_3)$

TABLE IV-III. ANALYSES OF SAMPLES[a]

Run No.	23		25		26		29	
	Control	Product	Control	Product	Control	Product	Control	Product
H_2				17.55		13.86	0.03	1.44
He			72.94	66.26	64.09	60.47	43.02	42.91
C_6H_6						0.03		
C_3H_8	0.07	0.07		0.02		0.04	0.04	
C_3H_6				0.02		0.07		0.14
C_2H_6	0.15	0.14	0.04	0.27	0.05	0.51	0.06	0.15
C_2H_4				0.24	0.02	0.35		0.27
C_2H_2				0.03		0.03		
CH_4	98.33	98.56	26.06	14.25	34.55	23.99	56.79	54.70
CO_2					0.02			
Air	0.91	0.96	0.17	1.24	0.45	0.41		0.22
H_2O	0.54	0.27	0.79	0.12	0.82	0.24	0.06	0.17

[a] Mole per cent, as reported by The Texas Company Montebello Laboratories

TABLE IV-III. ANALYSES OF SAMPLES (Cont.)

Run No.	31		33		35	
	Control	Product	Control	Product	Control	Product
H_2		9.79		3.02		11.45
He	58.17	54.87	62.90	16.20	71.24	65.64
C_6H_6		0.10		0.04		0.10
C_4H_8		0.04				
C_3H_8		0.08				
C_3H_6		0.11		0.04		0.06
C_2H_6	0.07	0.64	0.06	0.13	0.04	0.34
C_2H_4		0.46		0.14		0.44
CH_4	40.65	31.45	36.60	6.93	28.44	21.19
CO_2			0.02			
Air	0.87	1.94	0.20	73.26	0.10	0.44
H_2O	0.24	0.52	0.22	0.24	0.18	0.34

TABLE IV-III. ANALYSES OF SAMPLES (Cont.)

Run No.	86		87	
	Control	Product	Control	Product
H_2	0.06	7.85	0.05	15.66
He			39.17	36.63
N_2	65.70	63.84	40.03	36.71
C_6H_6		0.13		0.02
C_4H_8		0.02		
C_3H_6		0.10		0.02
C_2H_6	0.05	0.58	0.03	0.21
C_2H_4		0.46		0.17
CH_4	33.72	26.64	20.12	10.18
CO_2	0.05	0.04	0.03	0.02
Air	0.12	0.09	0.13	0.13
H_2O	0.30	0.25	0.44	0.25

TABLE IV-IV. ADJUSTED ANALYSES[a]

	Run No.	23	25	26	29	31
INITIAL	H_2				0.03*	
	He		74.84**	64.87**	44.88**	61.29**
	C_3H_8	0.07*			0.04*	
	C_2H_6	0.15*	0.04*	0.05*	0.06*	0.07*
	C_2H_4			0.02*		
	CH_4	99.78*	25.12**	35.06**	54.99**	38.64**
FINAL	H_2		17.80*	13.93*	1.44*	10.04*
	He		68.28***	60.55***	44.60***	58.53***
	C_6H_6			0.03*		0.10*
	C_4H_8					0.04*
	C_3H_8	0.07*	0.02*	0.04*		0.08*
	C_3H_6		0.02*	0.07*	0.14*	0.11*
	C_2H_6	0.14*	0.27*	0.51*	0.15*	0.65*
	C_2H_4		0.24*	0.35*	0.27*	0.47*
	C_2H_2		0.03*	0.03*		
	CH_4	99.79*	13.34***	24.49***	53.40***	29.98***
	Free C[b]	.00	9.26***	6.51***	0.23***	3.66***
	γ[c]	1.000	1.096***	1.071***	1.006***	1.047***

[a] Mole per cent
[b] Moles/100 moles initial
[c] Final moles gas/initial mole

* Mass spect. w/o Air, CO_2, H_2O
** By addition
*** Calculated by stoichiometry

TABLE IV-IV. ADJUSTED ANALYSES[a] (Cont.)

	Run No.	33	35	86	87
INITIAL	H_2			0.06*	0.05*
	He	64.83**	69.80**		39.93**
	N_2			66.71**	39.99**
	C_2H_6	0.06*	0.04*	0.05*	0.03*
	CH_4	35.17**	30.16**	33.18**	20.00**
FINAL	H_2	11.40*	11.51*	7.88*	15.54***
	He	61.34***	65.94***		36.88***
	N_2			64.37***	36.94***
	C_6H_6	0.15*	0.10*	0.13*	0.02*
	C_4H_8			0.02*	
	C_3H_8				
	C_3H_6	0.15*	0.06*	0.10*	0.02*
	C_2H_6	0.50*	0.34*	0.58*	0.21*
	C_2H_4	0.53*	0.44*	0.46*	0.17*
	CH_4	25.93***	21.60***	26.46***	10.22*
	Free C[b]	4.28***	4.90***	2.50***	7.98***
	γ[c]	1.057***	1.059***	1.036***	1.083***

TABLE IV-V. CONVERSION[a] OF METHANE

Run No.	25	26	29	31	33[b]	35	86	87
H_2	0.929	0.846	0.580	0.726	0.776	0.835	0.703	0.939
C_6H_6		0.022		0.087	0.122	0.087	0.140	0.014
C_4H_8				0.023			0.014	
C_3H_8	0.006	0.015		0.035				
C_3H_6	0.006	0.026	0.241	0.048	0.061	0.026	0.054	0.007
C_2H_6	0.048	0.112	0.145	0.168	0.120	0.087	0.191	0.044
C_2H_4	0.050	0.080	0.434	0.136	0.144	0.128	0.166	0.041
C_2H_2	0.006	0.007						
Free C	0.882	0.738	0.184	0.505	0.552	0.671	0.434	0.894
React[c]	0.418	0.252	0.023	0.187	0.221	0.242	0.174	0.447

[a] Fraction of reacted methane appearing as product, H_2 based on hydrogen, others based on carbon

[b] Sample for run 33 contaminated with 75 per cent air

[c] Fraction of methane reacted

TABLE IV-VI. CONDITIONS AND EFFECTIVE FRICTIONAL FORCE FOR RUNS WITHOUT REACTION

Run No.	Maximum Conditions		Effective Frictional Force (Lb.)
	Pressure (Lb./Sq.In.)	Temperature (°R.)	
23	63,419	2269	-13.45
24	75,234	2308	-42.62

TABLE IV-VII. CONDITIONS AND EFFECTIVE FRICTIONAL FORCE FOR RUNS WITH TIMING DATA

Run No.	h_2 (In.)	Conditions at h_2 (Isentropic) Temperature (°R.)	Conditions at h_2 (Isentropic) Pressure (Lb./Sq.In.)	Effective Frictional Force (Lb.)
86	0.1530	2884	7,572	9.69
87	0.1099	4707	17,360	-18.12

TABLE IV-VIII. RESULTS OF ISOTHERMAL PATH CALCULATIONS

Run No.	Effective Frictional Force (Lb.)	Assumed N_{av}/N_o	Initial Sample $N_o \times 10^4$ (Lb.Mole)	Results for Isothermal Reaction Assumption: Temp. T_1 (°R.)	Max.Press. P_2 (Lb./Sq.In.)	$(\Delta E_{o_R} - Q_o)$ (Btu/Lb.Mole)	Time At T_1 : $\Delta\Theta$ (Microsec.)	(PV/RT) At Max. Pressure
23	-13.45[a]	-	3.156	2269	63,419	0	0	2.557
24	-42.62[a]	-	3.205	2308	75,234	0	0	2.786
25	-28.03[b]	1.050	1.609	3308	102,792	27,011	818	1.618
26	-28.03[b]	1.036	1.923	2913	86,187	20,058	634	1.745
29	-28.03[b]	1.003	2.627	2497	50,069	9,877	412	1.757
31	-28.03[b]	1.025	2.100	2825	70,115	16,894	582	1.698
33	-28.03[b]	1.030	1.204	2452	81,777	23,440	1963	1.894
35	-28.03[b]	1.030	2.460	3254	22,765	10,692	731	1.115
86	9.69[c]	1.020	1.373	2695	92,710	15,917	347	2.666
87	-18.12[c]	1.040	1.397	3433	61,105	20,336	564	1.553

[a] Calculated for isentropic compression
[b] Average of values for runs 23 and 24
[c] From timing measurements

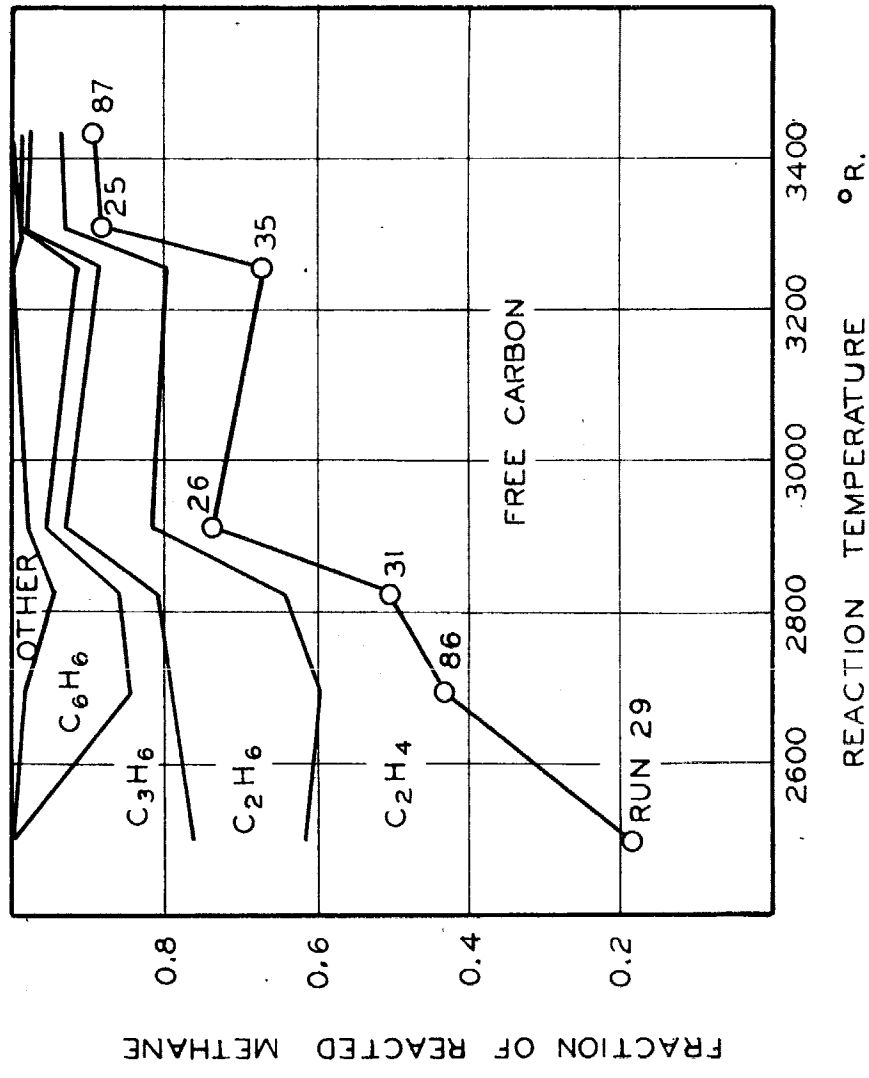

Fig. IV-1. Cumulative Product Distribution by Carbon Balance

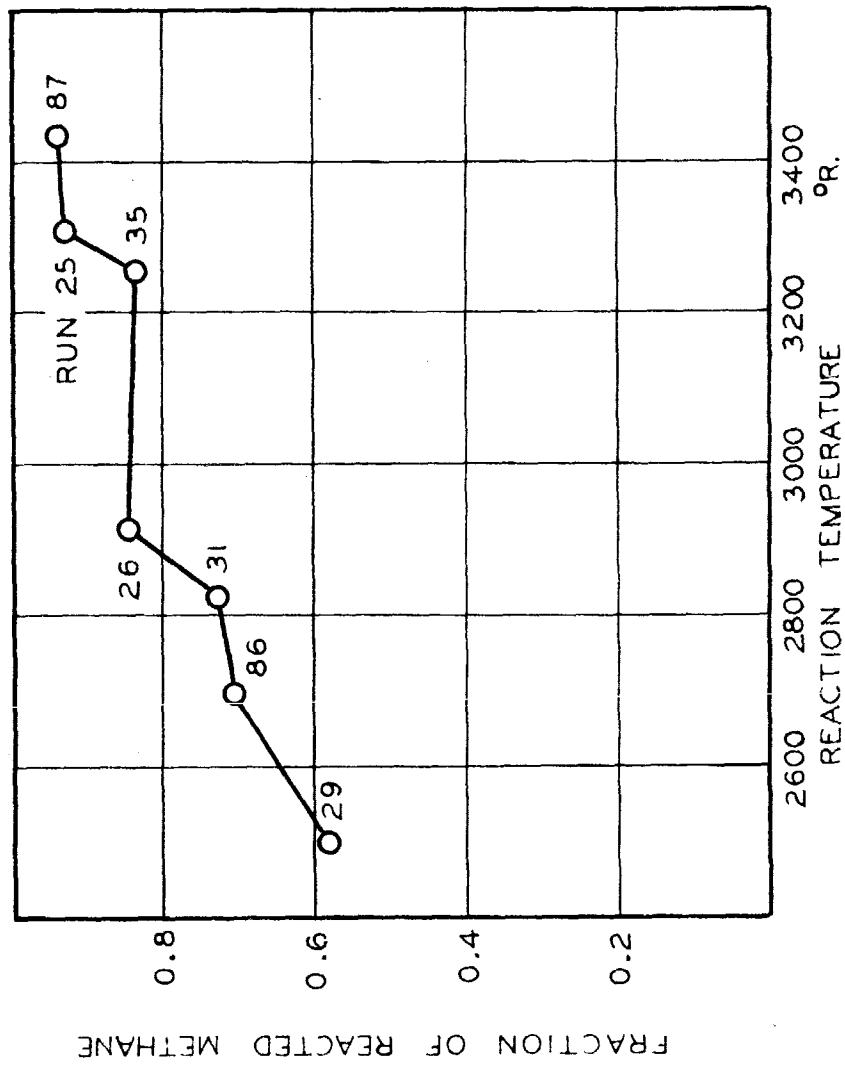

Fig. IV-2. Conversion of Methane to Hydrogen

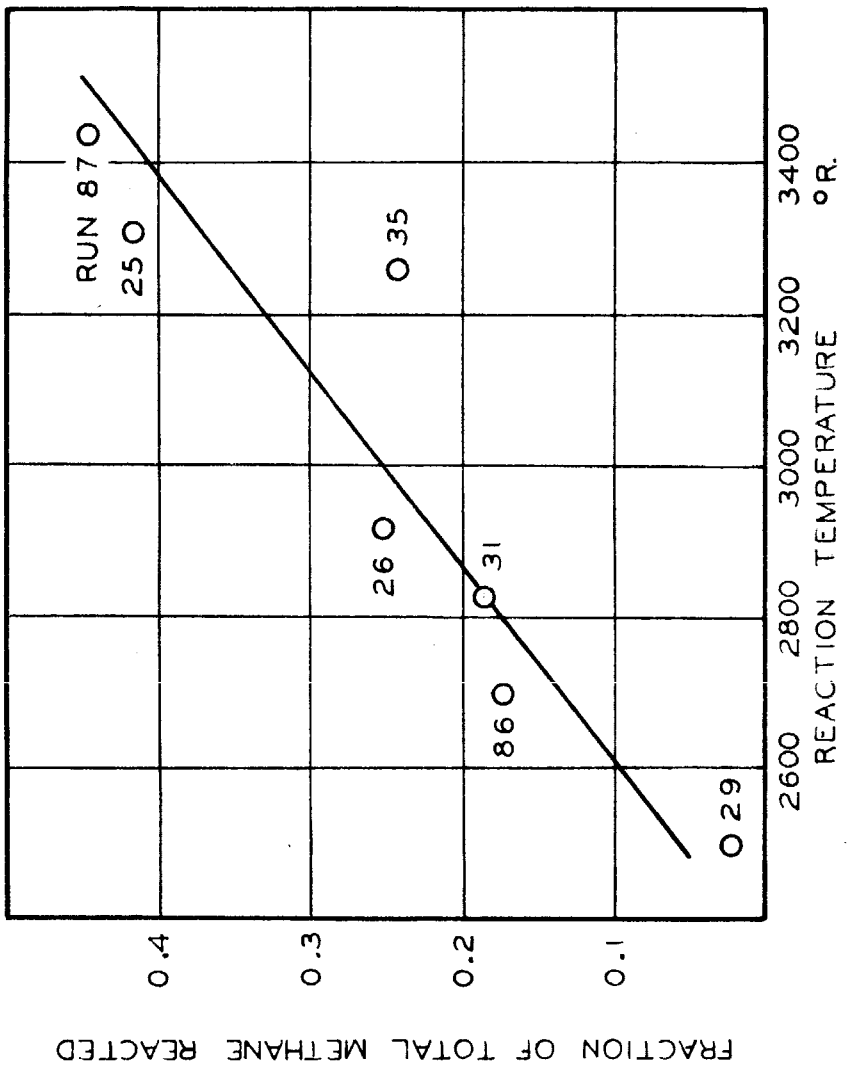

Fig. IV-3. Amount of Reaction

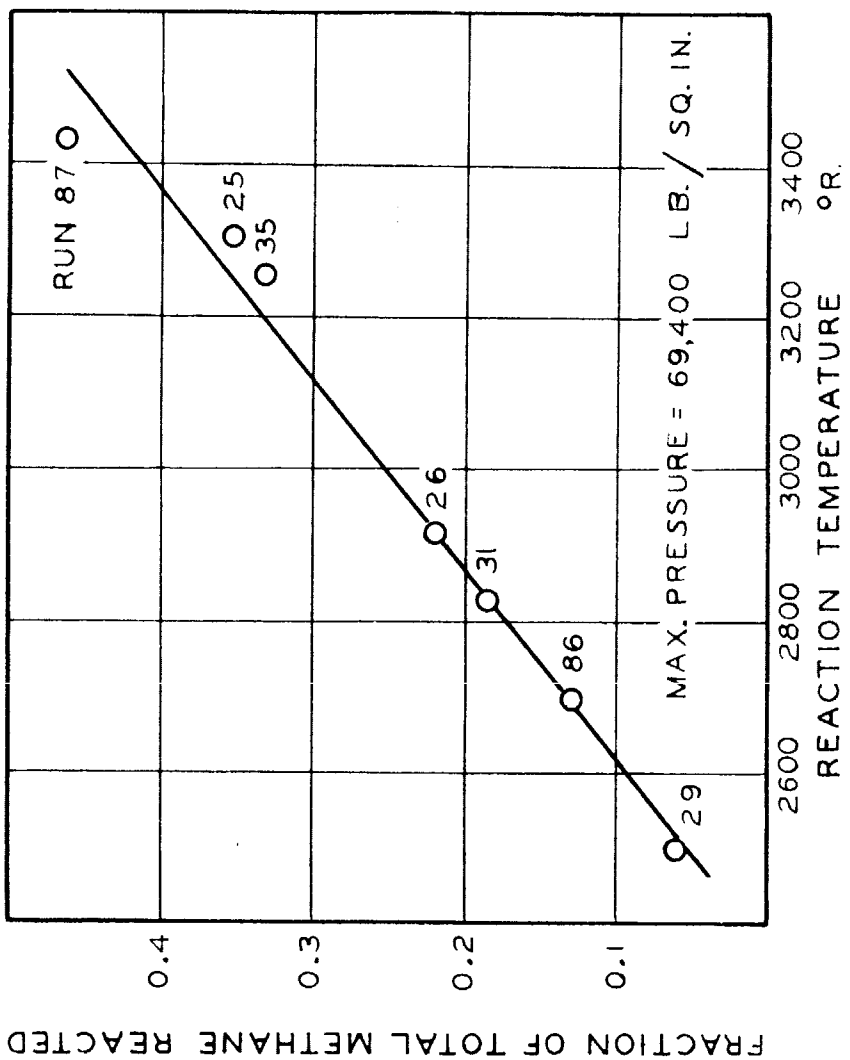

Fig. IV-4. Corrected Amount of Reaction

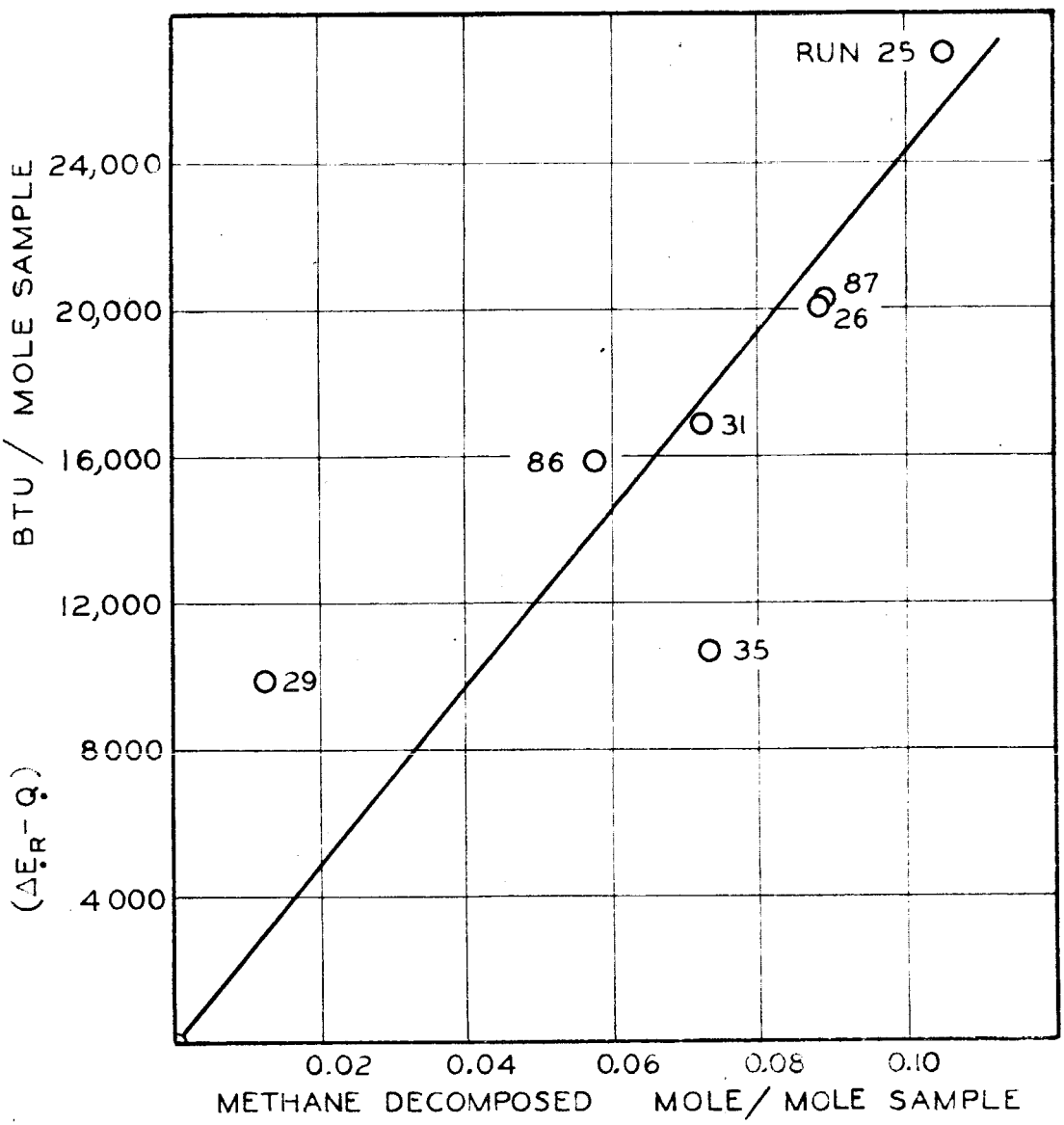

Fig. IV-5. $(\Delta E_{oR} - \frac{Q}{o})$ as Function of Methane Decomposed

V. CARBON-HYDROGEN SYSTEM: n-HEXANE

The products obtained from methane with the ballistic piston, as reported in Part IV of this thesis, were not of great interest, since when the conditions were made sufficiently severe to cause a moderate amount of methane to react, the products were mainly carbon and hydrogen. The higher hydrocarbons are less stable at these elevated temperatures than methane and so study of the reactions of a paraffin hydrocarbon of moderate molecular weight promised to be more interesting. n-Hexane was selected as having a vapor pressure sufficiently large to allow addition of the desired quantities in the vapor phase at room temperature.

It is necessary to dilute a material of high specific heat such as n-hexane with a gas of low specific heat in order that temperatures sufficiently high for reaction to take place will be attained. Hydrogen was selected as the diluent for one series of tests since it would be expected to react with unsaturated materials formed by breaking up n-hexane. Nitrogen was selected as an inert diluent for a second series of runs since its specific heat is similar to that of hydrogen.

Experimental Procedure

The ballistic piston apparatus as described in Part II was used for this investigation. A heavy piston having a stellite facing on the edge and sides of the sample end was employed for all runs. Procedure for a run was as follows:

The interior of the bottom closure was cleaned with acetone and

dried. Copper wires of appropriate height and either 0.025 inch or 0.013 inch in diameter were inserted in the contact holders, the larger diameter being used for wires extending more than 0.35 inch above the bottom. The heights of the wires were measured to 0.0002 inch with a depth micrometer registering on the top of the bottom closure, contact with the wire being determined by means of an electronic ohmmeter. A flattened lead shot was weighed, measured, and placed in the bottom of the closure to measure the closest approach of the piston.

The barrel was lubricated with graphite. The piston was assembled to the top closure with a 0.373 inch diameter brass shear pin, and a length of 0.020 inch piano wire in the form of a spiral helix was attached to the piston and to the top closure to ground the piston. The piston-top closure assembly was inserted in the barrel, the unsupported area seal tightened, and a ground wire attached to the top closure. The lower closure was next inserted in the bottom of the barrel, the unsupported area seal tightened, and vacuum line attached.

The lower chamber of the apparatus was evacuated to about 2 mm. pressure, then purged three times with one of the gases to be used in the sample, either nitrogen or hydrogen. This gas was passed through a trap immersed in a dry ice-trichlorethylene mixture to remove moisture. The apparatus was pumped down to a pressure of 10 mm. or less between purges; and to 1 to 2 mm. after the third purge when the pressure was recorded and chamber valves closed. The purging procedure was used

since the lines connecting the vacuum system to the apparatus are of small bore and obtaining a reasonable vacuum through them was wasteful of time.

The n-hexane was placed in one of the absorption bulbs in the sample addition system (Figure II-2) and the bulb pumped for 10-15 seconds to remove air. After evacuation of lines, hexane vapor was admitted to the chamber and addition continued by vaporization of hexane until the desired quantity had been added, then the chamber pressure was measured and the chamber valves closed. After evacuation of lines, sufficient of the diluent gas was added to bring the chamber pressure to about 800 mm. and the pressure measured. The diluent gas was introduced into the bottom of the chamber to aid mixing. After standing at least 30 minutes a control sample was drawn into an evacuated sample bulb, then the chamber pressure was reduced to that desired as an initial sample pressure. Meanwhile the time interval meters had been warmed up and checked out. Compressed air was admitted to the upper chamber, all valves closed, and the piston released.

After the shot, timing data were recorded, the air pressure remaining above the piston was vented, and the top closure removed. The distance to the top of the piston from the top of the apparatus was measured to 1/64 inch with a weighted steel tape, and the pressure of the sample measured by the mercury manometer. These measurements allowed estimation of final sample quantity and thus led to leakage estimates. Two product samples were taken in evacuated sample bulbs.

The piston and bottom closure were then removed and the lead gage recovered and measured.

Materials

The n-hexane used was Phillips Petroleum Company research grade n-hexane quoted as 99.85 mole per cent pure. Part of the runs were made with a sample which had been dried with sodium metal, however a new sample was used to finish the runs and drying was not considered necessary. Since the n-hexane was used as a calibration standard in the analysis of samples by mass spectrometer no independent measure of the purity is available.

The helium used (one run) was obtained from Air Reduction Company and represented as 99.97 per cent pure. A mass spectrometer analysis by The Texas Company showed 0.14 mole per cent nitrogen as an impurity.

The hydrogen was electrolytic hydrogen obtained from the Matheson Company. No analysis was obtained of the cylinder, however mass spectrometer analysis of a previous cylinder from this source showed as impurities (expressed in mole per cent) 0.04 nitrogen, 0.13 oxygen, 0.03 CO_2, and 0.02 methane. The analysis data for runs indicate about 0.11 mole per cent oxygen in the hydrogen used.

The nitrogen was obtained from Linde Air Products Company and was reported as 99.95 per cent pure. An analysis by mass spectrometer showed 0.04 mole per cent oxygen, 0.02 mole per cent argon, and 0.07 mole per cent water as impurities. The oxygen content is compatible with the analyses of control samples for runs.

All mass spectrometer analyses were performed by The Texas Company Montebello Laboratories.

Experimental Results

Sixteen runs were made, eight with hydrogen and eight with nitrogen as the diluent for the n-hexane. The conditions established for these runs are shown in Table V-I. The temperatures and pressures shown are those which would be reached by a perfect gas having the specific heat of the indicated mixture, if no chemical reaction or thermal transfer occurred and the piston reached the "predicted approach" as its minimum distance from the bottom of the chamber. Although the temperatures and pressures of Table V-I are not meaningful in an absolute sense, this set of conditions did yield a useful range of maximum temperatures and pressures. All runs used the same nominal initial sample pressure of 100 mm. and all were made at room temperature. The piston used weighed 30.98 pounds except for the last three runs numbers 140, 142 and 143 for which it weighed 32.09 pounds.

The initial conditions actually used are shown in Table V-II. The initial compositions shown were calculated from pressure measurements made during sample addition and deviations from perfect gas behavior were taken into account. The distance of closest approach of the piston to the bottom is also shown. V_2^*, the ratio of the minimum sample volume to initial sample volume, includes corrections for gage volume and the volume of timing contact holder and valve recesses. The figures for leakage are based on measurements of sample volumes,

temperatures and pressures made after the runs but before samples for analysis were taken. The leakage was very large for runs 131 and 142, and moderately large for several other of these relatively high pressure runs.

Table V-III shows the time data obtained by use of contact wires extending up from the bottom of the chamber. Berkeley Time Interval Meters were controlled by the grounding of these wires. The heights of the wires above the bottom of the chamber recorded in Table V-III were measured with a depth micrometer to 0.0002 inch and it is believed they are known to 0.001 inch at the time of piston contact in most cases. Times are accurate to $\pm$ 1 microsecond.

An attempt was made to use all four pieces of position-time data to determine the piston velocity at one of the positions by use of a four point formula derived for unequal time intervals. It was discovered however that the use of this third power polynomial gave illogical results in some cases, and that the use of three points was more reliable. Accordingly the velocities used were calculated at point h_2 by use of a three point unequal "lumping" formula

$$\left(\frac{dx}{d\theta}\right)_2 = -\frac{1}{\theta_3}\left[\frac{(\theta_3-\theta_2)}{\theta_2}(h_1-h_2) + \frac{\theta_2}{(\theta_3-\theta_2)}(h_2-h_3)\right] \qquad \text{(V-1)}$$

which is easily derived from Taylor's series. Accelerations at point h_2 were calculated from

$$\left(\frac{d^2x}{d\theta^2}\right) = \frac{2}{\theta_3}\left[\frac{(h_1-h_2)}{\theta_2} - \frac{(h_2-h_3)}{(\theta_3-\theta_2)}\right] \qquad (V\text{-}2)$$

which is similarly derived from Taylor's series. Velocities and accelerations are shown in Table V-III.

Side contacts were installed near the end of this program. Partial data on three runs were obtained and are shown in Table V-IV. The velocities shown are the average velocities between points 3 and 4. Timing data from both side and bottom contacts are shown for run 143 in Figure V-1. The flagged point is common to the two curves shown; the curve on the right is a magnification by a factor of 100 of the lower end of the curve on the left.

Representative samples of the gas mixture being investigated were taken for each run before and after the firing of the ballistic piston apparatus. These samples were analyzed by means of a mass spectrometer at the Montebello laboratories of The Texas Company. Analyses as reported by The Texas Company are shown in Table V-V. Analysis of complex mixtures of hydrocarbons such as occur in most of the product samples is difficult even with this instrument and the presence of some of the materials shown as traces is not certain. Also, the accuracy on the materials shown as present in large amounts is probably not better than 1.5 to 2 per cent of the amount present. However, despite these limitations, those analyses were very useful and

the assistance of The Texas Company in furnishing them is appreciated.

Qualitative observations of the movement of the apparatus during these firings led to the conclusion that the first stroke of the piston was the only one of consequence. The "feel" of the apparatus when fired was as though it had been hit with a sledge hammer, and it did not seem to oscillate up and down. This is in contradistinction to the behavior when fired on nitrogen-oxygen-helium mixtures for example, when the apparatus would oscillate perhaps 5 times.

The odor of the products was always observed when the piston was removed and was in qualitative agreement with the analyses shown in Table V-V. However in the case of run 128 the odor of napthalene was detected in the bottom closure when it was removed. There was a considerable amount of free carbon in this run and the odor was associated with the carbon. The odor disappeared in a few minutes. It is possible that other products were adsorbed on the carbon produced in other runs as well; this was not investigated.

Analysis of Composition Data

The analysis data of Table V-V do not balance stoichiometrically, for instance run 125 is out of balance on hydrogen by almost 8 per cent, nor do the control analyses agree precisely with the compositions computed from measurements made during addition of the sample. The latter disagreements are generally within the error to be expected with the mass spectrometer. Since a set of compositions which did balance stoichiometrically was required, such adjusted analyses were computed

and are shown in Table V-VI for the nitrogen-n-hexane runs and in Table V-VII for the hydrogen-n-hexane runs.

These adjusted analyses were computed by first eliminating the air, water, carbon dioxide and oxygen reported. It is not believed that the water and carbon dioxide figures are quantitatively significant since these materials appear as background in mass spectrometers, while the figures for oxygen and air are probably real. The initial composition was taken to be that determined by sample addition (except runs 128 and 129, see below). Material balances could be written for each atomic species present: carbon, hydrogen, nitrogen (when present) and helium (one run). One additional equation, the sum of mole per cent equals 100, was available. Unknowns equal in number to the equations available could of course be determined. In the case of the runs with nitrogen the unknowns included the ratio of final moles of gas to initial moles of gas, moles of free carbon per 100 initial moles of gas, the mole per cent nitrogen and the mole per cent for one other constituent. For the hydrogen runs the unknowns were the ratio of final moles of gas to initial moles of gas, the mole per cent hydrogen, and the mole per cent for one other constituent. The amounts of all other constituents in the final composition were set at the amount determined by mass spectrometer as corrected for air, water, carbon dioxide and oxygen and the equations solved for the unknowns. In general the component selected to be the unknown as described above was the one present in largest amount, however in a few cases an

adjusted analysis which was in better agreement with the mass spectrometer data was obtained by a different selection. In the case of runs 128 and 129 satisfactory agreement could not be obtained using the addition composition for initial composition, and the mass spectrometer control analyses, corrected for air, water etc., were used. The origin of each figure in Tables V-VI and V-VII is evident by footnotes to the tables.

The free carbon shown for the nitrogen runs in Table V-VI is in qualitative agreement with observation, with the exception of run 131, where no carbon was observed. Since there was graphite present as a lubricant, a small amount of carbon may have been undetected.

The distributions of the products of decomposition of the n-hexane were computed, using the adjusted analyses of Tables V-VI and V-VII. These product distributions were computed on the basis of the fraction of the carbon from the decomposed n-hexane appearing in each product (except that hydrogen was based on hydrogen), and are shown in Table V-VIII for nitrogen runs and in Table V-IX for hydrogen runs. Methane is a substantial portion of the product in most cases, otherwise unsaturates and aromatics predominate in the case of the nitrogen runs, while, as would be expected, saturates predominate for the hydrogen runs.

Analysis of Run Data

The run data were first subjected to an analysis to determine effective values of friction which could be used in conjunction with

the assumed behavior of the driving gas to determine the energy transferred to the sample gas. Piston velocities at the point h_2, the height of the second contact wire, are found in Table V-III. The pressure and temperature of the sample gas at this point were calculated on the assumption of an isentropic path using equations (III-31) and (III-32) which are

$$T^* = (v^* - \alpha)^{-R/\phi} \tag{V-3}$$

and

$$P^*(v^* - \alpha) = T^* \tag{V-4}$$

in combination with equations (III-49) and (AI-10);

$$\phi = \sum_{k=1}^{n} \eta_k \phi_k \tag{V-5}$$

and

$$b = \sum_{k=1}^{n} \eta_k b_k \tag{V-6}$$

and the values of ϕ_k and b_k tabulated in Appendix I. Compositions from Table V-II were used to make these calculations which are iterative in nature since ϕ is a function of temperature and b is a

function of temperature and pressure. The temperatures and pressures at h_2 are recorded in Table V-X. No corrections to the specific heat functions of the type described in Appendix I equations (AI-42) and (AI-48) were used in the calculations reported in this thesis since they are minor in nature and unwarranted by the real accuracy of the results.

The effective frictional force was calculated using equation (III-59)

$$F = m_p + \frac{A}{(1-V^*)}\left[\frac{P_{A0}}{K-1}\left[\beta-\beta^K(1+\beta-V^*)^{1-K}\right] - \frac{P_{B0}\Psi}{R} - \frac{m_p u^2}{2g\,V_{B0}}\right] \qquad (V\text{-}7)$$

with V^*, Ψ and u all for the point h_2. Since the temperatures were already calculated, the values of Ψ were easily obtained from those tabulated in Appendix I and equation (III-50)

$$\Psi = \sum_{K=1}^{n} n_{oK}\,\Psi_K \qquad (V\text{-}8)$$

A value of 1.424 as discussed in Appendix I was used for k for all the calculations on the n-hexane runs.

The calculated values of effective frictional force are shown in Table V-X. Those from the side contact velocity data were calculated as described above except that the point corresponding to the velocity was used.

The values of the effective frictional force are erratic. Part of the variation can be ascribed to the fact that numerically small differences of large numbers are involved for the runs considered, and the large numbers are subject to error. At most $|F - mp|$ amounts to 10 per cent of the largest number, corresponding to the energy from the driving air. However use of the calculated values of the effective frictional force will tend to correct for any errors, either systematic or random, in the assumed behavior of the driving gas and the calculated values were used in all subsequent calculations.

No correlations of the effective frictional forces of Table V-X with other variables were found, except for the last three runs. These were made after the ballistic piston apparatus was reassembled after the boring of the holes for the side contacts. Although the bore was thoroughly cleaned of oil and regraphited after reassembly, it was evident that the static friction of the piston in the bore was less than it had been previously. This does correlate with the calculated values.

The accelerations from Table V-III were used to calculate pressure using

$$P = \frac{m_p a}{g A} \qquad \text{(V-9)}$$

which neglects the small effects of the pressure of the driving gas and of frictional force at point h_2. These pressures are tabulated in

Table V-X and can be compared with the pressures calculated for the isentropic path. They demonstrate that the timing measurements are not sufficiently accurate to give good second derivatives, which fact was not unexpected.

The temperatures and pressures to which the samples were subjected were next estimated. It was assumed that the sample was compressed isentropically until it reached a certain temperature, and that endothermic reaction then took place at constant temperature until the minimum volume was reached. This path is discussed in detail in Part III and is shown diagramatically in Figure III-5.

The work done on the sample gas was calculated by use of equation (III-77)

$$\frac{W_B}{RT_{Bo}} = \frac{1}{P_{Bo}}\left\{\frac{F-m_p}{A}(1-V_2^*) - \frac{P_{Ao}}{K-1}\left[\beta - \beta^K(1+\beta-V_2^*)^{1-K}\right]\right\} \qquad (V\text{-}10)$$

and using values of the effective frictional force as determined from the velocity at h_2 as shown in Table V-X. For run 140 a value of -8.0 pounds was assumed. The calculated values for the dimensionless work $(W_B)/(RT_{Bo})$ are shown in Table V-XI. Equation (III-74) is a second relationship involving the temperature of the isothermal portion of the path:

$$\frac{W_B}{RT_{Bo}} = \left[\frac{N_{av}}{N_o}\ln(V_2^* - \alpha)\right]T_1^* + \left[\frac{N_{av}}{N_o}\frac{\phi_1}{R}T_1^*\right]\ln T_1^* - \frac{\psi_1}{R} \qquad (V\text{-}11)$$

It is necessary to assume values for the ratios $(N_{av})/(N_o)$ in order to use equation (V-11). Those assumed, which are approximately one half of the values of the figures for (moles/mole initial) in Tables V-VI and V-VII, are shown in Table V-XI.

Substitution of the numerical values of work from equations (V-10) and of (N_{av}/N_o) into equation (V-11) gives a transcendental equation which can be solved for T_1^*. If a value of T_1^* is assumed, α can be determined by use of the tables of the covolume b in Appendix I and equations (V-6) and (V-12)

$$P_2^* (V_2^* - \alpha) = \frac{N_2}{N_o} T_1^* \qquad \text{(V-12)}$$

by an iterative process. Values for ϕ_1/R and Ψ_1/R are obtained from Appendix I and by use of equations (V-5) and (V-8). Substitution of these in equation (V-11) gives a number to be compared to the work term, and the iteration is continued until a solution for T_1^* is obtained. The maximum pressure may then be obtained by use of equation (V-12). The temperatures and pressures so calculated are shown in Table V-XI.

By use of equation (III-78)

$$\frac{\Delta E_R - Q_o}{RT_{Bo}} = -\frac{W_B}{RT_{Bo}} - \frac{\Psi_1}{R} \qquad \text{(V-13)}$$

the term involving the change in internal energy due to reaction may be calculated. $(\Delta E_R - \frac{Q}{\sigma})$ was calculated in this manner and values are tabulated in Table V-XI. They indicate a rather sizable absorption of energy in reaction, or heat transfer, with the former much more probable.

The time interval during which this assumed isothermal compression occurs is given by equation (III-90)

$$\Delta\theta = 2C_3(V_2^* - \alpha)\int_0^{y_1} e^{y^2}\,dy \qquad (V\text{-}14)$$

where C_3, by equation (III-82) is

$$C_3 = \frac{1}{A}\left[\frac{m_p V_{Bo} N_o}{2g P_{Bo} T_1^* N_{av}}\right]^{\frac{1}{2}} \qquad (V\text{-}15)$$

and y is a variable defined by equation (III-85)

$$y = \left[\ln \frac{V^* - \alpha}{V_2^* - \alpha}\right]^{\frac{1}{2}} \qquad (V\text{-}16)$$

Time intervals calculated for the runs are shown in Table V-XI. Two other quantities are shown in this table, since they may be of interest. The total work done on the sample, given by

$$-W_B = -N_o R T_{Bo} \left[\frac{W_B}{R T_{Bo}} \right] \qquad \text{(V-17)}$$

indicates the rather small amounts of energy being used in the ballistic piston apparatus. The second is the compressibility factor at maximum compression

$$\frac{PV_o}{RT} = \frac{P_2^* V_2^* N_o}{T_1^* N_2} \qquad \text{(V-18)}$$

The values for the compressibility factor in Table V-XI show that the covolume equation of state employed predicts significant departure from perfect gas behavior under the conditions of these tests.

One can compare the values of the temperature T_1 for the isothermal portion of the assumed path with those shown in Table V-X as conditions at h_2. The latter should be the smaller in order that the assumption of isentropic compression to the point h_2 be consistent. This criterion is not satisfied for the first four runs where the height of bottom contact number 2 was less than for the rest of the runs, nor is it satisfied for run 127. However these deviations do not appear significant; at least the values of effective frictional force are not correlated with them.

The entries in Table V-XII show the effect of changing the numerical value of the effective frictional force on the calculated temperature

T_1 and on $(\Delta E_{oR} - \frac{Q}{o})$. Unfortunately the rate of change of calculated temperature with effective frictional force is large, of the order of 15° R. per pound, so that uncertainty in the value of effective frictional force to be employed causes relatively large uncertainty in the calculated temperature. The change in $(\Delta E_{oR} - \frac{Q}{o})$ is also sizable.

The data of Table V-VIII for conversion of n-hexane in the runs with nitrogen as a diluent are plotted as functions of the calculated reaction temperature in Figure V-2. There are marked shifts in the product distribution with temperature. At the lowest temperatures unsaturates predominate. In the middle range methane and free carbon predominate, but 0.15 of the hexane is converted to aromatics and 0.2 to C_2, C_3 and C_4 compounds. At the upper temperature range free carbon and methane are the major products. Hydrogen, which is also produced, is not shown in Figure V-2 but is included in Table V-VIII.

Similarly the conversion data of Table V-IX for the runs with hydrogen as a diluent are plotted in Figure V-3. The trends in this case are very definite. At the lowest temperature there is a somewhat uniform distribution of saturated hydrocarbons through propane with some high hydrocarbons. The amounts of unsaturates are small. In the middle and upper temperature ranges 0.85 to 0.9 of the n-hexane is converted to methane, with ethane accounting for most of the remainder.

It would appear that some of the runs, of which run 124 is the most evident, would fit the trends of Figures V-2 and V-3 better if they were plotted at different temperatures. However no account of

the possible effects of pressure or duration on the distribution of reaction products was taken in plotting these data and these factors, as well as inaccuracies in temperatures, may well account for some of the irregularities.

First Order Reaction Rate Coefficients

It was found possible to obtain some reaction rate coefficients for the decomposition of n-hexane from the results of these tests. It was assumed that the decomposition was irreversible and occurred only during the time represented by the isothermal path assumed for the calculations above. The mole fraction of n-hexane was then known at the beginning and at the end of this time since it was assumed to be equal to the initial and to the final mole fraction respectively.

Calculations were first made on the basis of a first order reaction, for which the equations are derived in Part III of this thesis. The reaction rate was taken as represented by equation (III-91)

$$-\frac{dN_R}{d\theta} = k_R \underline{V}_B (f_R) = k_R \underline{V}_B \eta_o f_R^\circ \qquad (V\text{-}19)$$

This is essentially a defining relationship for the reaction rate coefficient k_R. The reaction rate coefficient is obtained from equation (III-104)

$$\ln \frac{\eta_{o1}}{\eta_{o2}} = 2 k_R B_1 \int_0^{y_1} \left[\frac{\alpha}{V_2^* - \alpha} + \frac{P_2}{P} \right] \frac{f_R^\circ}{P} \, dy \qquad (V\text{-}20)$$

where, by equation (III-101)

$$B_1 = RT_1 (V_2^* - \alpha) C_3 \qquad (V\text{-}21)$$

by equation (III-103)

$$\frac{P_2}{P} = \frac{1.12838}{\Phi_1(y)} \qquad (V\text{-}22)$$

and, by equation (III-92)

$$\frac{f_R^\circ}{P} = \exp\left[\frac{P\bar{b}_R}{RT_1}\right] \qquad (V\text{-}23)$$

Values of $\bar{b}$ for n-hexane are tabulated in Appendix I.

Equation (V-20) was solved by numerical integration for all runs and the calculated values of the reaction rate coefficient k_R for first order reaction are shown in Table V-XIII. As a matter of interest, the maximum values of the ratio of fugacity to pressure for pure n-hexane (f_R°/P) which were obtained for each run by use of the equation of state in Appendix I are shown in Table V-XIII. It will be observed that these ratios, which are of course unity for ideal gases, become very large under these rather extreme conditions.

The calculated first order reaction rate coefficients are shown

in Figure V-4. Since reaction rate coefficients are often represented by the conventional Arrhenius equation (23)

$$\frac{d(\ln k_R)}{dT} = \frac{E'}{RT^2} \qquad \text{(V-24)}$$

in which $\ln k_R$ is a linear function of (1/T) if the activation energy E' is constant, a semilogarithmic plot if k_R against reciprocal temperature was used in Figure V-4. While there is perhaps a vague trend, the points do not make a good line even though data for two runs, numbers 131 and 143 were omitted on the basis of large (or suspected large) leakage. Inspection of the deviations of the points from a least squares line indicated considerable correlation with the value of maximum pressure. Accordingly a regression analysis of k_R as a linear function of P_2 and (1/T) was made (including all runs) giving as the result the equation

$$\ln k_R = 4.6665 - \frac{7639.4}{T_1} - 4.7801 \times 10^{-5} P_2 \qquad \text{(V-25)}$$

with temperature in degrees Rankine and pressure in pounds per square inch. The coefficient of the reciprocal temperature corresponds to an activation energy of 15,179 Btu/lb mole (8.43 Kcal/gm mole).

Variances were not calculated, but rather the calculated values of reaction rate coefficients were corrected to those which would presumably have been found if the maximum pressure had been equal to

the mean for the runs, 54,000 pounds per square inch. This correction was made by use of the coefficient of the pressure found in equation (V-25) in the form

$$(\ln k_R)_{corr.} = \ln k_R + 4.7801 \times 10^{-5}(P_2 - 54{,}000) \qquad (V\text{-}26)$$

The coefficients obtained in this manner are tabulated in Table V-XIII and are plotted in Figure V-5. The nature of this correction is such that all the variations of the actual calculated reaction rate coefficients from the relationship of equation (V-25) are shown as variations of the corrected coefficient from the line in Figure V-5. These variations are reasonably small, the maximum being a logarithm with absolute value corresponding to a ratio of 1.57.

In Figures V-4 and V-5 the points for the hydrogen and for the nitrogen runs have been distinguished, but no influence of the diluent on the reaction rate coefficient is detectable. This is in agreement with the assumption of a decomposition reaction with the reaction rate not being a function of the fugacity of components other than the n-hexane.

However, although the regression equation (V-25) gives a good fit of the data, it is incompatible with the basic premise that the reaction rate coefficient be a function only of the temperature. It must be concluded then that equation (V-19) does not describe the actual reaction rate, and the reaction is not first order.

One-Half Order Reaction Rate Coefficients

Calculations were next made for a one-half order reaction. The equations for the calculation are derived in Part III of this thesis. The defining equation for the case is that of equation (III-107):

$$-\frac{dN_R}{d\theta} = k_R \underline{V}_B (f_R)^{\frac{1}{2}} = k_R \underline{V}_B (\eta_o f_R^o)^{\frac{1}{2}} \qquad \text{(V-27)}$$

and the solution is equation (III-109)

$$(\eta_{o1})^{\frac{1}{2}} - (\eta_{o2})^{\frac{1}{2}} = k_R B_4 \int_0^{y_1} \left[\frac{\alpha}{V_2^* - \alpha} + \frac{P_2}{P}\right]\left[\frac{P_2}{P} + \frac{f_R^o}{P}\right]^{\frac{1}{2}} dy \qquad \text{(V-28)}$$

with

$$B_4 = \frac{\left[\underline{V}_{Bo}(V_2^* - \alpha)\right]^{\frac{3}{2}}}{A N_{av}} \left[\frac{m_p}{2g}\right]^{\frac{1}{2}} \qquad \text{(V-29)}$$

as given by equation (III-110). Numerical integrations of equation (V-28) were performed for all runs and the reaction rate coefficients calculated on the basis of this one-half order reaction are shown in Table V-XIV as "calculated" and are plotted in Figure V-6. A least squares line is shown on Figure V-6, corresponding to the equation.

$$\ln k_R = 2.6657 - \frac{2607.8}{T_1} \qquad \text{(V-30)}$$

The reciprocal temperature was taken as the independent variable for this regression.

The variations of the reaction rate coefficients from the regression line of equation (V-30) were carefully compared with run data in a search for further correlation. The variables examined included effective frictional force, maximum pressure, maximum ratio (f_R^o/P), time interval at reaction temperature, ($\Delta E_{oR} - Q_o^o$), the amount of n-hexane decomposed, the initial mole fraction n-hexane, the fraction of the n-hexane decomposed, the magnitude of y_1, the quantity $\left[(n_{o1})^{\frac{1}{2}} - (n_{o2})^{\frac{1}{2}} \right]$ used in equation (V-28) and the amount of leakage. No evidence of even weak correlation was found except with two variables, the time interval and the amount of n-hexane decomposed. The two runs showing the largest deviations from the line, numbers 127 and 142, had also the extremes in time interval $\Delta\theta$; however the other runs showed no trend and it appeared that regression with $\Delta\theta$ would not be profitable. The deviations of the reaction rate coefficients from the least squares line did show a somewhat weak correlation with the amount of n-hexane decomposed. A regression was therefore made with reciprocal temperature and amount of n-hexane decomposed as independent variables which yielded the equation

$$\ln k_R = 2.3227 - \frac{4648.4}{T_1} + 27.207 s \qquad \text{(V-31)}$$

The amount of n-hexane decomposed was determined by use of the equation

$$s = \eta_{o1} - \gamma \eta_{o2} \qquad \text{(V-32)}$$

and is shown in Table V-XIV.

Values of the reaction rate coefficients corrected to those which would presumably have been found if the amount of n-hexane decomposed has been constant at the mean of 0.04744 (moles)/(mole initial sample) were calculated by use of

$$(\ln K_R)_{corr.} = \ln K_R + 27.207(0.04744 - s) \qquad \text{(V-33)}$$

which uses the coefficient of s from equation (V-32). These corrected values are shown in Table V-XIV and are plotted in Figure V-7. Since all the variation of the data from the regression equation (V-31) is retained in Figure V-7, it can be seen by comparison with Figure V-6 that the fit has been improved. Two runs, numbers 142 and 143 show noticeably large deviations, while the rest of the data are much closer to the regression line.

Another significant fact is that the slopes of the regression lines in the two figures are quite different. Activation energies E' as defined in equation (V-24) were calculated for the data of Figures V-6 and V-7. The slope of Figure V-6 yields an activation energy of 5,180 Btu/lb mole (2.88 Kcal/gm mole) for the half order reaction (uncorrected) while from Figure V-7 an activation energy of 9,240 Btu/lb mole (5.13

Kcal/gm mole) is obtained for the one-half order reaction corrected for regression with s.

The mole fraction n-hexane and the quantity $(\Delta E_{oR} - Q_o)$ were calculated as functions of time for one run, number 128, which was selected as being representative. These were calculated by means of equations (III-106) and (III-111), which are respectively

$$(\Delta E_{oR} - Q_o)_{y-z} = \frac{N_{av}}{N_o} RT_1 y^2 \qquad (V-34)$$

and

$$(\eta_o)^{\frac{1}{2}} = (\eta_{o2})^{\frac{1}{2}} + k_R B_4 \int_o^y \left[\frac{\alpha}{V_2^* - \alpha} + \frac{P_2}{P}\right] \left[\frac{P_2}{P} \times \frac{f_R^o}{P}\right]^{\frac{1}{2}} dy \qquad (V-35)$$

and by use of equation (V-14). The mole fraction n-hexane and the quantity $(\Delta E_{oR} - Q_o)$ are shown as functions of time in Figure V-8 and $(\Delta E_{oR} - Q_o)$ is plotted against composition in Figure V-9. Interpretation of Figure V-9 is not straightforward. If it were assumed that $(\Delta E_{oR} - Q_o)$ should be linear with the mole fraction n-hexane; one could calculate the deviation of the temperature from the assumed isothermal state which would be necessary to account for the deviation of the calculated $(\Delta E_{oR} - Q_o)$ from the line. A straight line can be drawn through the curve of Figure V-9 so that the maximum deviations of the curve from the line are limited to about 1500 Btu/lb mole, corresponding

to 140° R. However, as will be discussed later, there is probably little justification for believing that the quantity $(\Delta E_{R} - Q)$ should be exactly linear with the mole fraction n-hexane. In any event it appears that the isothermal path assumption is a reasonable one.

Sources of Error

The calculated temperatures, pressures, times, reaction rates and other such quantities are subject to errors as the result of the assumptions necessarily made in deriving the relationships and in calculation. The sources of these errors will be considered in some detail.

Perhaps the most significant factor is the equation of state of the sample gases. The equation of state used is derived from data presented by Hirschfelder et al. (17) as discussed in Appendix I. Hirschfelder's equations of state which were used are based on theoretical considerations and have not been experimentally verified in the range of temperatures and pressures encountered in the ballistic piston. Furthermore, as discussed in Appendix I; it was necessary to bridge the gap between Hirshfelder's equations of state. The basic assumptions for the statistical mechanical model include that of spherically symmetric potentials and this assumption is probably poor in the case of n-hexane at least, since the n-hexane molecule is far from being spherical. For these reasons, while the use of the equation of state from Appendix I is considered to be considerably better than assumption of perfect gases, calculations must be considered as approximate only. Since the fugacity is very sensitive to the equation of

state, the reaction rate coefficients are probably less dependable than the pressures and temperatures.

While some estimated leakages are shown in Table V-II, all calculations were made assuming no leakage. No correlations of the observed over-all leakages with calculated conditions, reaction rates, etc. were found, which might be taken to mean that the leakages did not occur during the portion of the stroke of interest, but there is no real basis for concluding this. It is also possible that there is leakage past the piston head back into the groove for the O-ring seal during the high pressure part of the stroke, and that in most cases this gas returns to the sample side of the piston after the pressure there is reduced. This would not give over-all leakage as measured by the means described earlier, but would reduce the sample pressure markedly in cases where the piston approaches quite close to the bottom of the chamber. When pressure measurements become possible they may serve to resolve this leakage question.

The velocity of the piston at the point of measurement was known to within about 1 per cent for these runs in most cases, based on 1 microsecond maximum timing error and on positions being known to within 0.001 inch. This means that the energy transferred to the sample gas was probably known to within 2 per cent. This corresponds to about 6 pounds effective frictional force or, using the $(\Delta T_1/\Delta F)$ from Table VXII, about 90° R. on the calculated reaction temperature. The velocity may be subject to more error than indicated above in the case of runs 127 and 142 which showed absurd accelerations in Table V-III.

There is the possibility that hexane and other high molecular weight materials were adsorbed on the walls of the apparatus or on the free carbon produced in some runs. There is also the possibility of absorption of these materials in the hydrocarbon stopcock grease used in the glassware. No evidence to indicate that appreciable error was caused by these sources was found, but this possibility cannot be ignored.

The analyses of the sample gas, both before and after firing, are also subject to errors inherent in the mass spectrometer method, as was mentioned earlier when the analysis data were presented. While the adjusted analyses of Tables V-VI and V-VII are believed to be as good a representation of compositions as could be obtained from the data they certainly are not exact.

Inherent in all these calculations is the assumption that local equilibrium (18) exists. Since local equilibrium requires that the internal energy be distributed among the various degrees of freedom of the molecules in the equilibrium manner, local equilibrium is necessary in order that temperature be a meaningful concept. The rates of change of the internal energy of the sample gas are very high in these high pressure ballistic piston experiments and it becomes necessary to consider the "relaxation times" (24,25,26,27) of the molecular species present. Landau and Teller (24) considered theoretical aspects of the rate of transfer of energy between translational and vibrational degrees of freedom. Kantrowitz (25) and Huber (26) report relaxation

times for carbon dioxide, water, hydrogen and nitrogen while Lambert and Rowlinson (27) give data for hydrocarbons. Of the compounds encountered in these ballistic piston runs nitrogen has, by a factor of 10^4, the longest relaxation time, which is reported (26) as about 3×10^{-3} seconds at 700° K. and one atmosphere. It was found (26) that certain impurities serve to reduce this relaxation time markedly, for instance 2 per cent water reduces it by a factor of 10.

The number of collisions necessary to assure the "relaxation" between vibrational and translational degrees of freedom is considered (24) to be proportional to $\exp \left[T^{-\frac{1}{3}} \right]$ and the number of collisions per second is proportional (25) to the pressure and to the inverse of the square root of the temperature. Using these proportionalities a relaxation time of 3 microseconds is computed for nitrogen at 2000° R. and 20,000 pounds per square inch, and 0.6 microseconds at 2000° R. and 100,000 pounds per square inch. Those for other constituents will be less than 10^{-4} of these times. It can be concluded that nitrogen may possibly exhibit a small departure from local equilibrium under extreme ballistic piston conditions, although it is suspected that the presence of foreign molecules may serve to make this departure negligible. In any event the assumption of local equilibrium should be very good for the tests considered here.

It has been inherently assumed that the properties of the gas are uniform throughout the volume occupied. While the pressure can probably be assumed constant throughout the sample volume with small uncertainty,

the assumption of constant temperature is less valid. Since the walls are cold, there must be gas at temperatures ranging all the way from the temperature of the wall to that of the bulk of the gas. It is believed that heat transfer is quite small for the runs considered since the temperatures are moderate (as compared to those attainable with the ballistic piston apparatus) and the times during which the temperatures are in the upper range are very short. This belief is consistent with experimental observations but cannot be verified until measurements of thermal flux are made.*

The extent of heat transfer likewise directly affects the error introduced by the assumption of an isentropic path for the major portion of the compression. Shock waves, if existent, would also introduce error. It is believed that the latter are not likely with the relatively low piston velocities used, but verification was not obtained.

It has been assumed that the gases used form ideal solutions (20). They are well removed from the critical region, and thus could be expected (28) to approach ideal solutions; however the high pressures encountered may well negate the assumption. From the practical

---

* Subsequent to the preparation of this thesis, measurement of thermal transport was made on a run having a mixture of nitrogen, oxygen and helium as the sample gas. About 0.5 B.t.u. was transferred during the first stroke of this run, for which the maximum temperature was about 4500° R. and the maximum pressure about 6500 pounds per square inch. On this basis it is estimated that 0.01 to 0.05 B.t.u. was transferred in the runs made with n-hexane, since the temperatures in the latter were lower and the pressures much larger than in the run for which thermal transport was measured.

standpoint, since data were not available it was necessary to assume that ideal solutions were formed. The magnitude of error so introduced is not known.

The covolume is assumed constant in the derivations of most of the equations used (that for fugacity being the exception). This assumption has great practical merit in that it allows solutions to be in closed form in many cases, and when the uncertainties inherent in the equation of state used are considered it seems logical to accept the assumption. Actually, inspection of the covolumes in Appendix I reveals that they are surprisingly constant for hydrogen, helium, nitrogen and methane. The covolume of n-hexane does vary markedly for pressures less than 10,000 pounds per square inch, however. The assumption that the total covolume of the gas remains constant during chemical reaction, as is involved in the derivation of equation (V-11), is justified by the simplification involved in this case.

The derivation of equation (V-11) also involves the use of an average figure for the number of moles and use of this equation requires assumption of a numerical value for the ratio (N_{av}/N_o). Unfortunately this ratio has appreciable effect on the calculated temperature*, and there is not a firm basis for its selection. It is likely therefore that this is an appreciable source of error.

---

* For instance, in run 128 use of (N_{av}/N_o) equal to 1.12 instead of 1.06 gives a reaction temperature of 2011° R. instead of 2147° R.

The isothermal path for the reaction is discussed somewhat in Part III where the equations based on this assumption are derived. In the derivation of the relationships involving reaction rate coefficients it is assumed that the decomposition of the reactant (n-hexane in this case) is irreversible and occurs entirely during the isothermal portion of the compression. It is unlikely that all these assumptions are correct in detail. However the irreversibility of the decomposition reaction should be valid in the case of n-hexane as judged by free energies of formation (22). In some of the systems investigated in the ballistic piston the second bounce of the piston causes concern, however observation of the apparatus during these tests led to the conclusion that there was no second bounce of consequence, and that all decomposition occurred during the first stroke. Unfortunately there is no such evidence to show that decomposition of the n-hexane ceases at the instant of maximum compression as was assumed; on the contrary, while the temperature probably falls rapidly thereafter the free radical mechanisms of the type discussed below in conjunction with the $(\Delta E_{oR} - \frac{Q}{o})$ data would indicate that there were large numbers of hydrocarbon free radicals remaining at the instant of maximum compression, and that these radicals could attack more n-hexane thereafter. The amount of error so introduced is not known.

It would appear from the above discussion that the errors associated with the analysis of the results of these measurements made with the ballistic piston apparatus are sizable. While this is undoubtedly

true, it is considered that the results obtained are still meaningful, although measurement of pressure, thermal flux, temperature, etc., will certainly do much to decrease the errors.

Discussion of Results

The reaction rate coefficients for the apparent one-half order reaction (Table V-XIV and Figures V-6 and V-7) probably represent the situation as well as can be expected in the absence of measurements of additional quantities such as pressures and temperatures. It can certainly be concluded that the diluent gas does not enter chemically into the rate controlling steps of the decomposition of the n-hexane, since the calculated reaction rate coefficients for both first order and one-half order kinetics show no differences between nitrogen and hydrogen as the diluent. Since the reaction rate coefficients for one-half order kinetics show no correlation with either maximum pressure or the maximum ratio (f_R^o/P), it is believed that an apparent order of one half is correct for the decomposition reaction, presuming that the covolumes for n-hexane shown in Appendix I are reasonably correct. Unfortunately the calculated reaction rate coefficients are particularly sensitive to the equation of state of the normal hexane since the ratio (f_R^o/P), which assumes large values under the conditions encountered, is an exponential function of the covolume of the n-hexane. If the tabulated values of covolume for n-hexane in Table AI-IV (and $\bar{b}$ in Table AI-IX) should happen to be twice the true values, the ratios (f_R^o/P) calculated using

Table AI-IX would be equal to the squares of the true ratios. Although the calculation has not been made, it is believed that if covolumes equal to one half those shown in Appendix I for n-hexane were used, the reaction might appear to be closer to first order than to one half order. Thus, while it can be concluded that the decomposition reaction is probably of apparent one half order, there is some uncertainty herein.

A reaction mechanism involving free radicals which yields an apparent one half order is given by Laidler (29) and Steacie (30), along the lines first presented by Rice and Herzfeld (31). This is

$$M \xrightarrow{K_1} R_1 + R_1'$$

$$R_1 + M \xrightarrow{K_2} R_1H + R_2 \qquad \text{(V-36)}$$

$$R_2 \xrightarrow{K_3} R_1 + M'$$

$$2R_2 \xrightarrow{K_4} M''$$

The M's indicate molecules, the R's radicals. In the first step the reacting molecule M dissociates into two radicals by splitting a carbon-carbon bond. R_1' is assumed to play no part in the reactions of interest. R_1 reacts with the reacting molecule M by removing a hydrogen and yields a radical R_2, which then splits to yield R_1 and another molecule. Step (4) is the chain ending step. Using steady state assumptions (the rates of change of the concentration of R_1 and R_2 are zero) and assuming k_1 to be very small it is found that

$$-\frac{dM}{d\theta} \simeq K_3\left(\frac{K_1}{K_4}\right)^{\frac{1}{2}}(M)^{\frac{1}{2}} \qquad \text{(V-37)}$$

Similarly, if R_1 and R_2 combine as the chain ending step the reaction is of apparent first order, and if two R_1 combine as the chain ending step the reaction is of apparent 3/2 order.

While the exact mechanism of equation (V-36) will not give observed products (the molecule M'' would be $C_{12}H_{26}$, unlikely under the conditions), modifications of the mechanism can be written which are more plausible in this regard. They involve attack of the molecule by one radical obtained by splitting of another radical, with the chain ending step being combination of two of the second radicals. Thus, while the exact mechanisms considered seem somewhat unlikely, an apparent one-half order reaction is not unheard of and in this situation which probably involves free radicals the one half order need not cause undue concern. An apparent first order reaction might seem more likely however since the chain ending step then would be, for equation (V-36), combination of R_1 and R_2; and it would seem that $\frac{1}{2}$ order and 3/2 order chain endings could also occur and approximately average out at first order.

While the values of $(\Delta E_{oR} - Q_o)$ calculated for these runs and shown in Table V-XI do not correlate with other parameters, there is at least one significant observation to be made: they are large

positive numbers. If Q_o is assumed small, this large positive ΔE_{oR} indicates an appreciably endothermic reaction taking place. Calculations using heats of formation tabulated by Rossini (22) indicate that if the reaction of the initial sample to give the observed products took place at the calculated reaction temperature T_1, the ΔE_{oR} for the nitrogen runs would be close to zero and that for the hydrogen runs would be negative, or exothermic. As examples, run 128, having nitrogen as a diluent, gives + 65 (Btu/lb mole) and run 111, with hydrogen, gives -6075 (Btu/lb mole) for ΔE_{oR}. The values of $(\Delta E_{oR} - Q_o)$ from Table V-XI are respectively + 12,108 and +13,905 (Btu/lb mole). These indications of endothermic reaction are interpreted as showing that the final products are not all formed at the reaction temperature, but that rather at the instant of maximum compression, which is the end of the assumed isothermal process, a considerable quantity of free radicals remains.

The qualitative behavior of the apparatus during a shot sheds further light on the nature of the reaction subsequent to maximum compression. The reaction of the free radicals subsequent to maximum compression to give the final observed products is a highly exothermic reaction. If this reaction occurred sufficiently rapidly, for instance, to extend the assumed isothermal path beyond maximum compression until the reaction were complete, this energy would be available to be converted into kinetic energy of the piston and the piston would return with a velocity comparable to that with which it

descended. This would cause very noticeable oscillation of the apparatus such as is observed on firings on pure components like nitrogen, and on firings on nitrogen-oxygen mixtures. As a matter of fact practically no oscillations were observed; the apparatus behaved as though a sledge hammer had hit it and then exhibited essentially no further movement. It is concluded from these observations that the approximately isothermal portion of the path ended at maximum compression and that the temperature dropped very rapidly thereafter as the piston was accelerated upward. The free radicals finished the reactions sufficiently slowly so that in the main the energy from the exothermic reaction was not available to be converted to kinetic energy of the piston.

It is possible that the observed weak correlation of the one-half order reaction rate coefficients with the amount of n-hexane decomposed is caused by the reactions of the free radicals remaining after maximum compression. Some additional n-hexane could be attacked by the free radicals, which would invalidate to some degree the assumption that the decomposition of n-hexane was completed at the instant of maximum compression. While several mechanisms were considered, and some would yield correlation of the same sign as was observed, the observed correlation is sufficiently weak that it was not considered profitable to introduce additional assumptions in order to explain it.

The observed activation energies, as defined by equation (V-24),

are very low, being approximately 5200 and 9200 (Btu/lb mole) for the uncorrected and corrected half order reaction respectively. The apparent activation energy for the first order reaction as corrected for maximum pressure was 15,200 Btu/lb mole (8.4 Kcal/gm mole) which is also low. Jost (32) quotes a value of 64.5 Kcal/gm mole for the activation energy of the first order decomposition of n-hexane. This is for lower temperatures (about 500° C.) and of course much lower pressures. Hinshelwood et al. (33) found that the apparent activation energy for the first order decomposition of n-hexane shifted markedly with pressure in the subatmospheric range, and they quote apparent activation energies of 75 and 54 Kcal/gm mole for "low" and "high" pressures respectively. Pressures were not specifically defined, but "low" appeared to mean about 100 mm. of mercury, whereas "high" was probably atmospheric pressure or higher. Hinshelwood also found that added gases of certain kinds, such as propane, propylene and ethane behaved like n-hexane in lowering the activation energy while other gases such as methane, nitrogen, hydrogen, helium and CO_2 had no effect.

Activation energies and frequency factors for the first order decompositions of n-hexane from Jost (32) and Hinshelwood et al. (33) are shown in Table V-XV, along with reaction rate coefficients calculated for a temperature of 2200° R. using their data. These are compared with the reaction rate coefficient for that temperature taken from the line of Figure V-5, which represents the ballistic piston data corrected to a maximum pressure of 54,000 pounds per square inch. The agreement of

the reaction rate coefficients is surprisingly good, particularly when it is realized that the values from Jost and from Hinshelwood are based on work at considerably lower temperature and much lower pressure, and also that the reactions are not well represented by first order kinetics over the range of pressures involved.

The fact that extrapolation of literature data gives reaction rate coefficients similar to those estimated from ballistic piston data, while the activation energies determined from the latter data are markedly lower than those found by other investigations, tends to cast doubt on the apparent activation energies determined from ballistic piston data. However inasmuch as Hinshelwood found a marked influence of pressure on apparent activation energy in the low pressure region (see Table V-XV) and did not attempt an explanation, it appears that these complicated decomposition reactions are not well understood even when occurring under moderate conditions. Therefore the computed apparent activation energies for both first order and one half order may actually be of the right magnitude.

The literature contains little information on the products of decomposition of n-hexane. Pearce and Newsome (34) studied the decomposition of n-hexane at pressures of 14,000 to 15,000 pounds per square inch and temperatures between 430 and 520° C. for relatively long contact times. They found that the main products were methane and ethane with some aromatics and carbon at the higher temperatures. Little hydrogen was found. Kossiakoff and Rice (35) predicted

decomposition products for low pressure and short contact time on the basis of free radical mechanisms. They predicted approximately 5 per cent hydrogen, 22 per cent methane, 12 per cent ethane, 30 per cent ethylene, 20 per cent propylene, 8 per cent butene and 3 per cent pentane. The product distribution from the runs with nitrogen as a diluent does not agree with either reference. This is not unexpected however since their reaction conditions are grossly different. No data on the decomposition of n-hexane in the presence of hydrogen were found in the literature.

When the product distributions shown in Figures V-2 and V-3 are considered from a standpoint of the type of products, it appears that the lower temperature regions are the most interesting, except that the aromatics are found in the middle range of the nitrogen runs.

Conclusions

It is concluded that the thermal decomposition of n-hexane under conditions of high pressures and temperatures is of apparent order of approximately one half, and has a low apparent activation energy, of the order of 5,000 to 9,000 Btu/lb mole (2.8 to 5.0 Kcal/gm mole). The mechanism undoubtedly involves free radicals to a considerable extent, however some molecular reaction is not excluded. Hydrogen and nitrogen do not enter into any rate-controlling steps of the decomposition reaction. There are many fragments remaining at the instant of maximum compression in the ballistic piston apparatus, these react sufficiently slowly during the decompression so that the heat of

reaction involved does not contribute appreciably to the kinetic energy of the piston. The products of decomposition obtained by use of an inert diluent such as nitrogen are probably of most interest industrially since a large proportion of unsaturates can be obtained, or some aromatics can be obtained if desired.

The ballistic piston has shown that it can be a useful tool in investigating high pressure-high temperature reactions. With the addition of instrumentation for the measurement of pressure, temperature and thermal flux it can be used for quantitative measurements on such reactions, and for measurement of the pressure-volume-temperature properties required for establishment of the equations of state of gases under high pressure-high temperature conditions.

TABLE V-I. CONDITIONS ESTABLISHED FOR n-HEXANE RUNS

Maximum[a] Temperature (°R.)	Maximum[a] Pressure (Lb./Sq.In.)	Mole Fract. n-Hexane	Mole Fract. Hydrogen	Mole Fract. Nitrogen	Initial Air Pressure (Lb./Sq.In.)	Predicted Approach (In.)	Run Number
3800	55,000	0.0505	0.9495	-	637.1	0.025	(111)[b]
3400	55,000	0.0634	0.9366	-	605.0	0.022	142
3000	55,000	0.0805	0.9195	-	581.9	0.019	143
2600	55,000	0.1043	0.8957	-	556.3	0.017	119
3800	25,000	0.0375	0.9625	-	559.4	0.055	120
3400	25,000	0.0492	0.9508	-	543.9	0.049	132
3000	25,000	0.0648	0.9352	-	526.5	0.043	140
2600	25,000	0.0865	0.9135	-	506.5	0.037	121
3800	55,000	0.0450	-	0.9550	696.0	0.025	124
3400	55,000	0.0580	-	0.9420	659.1	0.022	129
3000	55,000	0.0752	-	0.9248	619.2	0.019	131
2600	55,000	0.0993	-	0.9007	559.2	0.017	125
3800	25,000	0.0321	-	0.9679	630.7	0.055	126
3400	25,000	0.0438	-	0.9562	598.4	0.049	(113)[b]
3000	25,000	0.0594	-	0.9406	563.7	0.043	128
2600	25,000	0.0814	-	0.9186	509.1	0.037	127

Initial sample pressure: 100 mm. mercury

[a] For isentropic compression of perfect gas to predicted approach

[b] These exact conditions not run, runs 111 and 113 with indicated maximum temperatures and pressures used

TABLE V-II. DATA FROM n-HEXANE RUNS

Run No.	Initial Air Pressure[a]	Initial Sample		Initial Sample Composition[b]			Closest Approach (In.)	Min.Vol. V_2^* x 10^4	Leakage Fract.
		Pressure[a]	Temperature (°R.)	n-Hexane	Nitrogen	Hydrogen			
111	618.6	1.9231	534.17	0.04973	-	0.95027	0.0188	2.503	0.050
113	618.4	1.9190	534.35	0.05005	0.83040[c]	-	0.0410	4.738	0.091
119	555.0	1.9263	528.86	0.10403	-	0.89597	0.0152	2.147	0.011
120	560.2	1.9225	528.05	0.03752	-	0.96248	0.0418	4.814	0.005
121	506.2	1.9183	526.52	0.08650	-	0.91350	0.0298	3.608	0.026
124	695.8	1.9249	529.31	0.04476	0.95524	-	0.0317	3.805	0.162
125	560.3	1.9216	529.90	0.09907	0.90093	-	0.0278	3.412	0.131
126	630.6	1.9241	529.40	0.03188	0.96812	-	0.0388	4.512	0.148
127	509.3	1.9221	523.28	0.08147	0.91853	-	0.0417	4.809	0.066
128	565.4	1.9250	530.17	0.05936	0.94064	-	0.0331	3.946	0.170
129	659.3	1.9262	526.97	0.06340	0.93660	-	0.0309	3.724	0.165
131	621.6	1.9233	528.68	0.07523	0.92477	-	0.0240	3.031	0.667
132	544.0	1.9039	529.49	0.04919	-	0.95081	0.0311	3.745	0.023
140	526.7	1.9202	531.47	0.06318	-	0.93682	0.0281	3.446	-
142	605.2	1.9233	537.59	0.06335	-	0.93665	0.0177	2.400	0.430
143	575.5	1.9063	530.48	0.08061	-	0.91939	0.0125	1.877	-

[a] (Lb./Sq.In.)

[b] Mole fraction

[c] Plus 0.11955 helium

TABLE V-III. BOTTOM CONTACT TIMING DATA

Run No.	Heights of Bottom Contacts (In.)				Times from h_1 (Microsec.)			Velocity at h_2 (Ft./Sec.)	Acceleration at $h_2 \times 10^{-3}$ (Ft./Sec.^{2})
	h_1	h_2	h_3	h_4	θ_2	θ_3	θ_4		
111	0.2528	0.1877	0.1223	0.0790	99	203	284	-53.63	23.6
113	0.2504	0.1913	0.1365	0.0727	102	213	363	-45.00	67.1
119	0.2486	0.1926	0.1303	0.0556	90	198	347	-50.14	50.6
120	0.2675	0.1667	0.1188	0.0719	190	285	407	-42.75	30.0
121	0.4990	0.3463	0.1913	0.1010	258	536	725	-47.95	10.7
124	0.5057	0.3537	0.2014	0.0970	210	454	630	-56.48	18.3
125	0.4984	0.3513	0.2142	0.0986	224	452	674	-52.44	20.4
126	0.4868	0.3476	0.2135	0.1022	195	394	584	-57.84	16.9
127	0.4876	0.3450	0.2068	0.1041	261	517	747	-45.26	2.1
128	0.4960	0.3303	0.1908	0.0933	249	474	657	-53.47	16.0
129	0.5012	0.3519	0.2085	0.1020	210	423	601	-57.69	14.9
131	0.5027	0.3344	0.2023	0.1119	236	431	580	-57.80	13.8
132	0.5121	0.3506	0.2108	0.1046	254	491	698	-51.00	15.6
140	0.5305	0.3734[a]	0.1928[a]	0.0968[a]	225	521	692	-	-
142	0.5186	0.3609	0.2073	0.1072	232	459	625	-56.51	1.1
143	0.5160	0.3577	0.2104	0.1100	224	440	606	-57.84	9.4

[a] Believed to be in error by constant amount

TABLE V-IV. SIDE CONTACT TIMING DATA

Run No.	140	142	143
Side contact 2 height (in.)	-	-	57.932
Side contact 3 height (in.)	37.892	37.892	37.892
Side contact 4 height (in.)	17.892	17.892	17.892
Bottom contact 2 height (in.)	0.3734	0.3609	0.3577
Side contact 2 time (millisec.)	-	-	0
Side contact 3 time (millisec.)	0	0	24.3
Side contact 4 time (millisec.)	24.0	22.7	47.9
Bottom contact 2 time (millisec.)	46.5	43.9	69.0
Velocity, 3 to 4 (ft./sec.)	69.44	73.42	70.63

TABLE V-V. ANALYSIS OF SAMPLES[a]

Run No.	111		113		119	
	Control	Product	Control	Product	Control	Product
H_2	95.31	72.53		1.39	89.80	77.53
He			11.52	11.18		
N_2			82.71	76.20		
n-C_6H_{14}	3.89	0.49	5.46	0.52	9.81	4.84
C_6H_{12}						0.12
C_5H_{12}						
C_5H_{10}						0.18
C_5H_8						
C_4H_{10}						0.44
C_4H_8				0.08		0.48
C_4H_6						
C_4H_2						
C_3H_8		0.09				2.27
C_3H_6		0.12		0.30		1.01
C_2H_6		0.78		0.40		5.10
C_2H_4				1.03		0.73
CH_4		25.50		8.12		6.92
C_6H_6				0.32		
C_7H_8				0.08		
Air	0.65	0.25				
H_2O	0.15	0.13	0.12	0.18	0.27	0.34
CO_2		0.11	0.08	0.18		
O_2			0.06	0.02	0.12	0.04

[a] Mole per cent, as reported by The Texas Company, Montebello Laboratories

TABLE V-V. ANALYSIS OF SAMPLES[a] (Cont.)

Run No.	120		121		124	
	Control	Product	Control	Product	Control	Product
H_2	96.16	80.02	91.72	68.03		5.85
He						
N_2	0.17				95.43	84.67
n-C_6H_{14}	3.47	0.22	8.04	2.33	4.47	0.46
C_6H_{12}						
C_5H_{12}		0.02				
C_5H_{10}				0.06		
C_5H_8						
C_4H_{10}				0.13		0.06
C_4H_8		0.04		0.23		
C_4H_6						
C_4H_2						
C_3H_8		0.16		0.70		
C_3H_6		0.06		0.38		0.19
C_2H_6		0.71		3.60		0.27
C_2H_4		0.12		0.53		0.67
CH_4		18.16		23.82		7.35
C_6H_6						0.25
C_7H_8						0.04
Air		0.35				
H_2O	0.10	0.14	0.12	0.19	0.10	0.19
CO_2						
O_2	0.10		0.12			

TABLE V-V. ANALYSIS OF SAMPLES[a] (Cont.)

Run No.	125		126		127	
	Control	Product	Control	Product	Control	Product
H_2		0.34		7.59		0.46
He						
N_2	90.57	84.21	96.68	87.13	92.07	85.90
n-C_6H_{14}	9.24	5.10	2.82	0.20	7.82	3.84
C_6H_{12}		0.04				0.21
C_5H_{12}						
C_5H_{10}		0.32				0.30
C_5H_8		0.15				0.16
C_4H_{10}						
C_4H_8		1.10				0.57
C_4H_6		0.10				0.14
C_4H_2						
C_3H_8		0.54				0.37
C_3H_6		2.02		0.04		1.58
C_2H_6		1.52		0.13		1.40
C_2H_4		2.50		0.46		3.01
CH_4		1.95		4.30		1.95
C_6H_6				0.04		
C_7H_8						
Air						
H_2O	0.17	0.09	0.48	0.09	0.09	0.07
CO_2						
O_2	0.02	0.02	0.02	0.02	0.02	0.04

TABLE V-V. ANALYSIS OF SAMPLES[a] (Cont.)

Run No.	128		129		131	
	Control	Product	Control	Product	Control	Product
H_2		3.02		3.85		1.17
A						0.07
N_2	94.25	84.42	93.88	83.62	92.10	82.64
n-C_6H_{14}	5.24	0.76	5.30	0.59	7.46	1.29
C_6H_{12}						0.22
C_5H_{12}						
C_5H_{10}		0.05				0.22
C_5H_8						0.15
C_4H_{10}						
C_4H_8				0.11		0.60
C_4H_6		0.08		0.06		0.26
C_4H_2		0.02		0.02		0.06
C_3H_8						0.32
C_3H_6		0.38		0.41		1.47
C_2H_6		0.83		0.56		2.19
C_2H_4		1.41		0.99		2.97
CH_4		8.21		8.64		5.17
C_6H_6		0.48		0.47		0.28
C_7H_8		0.20		0.15		0.21
Air						
H_2O	0.47	0.10	0.67	0.34	0.27	0.26
CO_2		0.02	0.13	0.15	0.13	0.10
O_2	0.04	0.02	0.02	0.04	0.04	0.35

TABLE V-V. ANALYSIS OF SAMPLES[a] (Cont.)

Run No.	132		140		142	
	Control	Product	Control	Product	Control	Product
H_2	95.02	74.02	95.57	68.12	93.78	68.00
CS_2				0.02		
N_2	0.11			0.21	0.10	0.42
$n\text{-}C_6H_{14}$	4.40	0.66	6.12	1.03	5.82	1.14
C_6H_{12}						
C_5H_{12}						
C_5H_{10}				0.04		0.02
C_5H_8						
C_4H_{10}				0.04		0.06
C_4H_8				0.06		0.10
C_4H_6						
C_4H_2						
C_3H_8		0.08		0.26		0.10
C_3H_6		0.11		0.17		0.04
C_2H_6		0.81		1.37		1.19
C_2H_4		0.21		0.32		0.25
CH_4	0.02	23.49		27.99		28.35
C_6H_6						
C_7H_8						
Air				0.09		0.23
H_2O	0.19	0.45	0.18	0.28	0.18	0.06
CO_2	0.13	0.13		Trace		0.04
O_2	0.13	0.04	0.13		0.12	

TABLE V-V. ANALYSIS OF SAMPLES[a] (Cont.)

Run No.	143	
	Control	Product
H_2	92.46	64.90
CS_2		
N_2	0.10	
n-C_6H_{14}	7.28	2.00
C_6H_{12}		
C_5H_{12}		
C_5H_{10}		0.04
C_5H_8		
C_4H_{10}		0.08
C_4H_8		0.10
C_4H_6		
C_4H_2		
C_3H_8		0.33
C_3H_6		0.25
C_2H_6		2.21
C_2H_4		0.18
CH_4		29.71
C_6H_6		
C_7H_8		
Air		0.10
H_2O	0.06	0.08
CO_2		0.02
O_2	0.10	

TABLE V-VI. ADJUSTED ANALYSES[a]: NITROGEN-n-HEXANE RUNS

	Run No.	113	124	125	126
INITIAL	He	11.96**			
	N_2	83.04**	95.52**	90.09**	96.81**
	$n\text{-}C_6H_{14}$	5.00**	4.48**	9.91**	3.19**
FINAL	H_2	1.40*	5.86*	0.34*	7.60*
	He	10.77***			
	N_2	74.75***	84.79***	84.31***	86.79***
	$n\text{-}C_6H_{14}$	0.52*	0.46*	5.10***	0.20*
	C_6H_{12}	-		0.04*	
	C_5H_{10}			0.32*	
	C_5H_8	-		0.15*	
	C_4H_{10}	-	0.06*		
	C_4H_8	0.08*		1.10*	
	C_4H_6	-		0.10*	
	C_3H_8	-		0.54*	
	C_3H_6	0.30*	0.19*	2.02*	0.04*
	C_2H_6	0.40*	0.27*	1.52*	0.13*
	C_2H_4	1.03*	0.67*	2.50*	0.46*
	CH_4	10.35***	7.41***	1.95*	4.74***
	C_6H_6	0.32*	0.25*		0.04*
	C_7H_8	0.08*	0.04*		
	Free C[b]	7.75***	10.39***	0.00***	10.80***
	γ[c]	1.111***	1.127***	1.069***	1.115***

[a] Mole per cent
[b] Moles/100 moles initial
[c] Final moles gas/initial mole

*Mass spect. w/o air, CO_2, H_2O, O_2
** By addition
*** Calculated by stoichiometry

TABLE V-VI. ADJUSTED ANALYSES[a]: NITROGEN-n-HEXANE RUNS (Cont.)

	Run No.	127	128	129	131
INITIAL	N_2	91.85**	94.73*	94.66*	92.48**
	$n\text{-}C_6H_{14}$	8.15**	5.27*	5.34*	7.52**
FINAL	H_2	0.46*	3.02*	3.87*	1.18*
	N_2	86.06***	84.99***	83.96***	83.12***
	$n\text{-}C_6H_{14}$	3.79***	0.76*	0.59*	1.30*
	C_6H_{12}	0.21*			0.22*
	C_5H_{10}	0.30*	0.05*		0.22*
	C_5H_8	0.16*			0.15*
	C_4H_8	0.57*		0.11*	0.60*
	C_4H_6	0.14*	0.08*	0.06*	0.26*
	C_4H_2		0.02*	0.02*	0.06*
	C_3H_8	0.37*			0.32*
	C_3H_6	1.58*	0.38*	0.41*	1.47*
	C_2H_6	1.40*	0.83*	0.56*	2.19*
	C_2H_4	3.01*	1.41*	0.99*	2.97*
	CH_4	1.95*	7.78***	8.81***	5.45***
	C_6H_6		0.48*	0.47*	0.28*
	C_7H_8		0.20*	0.15*	0.21*
	Free C[b]	0.00***	6.11***	8.01***	1.80***
	γ[c]	1.067***	1.115***	1.127***	1.113***

TABLE V-VII. ADJUSTED ANALYSES[a]: HYDROGEN-n-HEXANE RUNS

	Run No.	111	119	120	121
INITIAL	H_2 **	95.03	89.60	96.25	91.35
	$n\text{-}C_6H_{14}$ **	4.97	10.40	3.75	8.65
FINAL	H_2	73.87***	78.19***	80.12***	68.00***
	$n\text{-}C_6H_{14}$	0.49*	4.50***	0.22*	2.33*
	C_6H_{12}		0.12*		
	C_5H_{12}			0.02*	
	C_5H_{10}		0.18*		0.06*
	C_4H_{10}		0.44*		0.13*
	C_4H_8		0.48*	0.04*	0.23*
	C_4H_6				
	C_3H_8	0.09*	2.28*	0.16*	0.70*
	C_3H_6	0.12*	1.01*	0.06*	0.38*
	C_2H_6	0.78*	5.12*	0.71*	3.61*
	C_2H_4		0.73*	0.12*	0.53*
	CH_4	24.65***	6.95*	18.55***	24.03***
	γ[b]	1.001***	1.026***	1.002***	1.012***

[a] Mole per cent
[b] Final moles gas/initial mole
* Mass spect. w/o air, CO_2,H_2O,O_2
** By addition
*** Calculated by stoichiometry

TABLE V-VII. ADJUSTED ANALYSES[a]: HYDROGEN-n-HEXANE RUNS (Cont.)

	Run No.	132	140	142	143
INITIAL	H_2 **	95.08	93.68	93.67	91.94
	$n\text{-}C_6H_{14}$ **	4.92	6.32	6.33	8.06
FINAL	H_2	75.29***	70.54***	70.39***	66.18***
	$n\text{-}C_6H_{14}$	0.66*	1.04*	1.15*	2.00*
	C_6H_{12}				
	C_5H_{12}				
	C_5H_{10}		0.04*	0.02*	0.04*
	C_4H_{10}		0.04*	0.06*	0.08*
	C_4H_8		0.06*	0.10*	0.10*
	C_4H_6			0.10*	
	C_3H_8	0.08*	0.26*		0.33*
	C_3H_6	0.11*	0.17*	0.04*	0.25*
	C_2H_6	0.82*	1.38*	1.20*	2.22*
	C_2H_4	0.21*	0.32*	0.25*	0.18*
	CH_4	22.83***	26.15***	26.69***	28.62***
	γ[b]	1.003***	1.006***	1.006***	1.006***

TABLE V-VIII. CONVERSION[a] OF n-HEXANE: NITROGEN-n-HEXANE RUNS

Run No.	113	124	125	126	127	128	129	131
H_2	0.050	0.238	0.012	0.408	0.017	0.109	0.133	0.031
C_6H_{12}			0.010		0.055			0.040
C_5H_{10}			0.064		0.065	0.011		0.033
C_5H_8			0.030		0.035			0.022
C_4H_{10}		0.011						
C_4H_8	0.013		0.175		0.099		0.018	0.073
C_4H_6			0.016		0.024	0.013	0.009	0.032
C_4H_2						0.003	0.003	0.007
C_3H_8			0.065		0.048			0.029
C_3H_6	0.038	0.027	0.242	0.008	0.206	0.048	0.050	0.135
C_2H_6	0.033	0.026	0.121	0.016	0.121	0.070	0.045	0.134
C_2H_4	0.086	0.064	0.200	0.058	0.261	0.118	0.080	0.182
CH_4	0.433	0.351	0.078	0.297	0.084	0.327	0.354	0.167
C_6H_6	0.080	0.071		0.015		0.121	0.113	0.051
C_7H_8	0.023	0.013				0.058	0.042	0.044
Free C	0.292	0.437		0.607		0.230	0.285	0.049

[a] Fraction of decomposed n-hexane appearing as product, H_2 based on hydrogen, others based on carbon

TABLE V-IX. CONVERSION[a] OF n-HEXANE: HYDROGEN-n-HEXANE RUNS

Run No.	111	119	120	121	132	140	142	143
C_6H_{12}		0.021						
C_5H_{12}			0.005					
C_5H_{10}		0.027		0.008		0.007	0.003	0.006
C_4H_{10}		0.052		0.014		0.005	0.008	0.009
C_4H_8		0.057	0.007	0.025		0.007	0.013	0.011
C_4H_6							0.013	
C_3H_8	0.010	0.202	0.023	0.057	0.010	0.025		0.028
C_3H_6	0.014	0.090	0.009	0.031	0.013	0.016	0.004	0.021
C_2H_6	0.058	0.303	0.067	0.194	0.064	0.088	0.078	0.123
C_2H_4		0.043	0.011	0.028	0.016	0.020	0.016	0.010
CH_4	0.919	0.205	0.878	0.644	0.897	0.832	0.865	0.793

[a] Fraction of decomposed n-hexane appearing as product, based on carbon

TABLE V-X. CONDITIONS AT h_2 AND EFFECTIVE FRICTIONAL FORCE

Run No.	h_2 (In.)	Conditions at h_2			Effective Frictional Force (Lb.)	
		Isentropic		From Acceleration		
		Temp. (°R.)	Pressure (Lb./Sq.In.)	Pressure (Lb./Sq.In.)	From u At h_2	From u Side Contacts
111	0.1877	2612	5127	3220	10.36	-
113	0.1913	2583	5131	9134	61.55	-
119	0.1926	1800	3448	6898	48.51	-
120	0.1667	2967	6623	4086	12.23	-
121	0.3463	1763	1857	1453	44.56	-
124	0.3537	2268	2397	2490	79.48	-
125	0.3513	1644	1712	2782	55.57	-
126	0.3476	2555	2751	2299	13.14	-
127	0.3450	1789	1932	289	55.25	-
128	0.3303	2076	2339	2179	25.62	-
129	0.3519	1979	2100	2028	61.63	-
131	0.3344	1884	2089	1881	41.74	-
132	0.3506	2272	2338	2123	23.67	-
140	-	-	-	-	-	-16.05
142	0.3609	2065	2046	159	9.34	- 5.84
143	0.3577	1834	1834	1322	-4.33	6.98

TABLE V-XI. RESULTS FOR ISOTHERMAL PATH CALCULATIONS

Run No.	Initial Sample $N_o \times 10^4$ (Lb.Mole)	$\frac{W_B}{RT_{Bo}}$	Work Done On Sample $-W_B$ (Btu)	Assumed $\frac{N_{av}}{N_o}$	Results for Isothermal Reaction Assumption: Temp. T_1 (°R.)	Max.Press. P_2 (Lb./Sq.In.)	$(\Delta E_{oR} - Q)$ (Btu/Lb.Mole)	Time At Temp. T_1 $\Delta\Theta$ (Microsec.)	$(PV)/(RT)$ At Max. Pressure
111	1.3663	-28.632	4.152	1.000	2524	67,050	13,905	423	1.844
113	1.3629	-24.911	3.605	1.060	2288	32,180	12,106	720	1.670
119	1.3829	-23.000	3.342	1.013	1640	81,590	12,681	664	2.859
120	1.3816	-25.941	3.760	1.000	2757	27,090	10,111	524	1.296
121	1.3832	-21.242	3.074	1.006	1890	30,630	8,885	567	1.585
124	1.3801	-26.906	3,905	1.065	2293	52,630	13,850	615	2.132
125	1.3768	-22,769	3.301	1.035	1861	55,550	9,710	374	2.629
126	1.3791	-28.937	4.198	1.060	2764	44,950	13,156	466	1.810
127	1.3944	-20.549	2.979	1.035	1738	26,200	9,701	966	1.850
128	1.3781	-25.152	3.651	1.060	2147	47,480	12,108	557	2.156
129	1.3874	-26.602	3.865	1.065	2381	62,510	10,438	274	2.372
131	1.3809	-26.452	3.837	1.060	2088	84,270	12,571	347	3.022
132	1.3646	-24.628	3.536	1.000	2283	31,550	11,725	705	1.435
140	1.3806	-24.650	3.594	1.000	2381	38,580	9,384	384	1.535
142	1.3568	-26.570	3.851	1.000	2234	66,610	13,376	216	1.988
143	1.3629	-26.590	3.820	1.000	1945	115,160	14,526	473	3.074

TABLE V-XII. SENSITIVITY OF ISOTHERMAL CALCULATION TO VALUE OF EFFECTIVE FRICTIONAL FORCE

	Using F From Velocities				Using F = 50 lb.				
Run No.	F (Lb.)	$\frac{W_o}{RT_{Bo}}$	Temp. T_1 ($^oR.$)	$(\Delta E_{oR}-Q_o)^a$	$\frac{W_o}{RT_{Bo}}$	Temp. T_1 (^oR)	$(\Delta E_{oR}-Q_o)^a$	$\frac{\Delta T_1}{\Delta F}$ ($^oR./Lb.$)	$\frac{\Delta(\Delta E_{oR}-Q_o)^b}{\Delta F}$
111	10.36	-28.63	2524	13,905	-25.72	2043	15,358	-12.1	36.7
113	61.55	-24.91	2288	12,106	-25.76	2469	11,231	-15.7	75.8
120	12.23	-25.94	2757	10,111	-23.16	2139	12,547	-16.4	64.5
124	79:48	-26.91	2293	13,850	-29.07	2728	11,828	-14.9	68.5
125	55.57	-22.77	1861	9,710	-23.18	1932	9,209	-12.7	89.8

[a] (Btu/Lb.Mole)

[b] (Btu)/(Lb.Mole)(Lb.)

TABLE V-XIII. FIRST ORDER REACTION RATE COEFFICIENTS

Run No.	Diluent	Temp. T_1 ($^oR.$)	$\frac{1}{T_1} \times 10^4$ ($^oR.^{-1}$)	Maximum Pressure P_2 (Lb./Sq.In.)	Maximum Ratio f_R^o/P	First Order Reaction Rate Coefficient[a]	
						Calculated	Corrected To P_2 = 54,000
111	H_2	2524	3.962	67,050	60.3	0.285	0.531
113	N_2- He	2288	4.371	32,180	7.05	0.723	0.255
119	H_2	1640	6.098	81,590	723.	0.023	0.098
120	H_2	2757	3.627	27,090	4.45	1.155	0.319
121	H_2	1890	5.291	30,630	7.00	0.658	0.215
124	N_2	2293	4.361	52,630	28.8	0.358	0.335
125	N_2	1861	5.373	55,550	51.9	0.092	0.099
126	N_2	2764	3.618	44,950	13.5	0.588	0.382
127	N_2	1738	5.754	26,200	4.89	0.342	0.091
128	N_2	2147	4.658	47,480	22.9	0.370	0.284
129	N_2	2381	4.200	62,510	52.0	0.239	0.359
131	N_2	2088	4.789	84,270	314.	0.054	0.230
132	H_2	2283	4.380	31,550	6.73	0.740	0.253
140	H_2	2381	4.200	38,580	10.7	0.646	0.310
142	H_2	2234	4.476	66,610	80.6	0.193	0.353
143	H_2	1945	5.141	115,160	4300.	0.0063	0.118

[a] (Lb.mole)/(Cu.ft.)(Atm.)(Sec.)

TABLE V-XIV. ONE HALF ORDER REACTION RATE COEFFICIENTS

Run No.	Diluent	$\frac{1}{T_1} \times 10^4$ ($^\circ R.^{-1}$)	Amount n-Hexane Decomposed s[a]	One-Half Order Reaction Rate Coefficient[b]	
				Calculated	Corrected To s = 0.04744
111	H_2	3.962	0.0448	5.26	5.65
113	N_2- He	4.371	0.0442	3.60	3.93
119	H_2	6.098	0.0578	3.08	2.32
120	H_2	3.627	0.0353	4.93	6.86
121	H_2	5.291	0.0629	5.70	3.74
124	N_2	4.361	0.0396	3.52	4.35
125	N_2	5.373	0.0446	3.77	4.08
126	N_2	3.618	0.0297	4.02	6.52
127	N_2	5.754	0.0410	1.95	2.33
128	N_2	4.658	0.0442	4.17	4.55
129	N_2	4.200	0.0467	6.44	6.57
131	N_2	4.789	0.0607	4.84	3.37
132	H_2	4.380	0.0426	3.48	3.97
140	H_2	4.200	0.0527	7.05	6.11
142	H_2	4.476	0.0517	8.39	7.47
143	H_2	5.141	0.0605	2.82	1.97

[a] Lb.mole/lb.mole initial sample

[b] $(Lb.mole)/(Cu.ft.)(Atm.^{\frac{1}{2}})(Sec.)$

TABLE V-XV. REACTION RATE DATA FROM LITERATURE

Source	Activation Energy E' Kcal./gm.mole	Log A'	First Order Reaction Rate Coefficients[a] k_c[b]	k_R[c]
Jost (32)	64.5	14.58	1110	0.69
Hinshelwood: (33)				
"Low Pressure"	75.	17.0	3800	2.38
"High Pressure"	54.	12.2	368	0.23
Figure V-5[d]	8.4	-	-	0.25

[a] At 2200°R.

[b] $k_c = A' e^{-E'/RT}$ sec.$^{-1}$

[c] (Lb.mole)/(Cu.ft.)(Atm.)(Sec.)

[d] For maximum pressure of 54,000 pounds per square inch

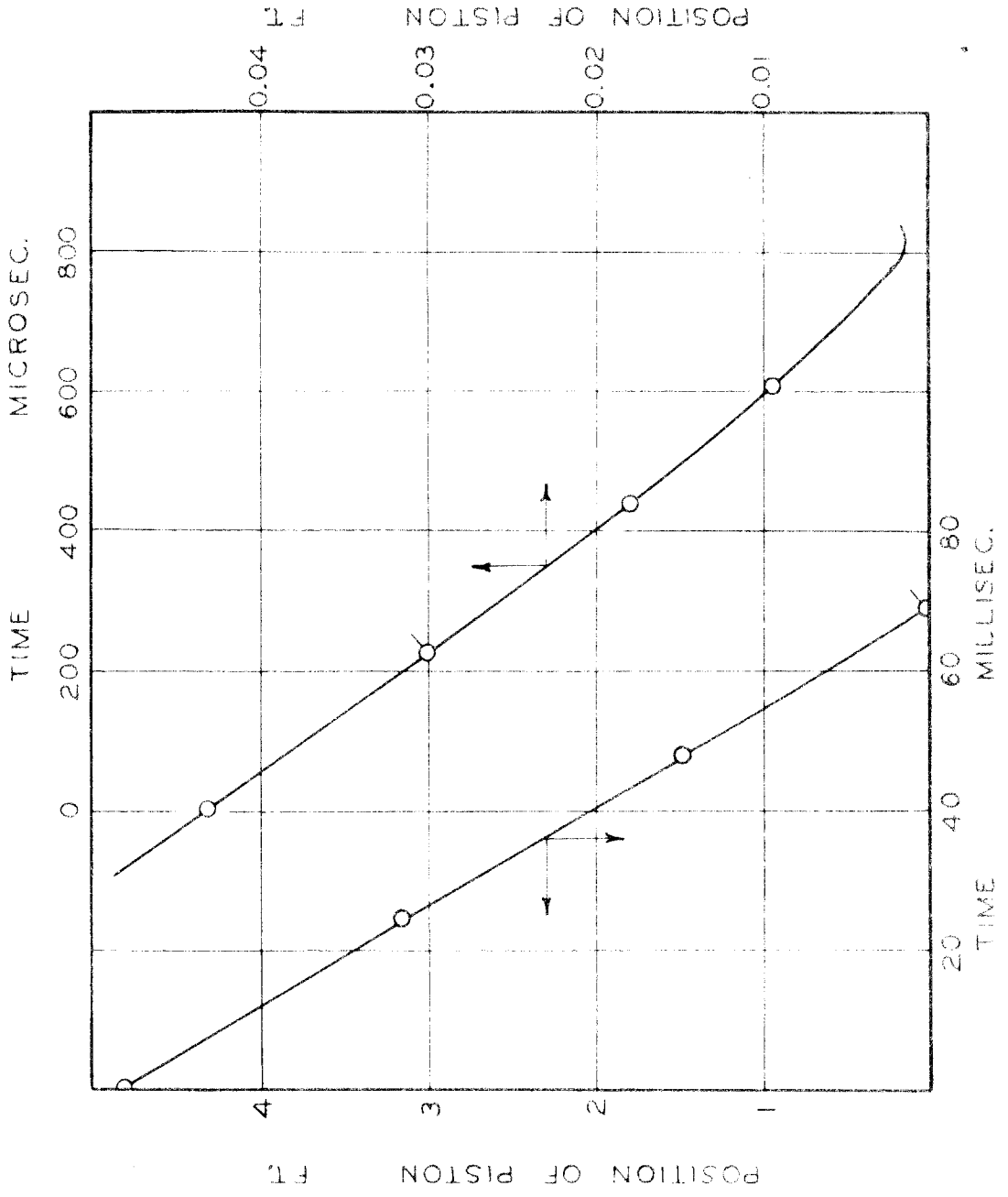

Fig. V-1. Position-Time Data, Run 143

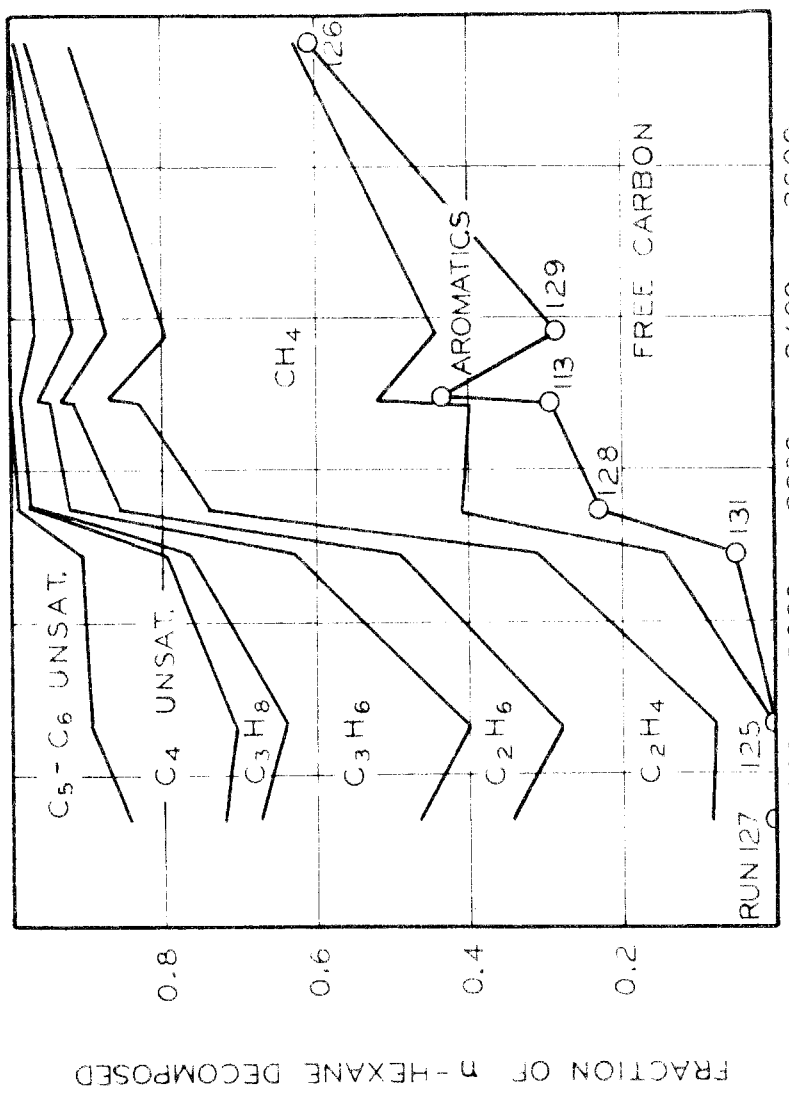

Fig. V-2. Cumulative Product Distribution: Nitrogen-n-Hexane Runs

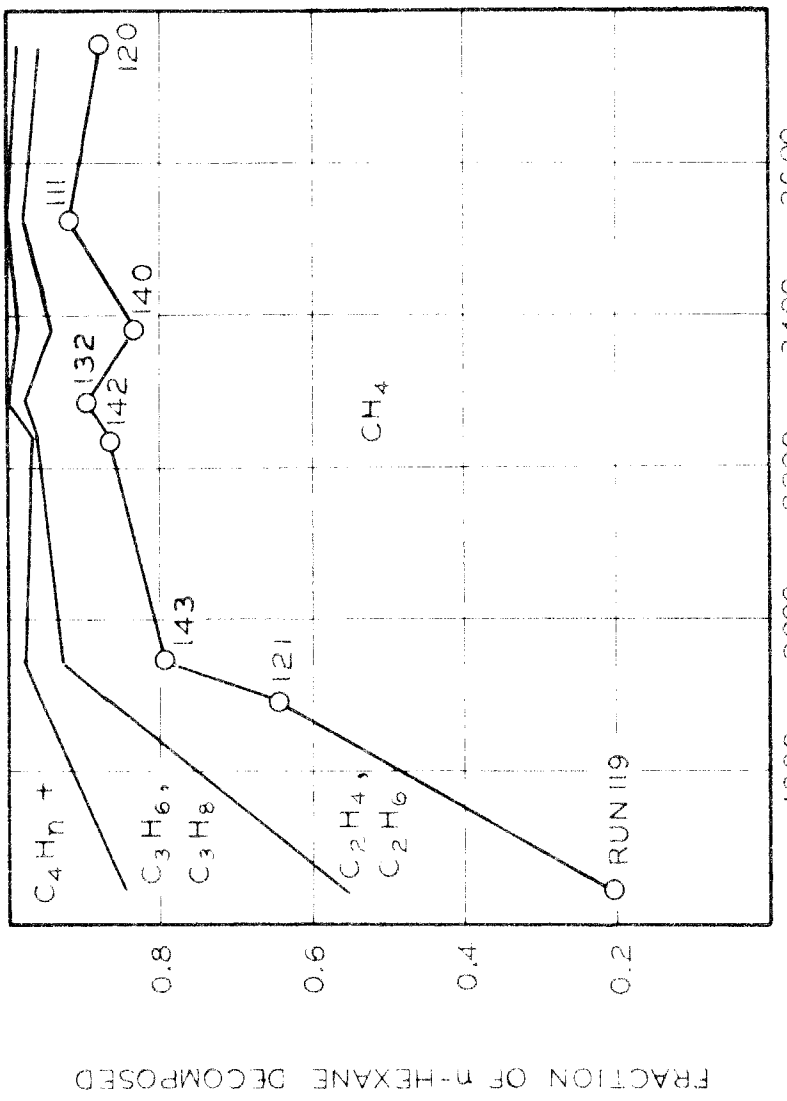

Fig. V-3. Cumulative Product Distribution: Hydrogen-n-Hexane Runs

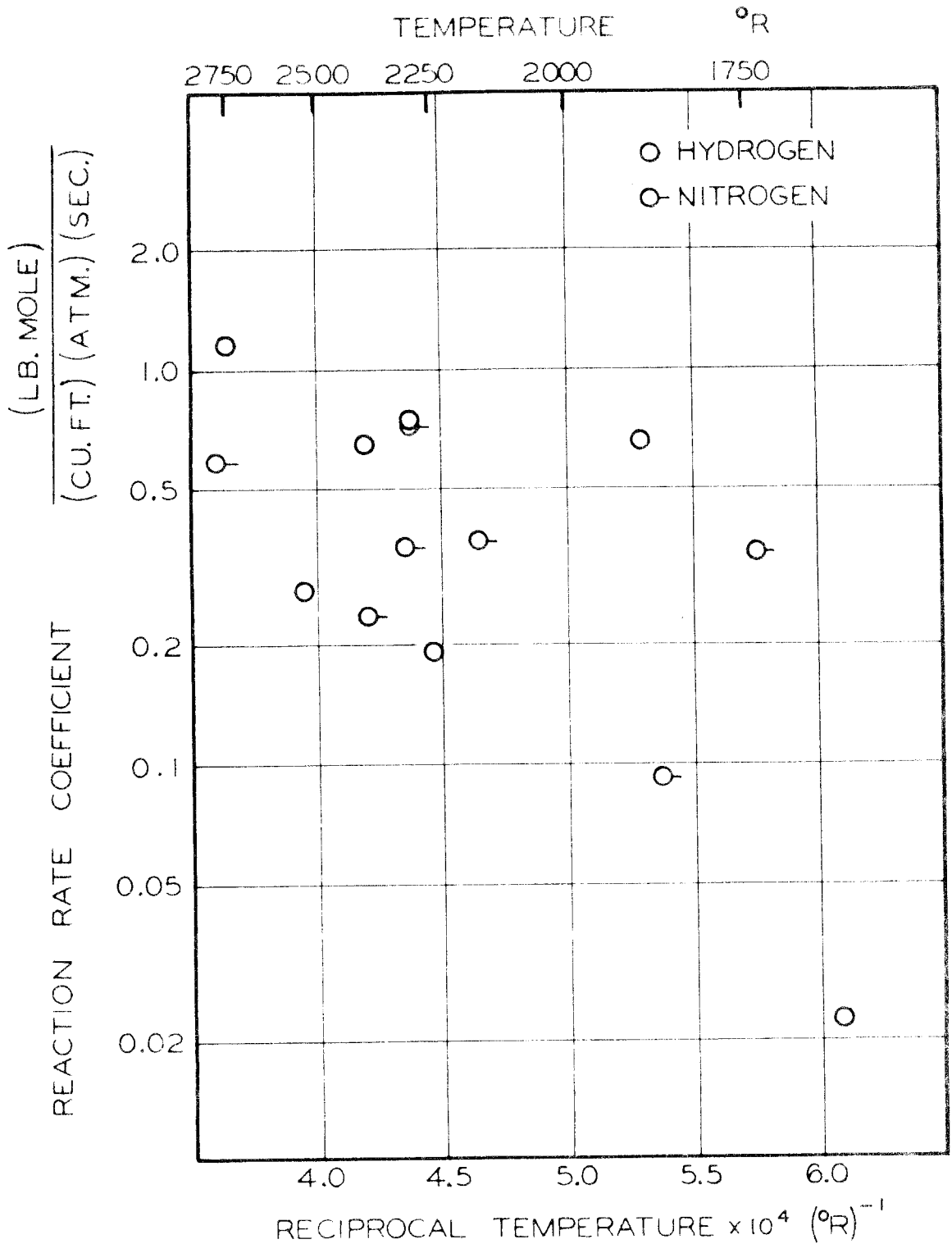

Fig. V-4. First Order Reaction Rate Coefficients

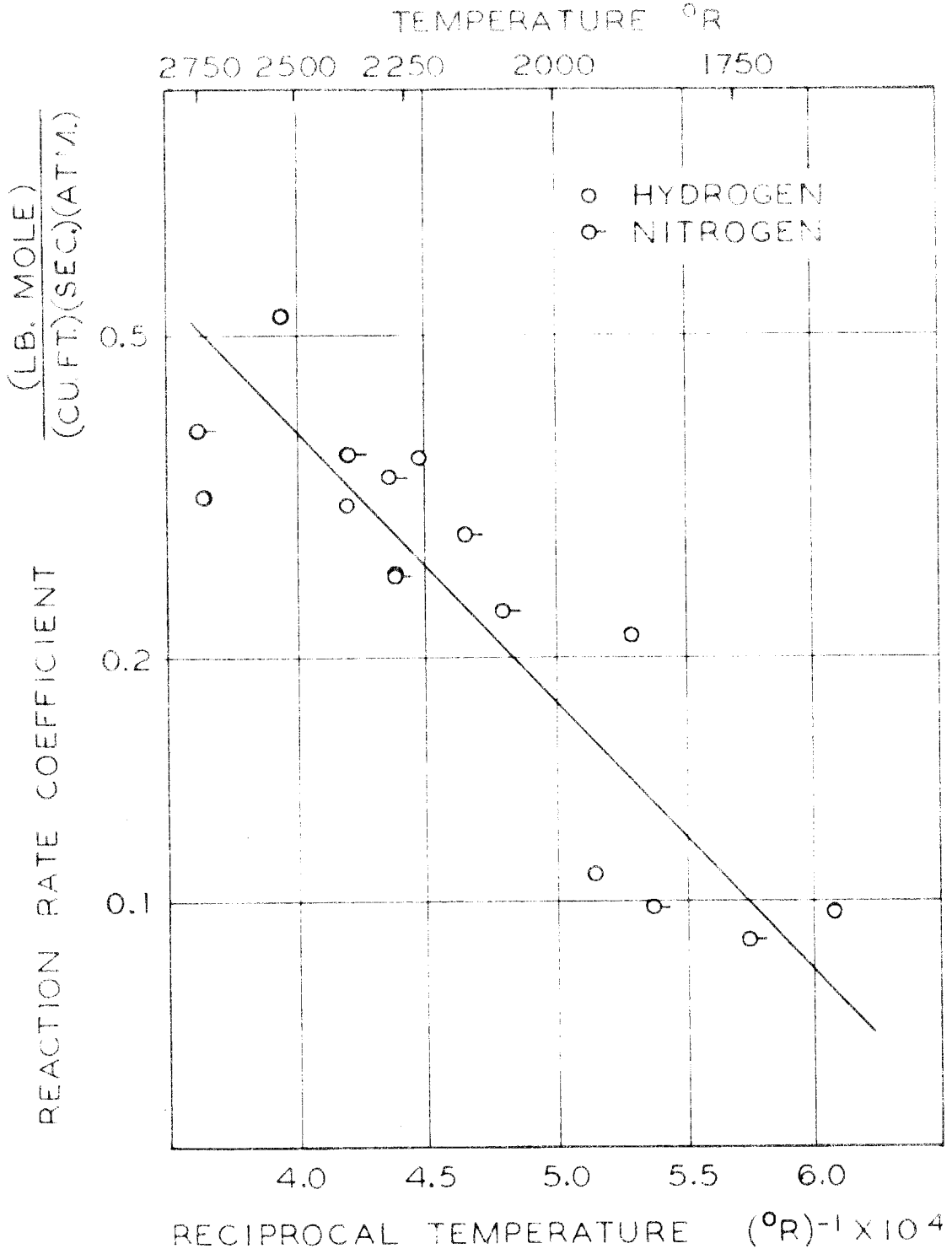

Fig. V-5. First Order Reaction Rate Coefficients Corrected to 54,000 lb./sq. in. Maximum Pressure

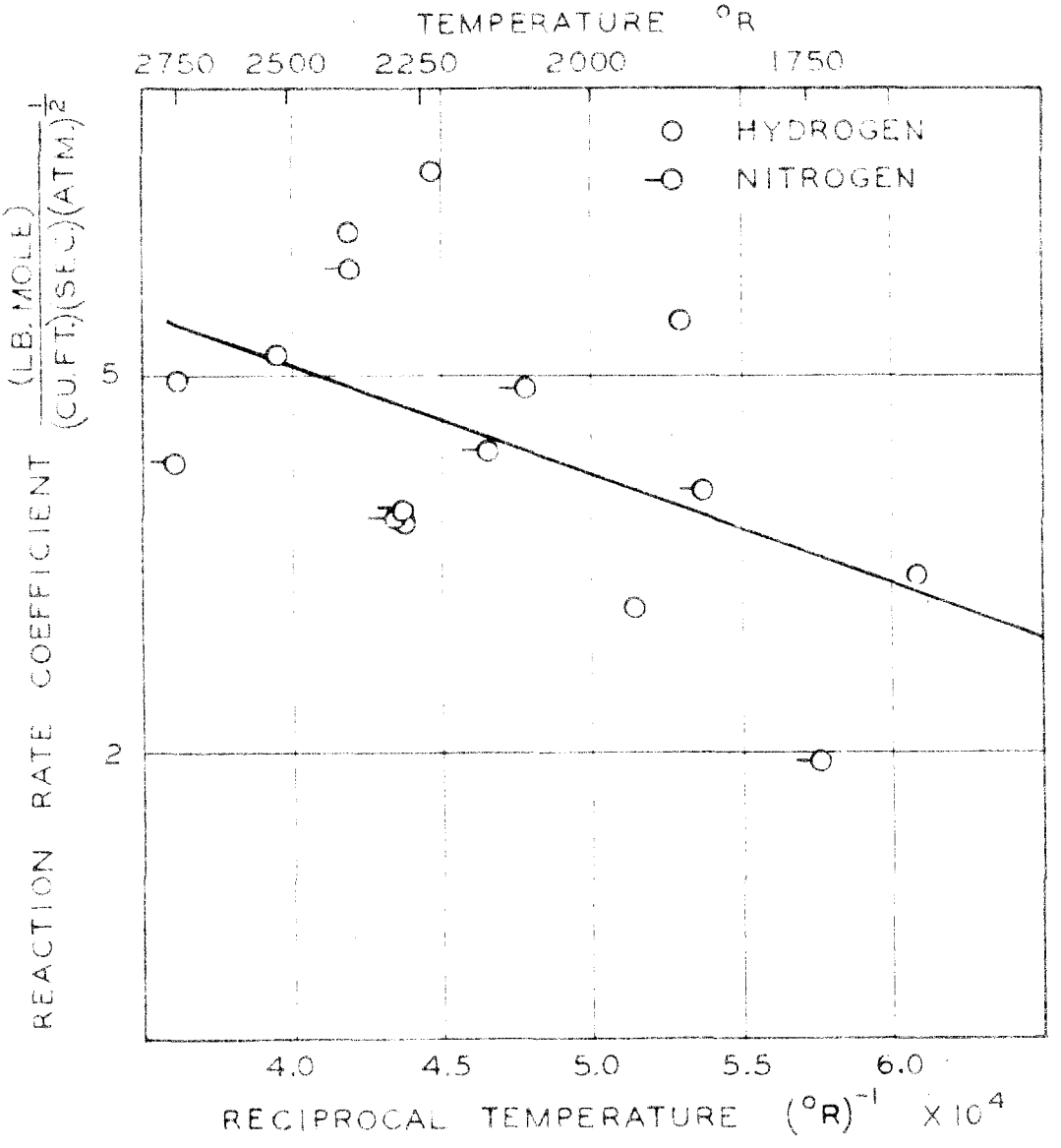

Fig. V-6. One Half Order Reaction Rate Coefficients

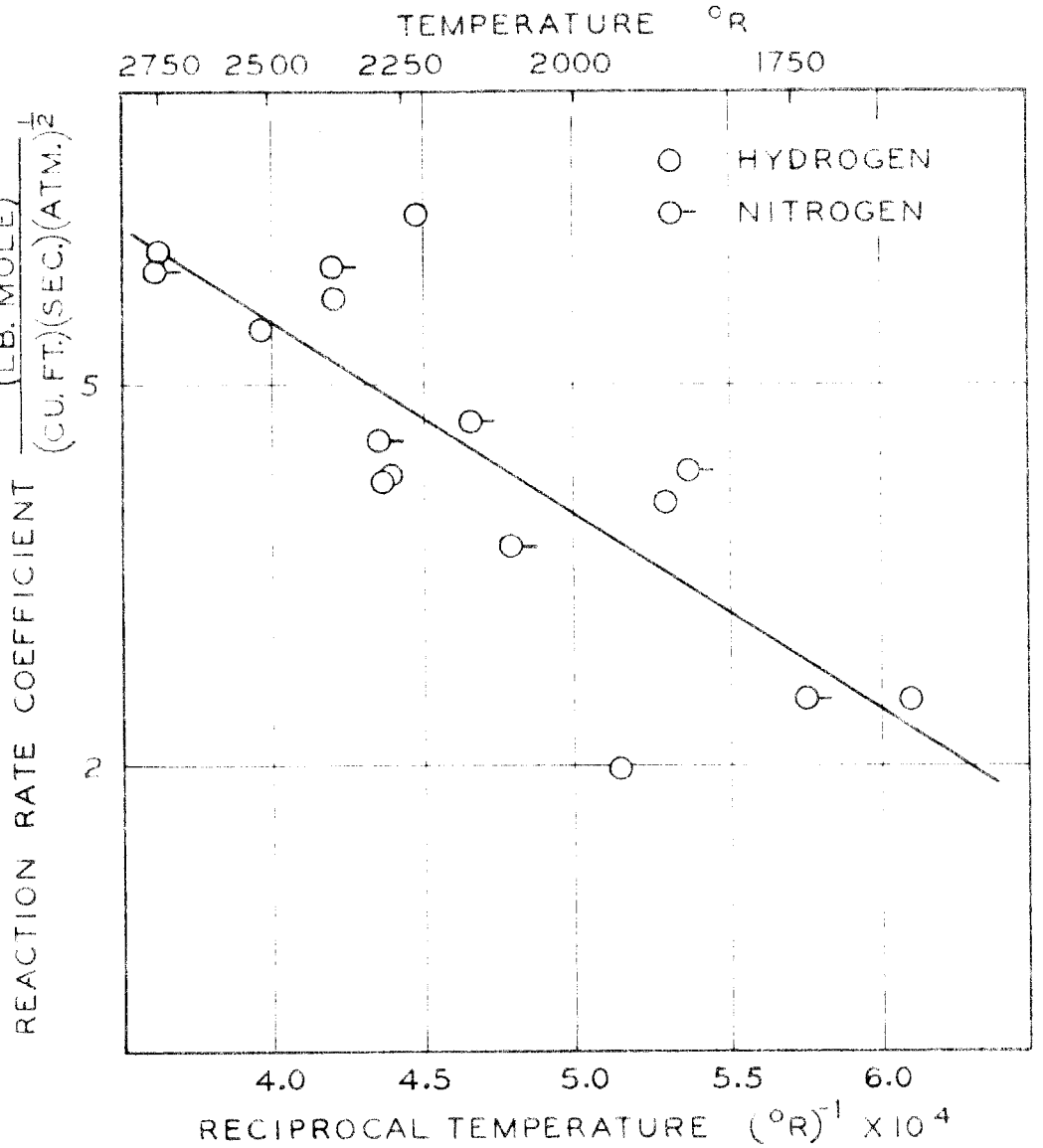

Fig. V-7. One Half Order Reaction Rate Coefficients Corrected to Average Amount of Reaction

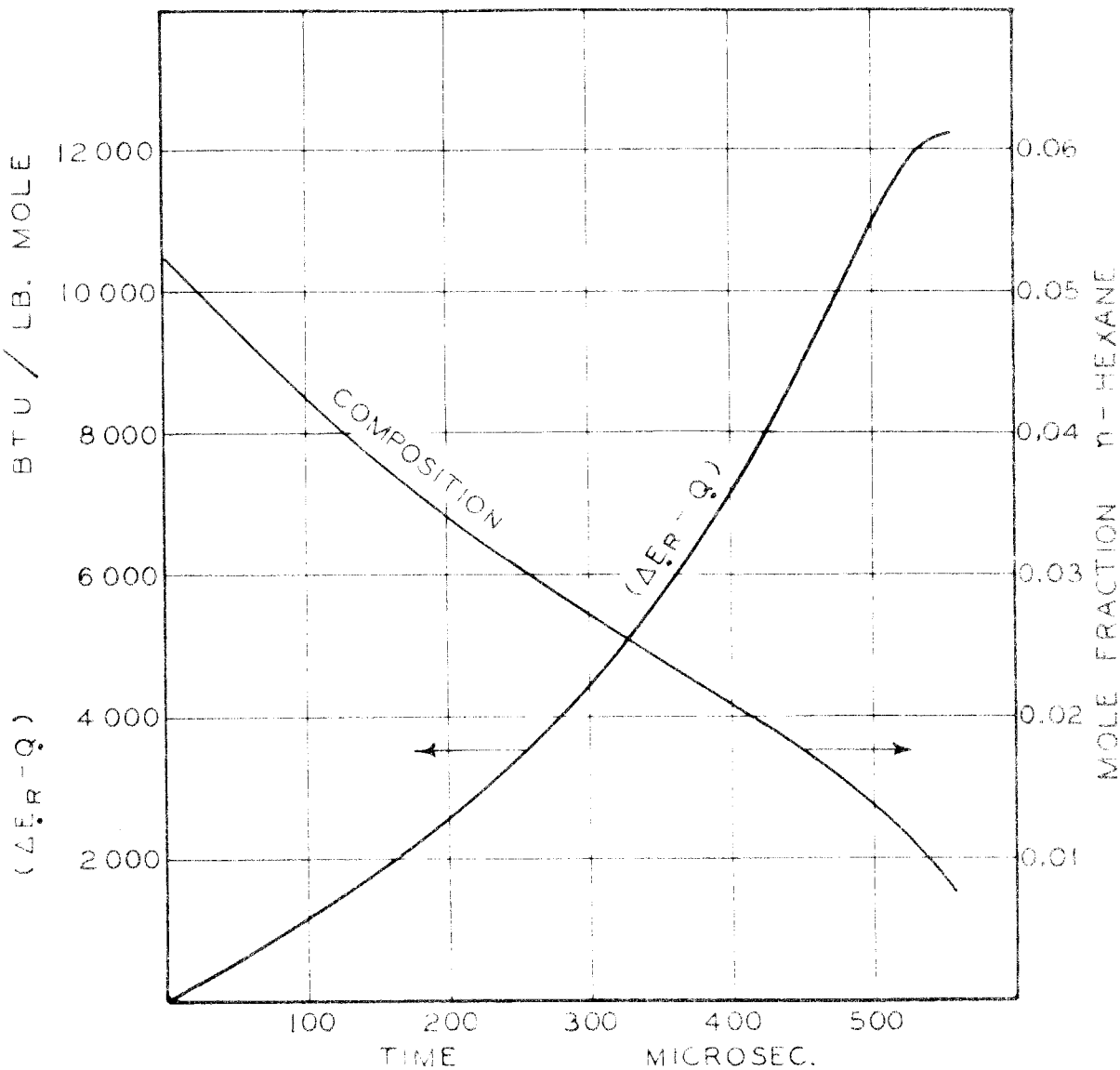

Fig. V-8. Composition and Change in Internal Energy as Functions of Time, Run 128

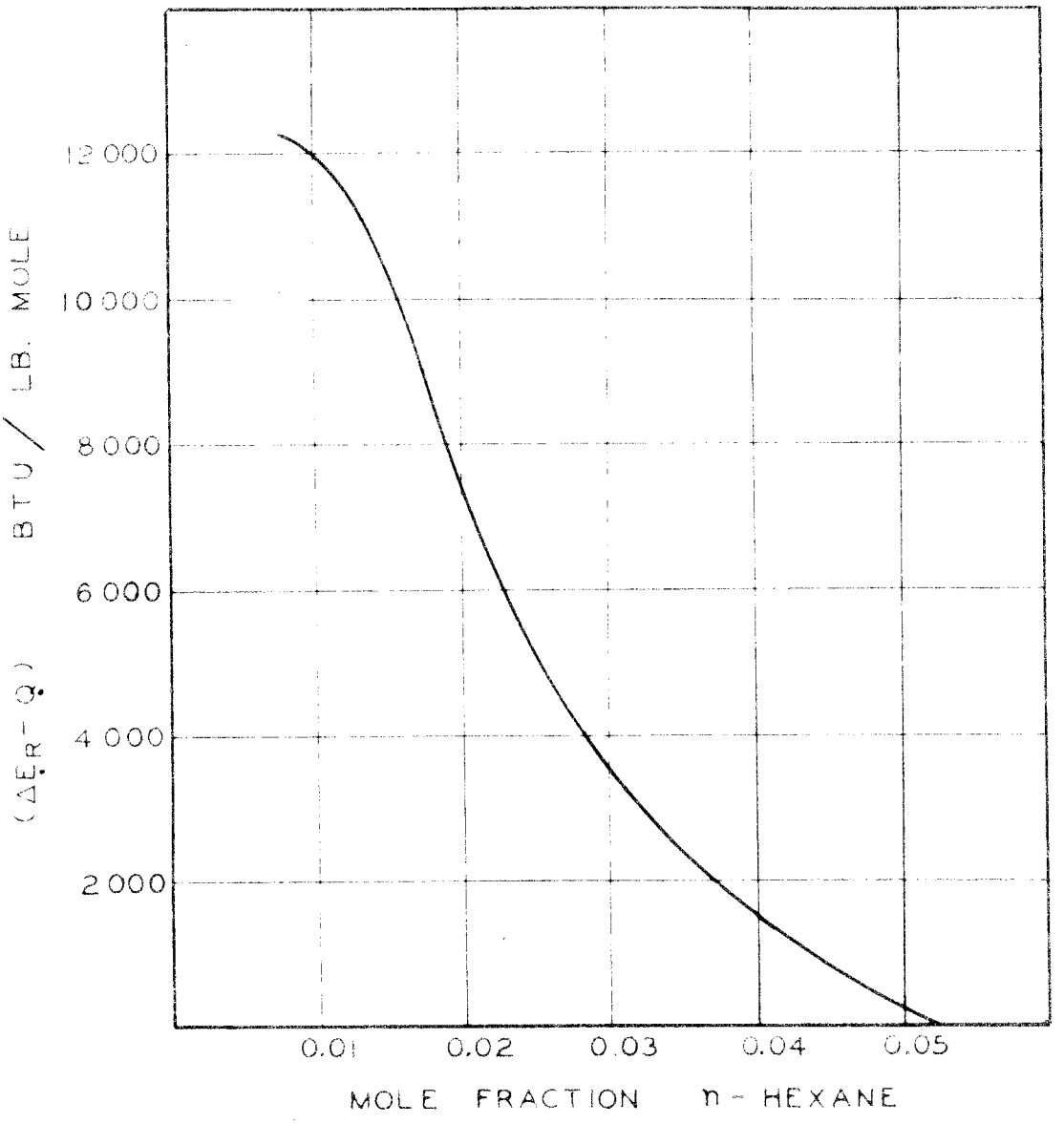

Fig. V-9. Composition and Change in Internal Energy, Run 128

Appendix I.

THERMODYNAMIC PROPERTIES OF VARIOUS GASES

It is necessary to use the thermodynamic properties of the gases concerned in order to obtain any type of solution of the equations describing sample behavior in the ballistic piston apparatus. These conditions range from room temperature at low (generally subatmospheric) pressure up to pressures of 10,000 to 150,000 pounds per square inch at temperatures ranging from 1,500 to 15,000 degrees Rankine, depending on the particular gases. This range of conditions is greater than that encountered in interior ballistics work, and is of course at lower pressures than are of interest in the detonation of condensed explosives, although the temperatures of detonation are included in the range of interest for ballistic piston work. However, since the fields of interior ballistics and condensed explosives are the ones which have been concerned with the properties of gases at high temperatures and pressures, it is logical to look to workers in these fields for information. Since a considerable amount of work in these fields has been done during and since World War II, it was not considered profitable to explore work prior to that time.

Caldirola (36) presented a three constant equation of state for the detonation products of solid explosives of the form

$$P\left(\frac{V}{} - \frac{b'}{1 + \frac{c}{V}}\right) = N R T \qquad \text{(AI-1)}$$

and listed values of the constants for various solid explosives. The range of validity was claimed to be from 30,000 to 300,000 atmospheres and 3,000 to 7,000° K. Hirschfelder and Roseveare (37) proposed a modified virial type equation of state for gases at moderately high pressures.

$$PV_o = RT\left[1 + \frac{B(T)}{V_o} + 0.625\left(\frac{b_o}{V_o}\right)^2 + 0.2869\left(\frac{b_o}{V_o}\right)^3 + 0.1928\left(\frac{b_o}{V_o}\right)^4\right] \qquad \text{(AI-2)}$$

This equation is applicable to interior ballistics conditions. Corner (38) considered equations of state for use in interior ballistics calculations. He found that a simple covolume two constant equation (Noble-Abel equation)

$$P(V - \eta) = (\text{Constant}) \times T \qquad \text{(AI-3)}$$

with the specific covolume η taken as constant has been used with considerable success. Corner also presented a truncated virial coefficient type of equation of state having one constant and two parameters which are functions of temperature

$$PV_o = RT\left[1 + \frac{B(T)}{V_o} + \frac{C(T)}{V_o^2}\right] \qquad \text{(AI-4)}$$

and tabulated these parameters for various gases encountered in interior ballistics.

Wentorf et al. (39) utilized high speed digital computing equipment to calculate the equation of state utilizing a 3 shell modification of the Lennard-Jones and Devonshire (40) equation of state. In these calculations a spherical molecule was considered to be confined to a cell and interactions with the three neighboring shells of molecules were taken into account. Fickett and Wood (40) extended these calculations into the region of interest in the detonation of solid high explosives. Zwanzig (42) reported an equation of state for argon and nitrogen at high pressures and temperature.

Hirschfelder, Curtiss and Bird (17) treated rather thoroughly the subject of the calculation of equations of state on the basis of statistical mechanical models and presented several equations of state obtained in this manner. They presented two which seem suitable for nonpolar gases in the range of conditions of interest. One using a 3 shell modification (39) of the Lennard-Jones and Devonshire equation of state is suitable for the dense gas region, while a virial equation of state with the second and third virial coefficients calculated from the Lennard-Jones (6-12) potential (43,44) is suitable for the region of lower densities. Both are based on spherically symmetrical potentials. It was decided to use the results summarized by Hirschfelder (17) to estimate the equations of state for the various gases used in this investigation.

Equations of State Used

The virial equation of state as presented by Hirschfelder (17) is

$$\frac{PV_o}{RT} = Z = 1 + \frac{B^* b_o}{V_o} + \frac{C^* b_o^2}{V_o^2} + \frac{0.2869\, b_o^3}{V_o^3} + \frac{0.1928\, b_o^4}{V_o^4} \qquad \text{(AI-5)}$$

and he tabulated B^* and C^* as functions of t^* where

$$t^* = \frac{T}{(\epsilon/k)} \qquad \text{(AI-6)}$$

Values of the force constants b_o and (ϵ/k) for a number of gases taken from Hirschfelder have been converted to engineering units and are shown in Table AI-I. Where there was a choice, values derived from equation of state data were selected as most applicable.

The equation of state for dense gases based on the 3 shell modifications of the Lennard-Jones and Devonshire equation of state was presented (17) in tabular form. The compressibility factor Z was tabulated as a function of t^* and $(a^*)^3$, where

$$(a^*)^3 = \frac{2\sqrt{2}\,\pi}{3\, b_o} V_o \qquad \text{(AI-7)}$$

A covolume equation of state such as that considered by Corner (38) has considerable advantage for use in equations of the type developed in Part III of this thesis, particularly if the covolume remains approximately constant. It was therefore decided to utilize the covolume equation of state

$$P(V_o - b) = RT \tag{AI-8}$$

and to determine values of the molal covolume b in accordance with Hirschfelder's calculations. The covolume is easily obtained from compressibilities, since

$$b = \left[\frac{Z-1}{Z}\right] V_o = \frac{Z-1}{Z\rho_o} \tag{AI-9}$$

It is necessary to know covolumes as functions of pressure and temperature in order to determine the covolume of a mixture, using the ideal solution assumption. Using this latter assumption

$$b = \sum_{K=1}^{n} \eta_K b_K \tag{AI-10}$$

The procedure used to obtain covolumes for pure gases as functions of pressure and temperature was in general as outlined below. Special

points will be mentioned in discussing individual gases.

1. Using force constants from Table AI-I, compressibility factors Z were calculated for the lower range of the reciprocal molal volume at various temperatures by means of equation (AI-5) and Hirschfelder's B^* and C^*. Z's at higher values of reciprocal molal volume were obtained for temperatures in the region of interest from the tabular data for the 3 shell modification of the Lennard-Jones and Devonshire equation of state.
2. Covolumes b were calculated for both sets of data obtained above by means of equation (AI-9)
3. Plots of b versus $\sqrt{T}_o$ at constant temperature were made, with the values from both the virial and the 3 shell equations of state on one plot. Since the virial equation was poor at high densities and the 3 shell equation was poor at lower densities, it was necessary to draw in a transition curve between the two curves. This step in some cases left a good deal to the imagination and is probably the source of considerable uncertainty in these cases. Figure AI-1 shows an example wherein the transition between the two curves was quite simple and probably introduces little error beyond that of the two equations of state in their respective domains. On the other hand Figure AI-2 shows a case where the proper position of the

line bridging the gap between the two curves is subject to considerable uncertainty.

4. The pressure was calculated for various values of reciprocal molal volume at constant temperature using the final smoothed-in curve arrived at in step 3 in each case. Equation (AI-8) was used for these calculations.
5. The covolume b was plotted versus log P at constant temperature and smooth curves drawn.
6. The curves of step 5 were used to crossplot b versus log T at constant pressure.
7. Values of b were read at even temperatures and pressures and tabulated.

Hydrogen

Covolumes for hydrogen were calculated at temperatures of 1332, 3330, 6660 and 26,640° R. and treated as outlined. The curves of b versus $\sqrt{\rho_o}$ were easily joined for the two lower temperatures, while those for the upper two temperatures were tending towards the type shown in Figure AI-2. However, for the latter two cases the pressures at which the smoothed curves depart from the low density virial equations of state are in excess of 150,000 pounds per square inch and are thus out of the range normally used. It is believed that little added uncertainty is introduced by the smoothing between the two equations of state for hydrogen. The covolumes resulting are shown in Table AI-II for a temperature range of 1500 to 20,000° R. and pressures

from zero to 200,000 pounds per square inch absolute. It will be noted that the covolume for hydrogen varies only from 0.192 to 0.282 cubic foot per pound mole in this rather large range.

Helium

For helium, the data (17) were so spaced that covolumes were obtained from the 3 shell modification of the Lennard-Jones and Devonshire equation of state only at 1840 and 7358° R. Values from the low density virial equation of state were calculated at 1472, 1840, 3679, 5519 and 7358° R. The smoothing between the two curves at 1840° R. was over a moderate range while the curves for 7358° R. are shown in Figure AI-2 as an example in which considerable uncertainty may be introduced. Since it was desired to compute covolumes over a full range of temperatures and pressure, plots of b versus log T at constant $\sqrt{\ }_o$ were used both for interpolation and extrapolation. Fortunately these lines were almost straight so interpolation and extrapolation to 20,000° R. seemed reasonable. However only for temperatures less than 7500° R. was it necessary to depart from the curve for the virial equation of state in order to reach pressures of 200,000 pounds per square inch. Thus the extrapolations to the higher temperatures were really merely extrapolations of the virial equation of state. It is not known how accurately these extrapolations match theory. Although Fickett and Wood (41) made calculations for higher temperatures, their densities were much greater and so these results are not applicable. In any event the covolumes for helium are small

and errors in them are of relatively less importance than are errors in those for the other gases. The covolumes for helium are shown in Table AI-III for temperatures from 1500 to 20,000° R. and pressures up to 200,000 pounds per square inch.

n-Hexane

Covolumes were calculated from the two equations of state for temperatures of 1487, 2230, 2974 and 3717° R. and handled in the normal manner. The transition between the two curves was in every case over a relatively short range. Covolumes are tabulated in Table AI-IV for the range of 1500 to 4000° R. and pressures up to 200,000 pounds per square inch. The variation in covolumes is large in this range. Because the n-hexane molecule is far from spherical, the covolumes are probably less accurate than for the other gases considered.

Methane

Covolumes were calculated at temperatures 1334, 1868, 2668 and 5336° R. The transitions between the curves for the two equations of state were in all cases over very small ranges. The covolumes were handled in the established manner and are shown for a range of 1500 to 5000° R. and for pressures up to 200,000 pounds per square inch in Table VI-V.

Nitrogen

Covolumes were calculated at temperatures of 1710, 3420, 8550 and 17,100° R. Transitions between curves were over small ranges in

all cases and no unusual techniques were used in handling the data. Covolumes for the range 1500 to 20,000° R. and pressures up to 200,000 pounds per square inch are found in Table AI-VI.

Specific Heat Functions

Two specific heat functions have been defined in Part III of this thesis. These are

$$\phi = \frac{1}{\ln T^*} \int_0^{\ln T^*} C_v^\circ \, d(\ln T^*) \qquad \text{(AI-11)}$$

and

$$\psi = \int_1^{T^*} C_v^\circ \, dT^* \qquad \text{(AI-12)}$$

Both equations (AI-11) and (AI-12) were derived using an equation of state for which the specific heat at constant volume is a function of temperature alone.

Specific heats at constant pressure and infinite attenuation for hydrogen, n-hexane, methane and nitrogen were taken from Rossini (22). The specific heat at constant volume of helium was taken as constant at 3/2 R. The functions ϕ and ψ were calculated by conventional graphical and numerical methods using these specific heats at infinite attentuation. In most cases values for the functions were

desired for temperatures higher than those for which the specific heats were available, and the specific heats were extrapolated on plots against T^* and against log T^*. Smooth curves which used as asymptotes the values given by Rossini (45) for excitation of all degrees of freedom were drawn on both plots.

The functions (ϕ/R) and $(\psi/(T^* - 1)R)$ were selected for tabulation since (ϕ/R) and (ψ/R) are the forms generally used in calculation. Division of (ψ/R) by $(T^* - 1)$ makes it more convenient for tabulation and interpolation. The functions as calculated are based on a reference temperature of 536.7° R. (77° F.)

The specific heat functions for hydrogen and nitrogen are shown in Table AI-VII for T^* from 1 to 20. Those for the hydrocarbons, methane and n-hexane, are shown in Table AI-VIII for T^* from 1 to 10. The regions of extrapolation of the specific heats are indicated.

Properties of Covolume Equation of State

The equation of state is given by equation (AI-8) as

$$P(V_o - b) = RT \qquad \text{(AI-13)}$$

where

$$b = f(P,T) = -\underset{\sim}{V_o} \qquad \text{(AI-14)}$$

The standard derivatives are

$$\left(\frac{\partial V_o}{\partial T}\right)_P = \frac{R}{P} + \left(\frac{\partial b}{\partial T}\right)_P \qquad \text{(AI-15)}$$

$$\left(\frac{\partial V_o}{\partial P}\right)_T = -\frac{RT}{P^2} + \left(\frac{\partial b}{\partial P}\right)_T \qquad \text{(AI-16)}$$

$$\left(\frac{\partial P}{\partial T}\right)_{V_o} = \frac{1}{V_o - b}\left[R + P\left(\frac{\partial b}{\partial T}\right)_{V_o}\right] \qquad \text{(AI-17)}$$

Thus

$$\left(\frac{\partial E_o}{\partial P}\right)_T = -T\left(\frac{\partial V_o}{\partial T}\right)_P - P\left(\frac{\partial V_o}{\partial P}\right)_T = -T\left(\frac{\partial b}{\partial T}\right)_P - P\left(\frac{\partial b}{\partial P}\right)_T \qquad \text{(AI-18)}$$

and the change in internal energy due to gas imperfection is

$$E_o - E_o^\circ = -T\int_o^P \left(\frac{\partial b}{\partial T}\right)_P dP - \int_o^P P\left(\frac{\partial b}{\partial P}\right)_T dP \qquad \text{(AI-19)}$$

when the integration is performed at constant temperature. Differentiation of equation (AI-18) with respect to temperature at constant gives

$$\left(\frac{\partial^2 E_o}{\partial P \partial T}\right) = \left(\frac{\partial C_{v_o}}{\partial P}\right)_T = -\left[\left(\frac{\partial V_o}{\partial T}\right)_P + T\left(\frac{\partial^2 V_o}{\partial T^2}\right)_P + P\left(\frac{\partial^2 V_o}{\partial P \partial T}\right)\right]$$

(AI-20)

$$= -\left[\left(\frac{\partial b}{\partial T}\right)_P + T\left(\frac{\partial^2 b}{\partial T^2}\right)_P + P\left(\frac{\partial^2 b}{\partial P \partial T}\right)\right]$$

For isentropic processes one is interested in

$$\left(\frac{\partial V_o}{\partial T}\right)_S = \frac{C_{o_P}\left(\frac{\partial V_o}{\partial P}\right)_T + T\left(\frac{\partial V_o}{\partial T}\right)_P^2}{T\left(\frac{\partial V_o}{\partial T}\right)_P} \qquad \text{(AI-21)}$$

and since

$$C_{o_P} - C_{v_o} = -T\frac{\left(\frac{\partial V_o}{\partial T}\right)_P^2}{\left(\frac{\partial V_o}{\partial P}\right)_T} \qquad \text{(AI-22)}$$

$$\left(\frac{\partial V_o}{\partial T}\right)_S = \frac{C_{v_o}\left(\frac{\partial V_o}{\partial P}\right)_T}{T\left(\frac{\partial V_o}{\partial T}\right)_P} \qquad \text{(AI-23)}$$

Substitution of equations (AI-15) and (AI-16) gives

$$\left(\frac{\partial V_o}{\partial T}\right)_S = \frac{C_{v_o}\left[-\frac{RT}{P^2}+\left(\frac{\partial b}{\partial P}\right)_T\right]}{T\left[\frac{R}{P}+\left(\frac{\partial b}{\partial T}\right)_P\right]} = \frac{-C_{v_o}\left[1-\frac{P^2}{RT}\left(\frac{\partial b}{\partial P}\right)_T\right]}{P\left[1+\frac{P}{R}\left(\frac{\partial b}{\partial T}\right)_P\right]} \qquad \text{(AI-24)}$$

The fugacity is useful for chemical reactions

$$\left(\frac{\partial \ln f^\circ}{\partial P}\right)_T = \frac{1}{RT}V_o = \frac{1}{RT}\left(b+\frac{RT}{P}\right) = \frac{b}{RT}+\frac{1}{P} \qquad \text{(AI-25)}$$

so

$$\left(\frac{\partial \ln \frac{f^\circ}{P}}{\partial P}\right)_T = \frac{b}{RT} \qquad \text{(AI-26)}$$

and integration from zero pressure at constant temperature gives

$$\ln \frac{f^\circ}{P} = \frac{1}{RT}\int_0^P b\, dP \qquad \text{(T)} \qquad \text{(AI-27)}$$

An average "b" is useful for tabulation when

$$\bar{b} = \frac{1}{P}\int_{0}^{P} b \, dP \qquad \text{(AI-28)}$$

and

$$\ln \frac{f^{\circ}}{P} = \frac{P\bar{b}}{RT} \qquad \text{(AI-29)}$$

Values of $\bar{b}$ as defined in equation (AI-28) were calculated for n-hexane and are shown in Table AI-IX. If an ideal solution is assumed, the fugacity of a component is calculated by multiplying the fugacity obtained from equation (AI-27) or (AI-29) by the mole fraction of the component.

The Joule-Thomson coefficient is given by

$$\mu = \left(\frac{\partial T}{\partial P}\right)_H = \frac{-V_o + T\left(\frac{\partial V_o}{\partial T}\right)_P}{C_{oP}} = \frac{-b + T\left(\frac{\partial b}{\partial T}\right)_P}{C_{oP}} \qquad \text{(AI-30)}$$

The last relationship of equation (AI-30) is obtained by use of equation (AI-15).

Inspection of Tables AI-II through AI-VI and calculation of

questionable cases reveals that the Joule-Thomson coefficient, as given by the data used herein, is negative for hydrogen, helium, and nitrogen in the ranges covered by the tables, and is negative for methane except for the low temperature and low pressure portion of the range. The Joule-Thomson coefficient for n-hexane assumes both positive and negative values.

Properties for Constant Covolume

If the covolume "b" is constant, it is evident that most of the relationships considered above are markedly simplified. One finds from equations (AI-15) and (AI-16) that

$$\left(\frac{\partial V_o}{\partial T}\right)_P = \frac{R}{P} \qquad \text{(AI-31)}$$

and

$$\left(\frac{\partial V_o}{\partial P}\right)_T = -\frac{RT}{P^2} \qquad \text{(AI-32)}$$

Equation (AI-18) gives

$$\left(\frac{\partial E_o}{\partial P}\right)_T = 0 \qquad \text{(AI-33)}$$

and equation (AI-20) reduces to

$$\left(\frac{\partial C_{v}^{\circ}}{\partial P}\right)_{T} = 0 \qquad \text{(AI-34)}$$

Equation (AI-24) becomes

$$\left(\frac{\partial V_{o}}{\partial T}\right)_{S} = -\frac{C_{v}^{\circ}}{P} \qquad \text{(AI-35)}$$

and equations (AI-27) and (AI-31) reduce to

$$\ln \frac{f^{\circ}}{P} = \frac{bP}{RT} \qquad \text{(AI-36)}$$

and

$$\mu = \frac{-b}{C_{P}^{\circ}} \qquad \text{(AI-37)}$$

Corrections to Specific Heat Functions

The specific heat functions ϕ and ψ defined in equations (AI-11) and (AI-12) were calculated for a reference temperature of 536.7° R. (77° F.). They are however used for initial temperatures differing slightly from this reference temperature and it is of interest to estimate the error so introduced. If the reference

temperature of 536.7° R. is designated as T_r and the actual initial temperature by T_o one can write

$$\frac{T'}{T_r} = \frac{T}{T_o} = T^* \qquad \text{(AI-38)}$$

One may actually use at T a value of ϕ or ψ calculated for T' when functions are used as functions of T^*.

Equation (AI-11) can be written as

$$\phi' = \frac{1}{\ln T^*} \int_{\ln T_r}^{\ln T'} C_v^\circ \, d \ln T \qquad \text{(AI-39)}$$

and

$$\phi = \frac{1}{\ln T^*} \int_{\ln T_o}^{\ln T} C_v^\circ \, d \ln T \qquad \text{(AI-40)}$$

Subtracting (AI-40) from (AI-39)

$$(\ln T^*)(\phi' - \phi) = \int_{\ln T}^{\ln T'} C_v^\circ \, d \ln T - \int_{\ln T_o}^{\ln T_r} C_v^\circ \, d \ln T \qquad \text{(AI-41)}$$

Using average specific heats in small intervals, the error is

$$\phi' - \phi = \frac{\ln \frac{T_r}{T_o}}{\ln T^*} \left[(C_v)_T - (C_v)_r \right] \qquad \text{(AI-42)}$$

in which the specific heats are those at T and at T_r respectively.

The error in ψ can be obtained somewhat similarly. Equation (AI-12) can be written as

$$\psi' = \frac{1}{T_r} \int_{T_r}^{T'} C_v \, dT \qquad \text{(AI-43)}$$

and

$$\psi = \frac{1}{T_o} \int_{T_o}^{T} C_v \, dT \qquad \text{(AI-44)}$$

Subtracting:

$$T_r \psi' - T_o \psi = \int_{T}^{T'} C_v \, dT - \int_{T_o}^{T_r} C_v \, dT \qquad \text{(AI-45)}$$

Using average specific heats

$$T_r \psi' - T_o \psi = (c_{ov})_T (T' - T) - (c_{ov})_r (T_r - T_o) \qquad \text{(AI-46)}$$

Dividing by T_o and using equation (AI-38) there is obtained

$$\frac{T_r}{T_o} \psi' - \psi = \left[\frac{T_r}{T_o} - 1\right]\left[(c_{ov})_T T^* - (c_{ov})_r\right] \qquad \text{(AI-47)}$$

If equation (AI-47) is solved for ψ, and the result is subtracted from ψ', the error is obtained:

$$\psi' - \psi = \left[\frac{T_r}{T_o} - 1\right]\left\{\left[(c_{ov})_T T^* - (c_{ov})_r\right] - \psi'\right\} \qquad \text{(AI-48)}$$

Determination of Polytropic Expansion Exponent for Air

In order to use an equation of the form

$$PV^K = \text{constant} \qquad \text{(AI-49)}$$

for the air acting as a driving gas, the temperature-entropy diagram given by Williams (46) was used. Upon assumption of perfect gas behavior and isentropic expansion, the exponent can be calculated from

$$\frac{K}{K-1} = \frac{\log \frac{P}{P_o}}{\log \frac{T}{T_o}} \qquad \text{(AI-50)}$$

Pressure was plotted as a function of temperature on log-log paper for several initial pressures and an initial temperature of 540° R., and straight lines were obtained. Values for k of 1.404, 1.425, 1.423 and 1.424 were obtained for initial pressures of 440, 1000, 2000 and 3000 pounds per square inch respectively. Neither the isentropic path nor the perfect gas behavior is a good assumption; however, the value of k used does not influence calculated energy transfer to the sample gas significantly if corresponding values of the effective friction F are used. A value for k of 1.424 was selected for use.

TABLE AI-I. FORCE CONSTANTS FOR VARIOUS GASES[a]

Gas	b_o (Cu.Ft./Lb.Mole)	(ϵ/k) ($^oR.$)
A	0.7977	215.6
Air	0.8828	178.6
CH_4	1.1238	266.8
C_2H_4	1.8693	358.6
C_2H_6	1.2494	437.
C_3H_8	3.6201	436.
$n\text{-}C_4H_{10}$	2.4828	535.
$N\text{-}C_5H_{12}$	3.880	621.
$n\text{-}C_6H_{14}$	4.169	743.
CO	1.0767	180.4
CO_2	1.8245	340.
H_2	0.5073	66.60
He	0.3375	18.40
N_2	1.0202	171.09
NO	0.6407	236.
N_2O	1.9542	340.
O_2	0.9250	211.5

[a] Converted from Table 1-A Hirshfelder, Curtis and Bird (17)

TABLE AI-II. COVOLUMES "b" FOR HYDROGEN[a]

T°(R)	1500	2000	2500	3000	4000	5000	6000	8000	10,000	12,500	15,000	20,000
P(Lb./Sq.In.)												
0	0.267	0.265	0.262	0.258	0.250	0.243	0.237	0.227	0.219	0.210	0.203	0.192
5,000	"	"	"	"	"	"	"	"	"	"	"	"
7,000	0.268	0.266	"	"	"	"	"	"	"	"	"	"
10,000	0.269	"	"	"	"	"	"	"	"	"	"	"
15,000	0.271	0.267	"	"	"	"	"	"	"	"	"	"
20,000	0.273	0.268	0.263	0.259	"	"	"	"	"	"	"	"
30,000	0.278	0.272	0.266	0.261	0.251	0.244	"	"	"	"	"	"
50,000	0.282	0.277	0.272	0.266	0.256	0.247	0.239	"	"	"	"	"
70,000	0.279	0.278	0.275	0.271	0.261	0.251	0.243	0.230	0.221	0.211	0.204	"
100,000	0.268	0.276	0.277	0.274	0.266	0.257	0.250	0.236	0.225	0.214	0.206	0.194
150,000	0.231	0.249	0.261	0.269	0.268	0.261	0.255	0.242	0.232	0.221	0.212	0.198
200,000	0.216	0.235	0.248	0.258	0.265	0.260	0.254	0.244	0.236	0.227	0.219	0.204

[a] Cu.ft./lb.mole

TABLE AI-III. COVOLUMES "b" FOR HELIUM[a]

$T^{\circ}(R)$	1500	2000	2500	3000	4000	5000	6000	8000	10,000	12,500	15,000	20,000
P(Lb./Sq.In.)												
0	0.162	0.155	0.150	0.145	0.137	0.132	0.127	0.120	0.113	0.107	0.103	0.095
5,000	0.160	0.153	0.148	0.143	0.136	0.131	0.126	0.119	"	"	"	"
7,000	"	"	"	"	"	"	"	"	"	"	"	"
10,000	"	"	0.147	"	"	0.130	"	"	"	"	"	"
15,000	0.161	"	"	0.142	0.135	"	"	"	"	"	"	"
20,000	0.162	0.154	0.148	0.143	"	"	"	"	"	"	"	"
30,000	0.166	0.156	0.149	0.144	0.136	"	"	"	"	"	"	"
50,000	0.170	0.162	0.155	0.149	0.139	0.132	0.127	"	"	"	"	"
70,000	0.171	0.166	0.160	0.154	0.144	0.136	0.130	0.121	0.114	0.108	0.104	0.096
100,000	0.167	0.166	0.164	0.160	0.150	0.141	0.134	0.124	0.116	0.109	0.104	0.097
150,000	0.158	0.161	0.161	0.159	0.155	0.149	0.143	0.130	0.121	0.113	0.107	0.098
200,000	0.145	0.153	0.155	0.156	0.154	0.151	0.147	0.137	0.127	0.117	0.110	0.100

[a] Cu.ft./lb.mole

TABLE AI-IV. COVOLUMES "b" FOR n-HEXANE[a]

T °R.	1500	1750	2000	2250	2500	2750	3000	3250	3500	3750	4000
P(Lb./Sq.In.)											
0	-2.53	-1.83	-1.10	-0.42	0.00	0.28	0.49	0.71	0.88	1.03	1.17
1,000	-2.08	-1.45	-0.74	-0.10	0.27	0.50	0.68	0.87	1.02	1.13	1.25
1,500	-1.70	-1.09	-0.43	0.08	0.40	0.62	0.80	0.95	1.09	1.20	1.32
2,000	-1.28	-0.70	-0.17	0.23	0.53	0.73	0.88	1.03	1.15	1.25	1.35
2,500	-0.63	-0.26	0.10	0.44	0.69	0.86	0.96	1.10	1.21	1.30	1.38
3,000	-0.08	0.16	0.40	0.60	0.80	0.96	1.06	1.17	1.27	1.35	1.43
4,000	0.55	0.65	0.77	0.89	1.02	1.17	1.25	1.32	1.40	1.45	1.50
5,000	0.935	0.992	1.053	1.135	1.250	1.390	1.480	1.508	1.525	1.534	1.536
7,000	1.230	1.290	1.360	1.445	1.550	1.625	1.667	1.682	1.688	1.688	1.688
10,000	1.382	1.475	1.562	1.640	1.710	1.780	1.822	1.842	1.850	1.851	1.848
15,000	1.472	1.575	1.665	1.748	1.815	1.880	1.938	1.970	1.993	2.002	2.005
20,000	1.515	1.605	1.688	1.765	1.840	1.912	1.965	2.002	2.027	2.040	2.050
30,000	1.560	1.605	1.660	1.725	1.802	1.880	1.940	1.980	2.005	2.020	2.030
50,000	1.582	1.595	1.615	1.645	1.688	1.735	1.780	1.822	1.860	1.894	1.925
70,000	1.568	1.573	1.585	1.600	1.622	1.648	1.675	1.703	1.732	1.760	1.787
100,000	1.532	1.540	1.547	1.555	1.562	1.567	1.579	1.593	1.610	1.633	1.660
150,000	1.483	1.483	1.485	1.490	1.493	1.498	1.502	1.508	1.512	1.520	1.525
200,000	1.460	1.460	1.460	1.460	1.460	1.460	1.460	1.460	1.460	1.460	1.460

[a] Cu.ft./lb.mole

TABLE AI-V. COVOLUMES "b" FOR METHANE[a]

T °R.	1500	1750	2000	2250	2500	2750	3000	3250	3500	4000	4500	5000
P(Lb./Sq.In.)												
0	0.330	0.399	0.445	0.481	0.504	0.522	0.536	0.550	0.559	0.572	0.583	0.589
2,000	0.368	0.422	0.464	0.494	0.517	0.532	0.544	0.553	0.561	0.573	0.581	0.589
5,000	0.427	0.465	0.492	0.513	0.530	0.542	0.551	0.558	0.565	0.574	0.581	0.587
7,000	0.460	0.490	0.510	0.526	0.538	0.548	0.556	0.563	0.568	0.577	0.583	0.588
10,000	0.498	0.518	0.533	0.543	0.551	0.558	0.563	0.569	0.573	0.580	0.585	0.589
15,000	0.540	0.552	0.559	0.565	0.569	0.572	0.575	0.578	0.581	0.585	0.589	0.592
20,000	0.565	0.573	0.578	0.581	0.583	0.585	0.587	0.588	0.590	0.592	0.594	0.595
30,000	0.585	0.594	0.600	0.603	0.605	0.606	0.607	0.607	0.607	0.607	0.606	0.605
50,000	0.568	0.592	0.606	0.614	0.620	0.622	0.623	0.624	0.624	0.623	0.621	0.619
70,000	0.524	0.552	0.575	0.594	0.608	0.618	0.622	0.625	0.626	0.627	0.626	0.625
100,000	0.481	0.501	0.522	0.543	0.558	0.571	0.581	0.589	0.595	0.606	0.614	0.620
150,000	0.438	0.452	0.467	0.482	0.496	0.508	0.520	0.530	0.541	0.559	0.575	0.590
200,000	0.417	0.423	0.438	0.450	0.460	0.471	0.481	0.491	0.500	0.517	0.532	0.546

[a] Cu.ft./lb.mole

TABLE AI-VI. COVOLUMES "b" FOR NITROGEN[a]

T°(R)	1500	2000	2500	3000	4000	5000	6000	8000	10,000	12,500	15,000	20,000
P(Lb./Sq.In.)												
0	0.443	0.493	0.518	0.531	0.538	0.538	0.534	0.521	0.508	0.493	0.481	0.462
5,000	0.488	0.511	0.525	0.533	0.538	0.535	0.530	0.517	0.504	0.490	0.478	0.458
7,000	0.500	0.520	0.531	0.537	0.540	0.536	"	"	"	"	"	"
10,000	0.517	0.529	0.537	0.541	0.541	"	"	"	"	"	"	"
15,000	0.537	0.542	0.545	0.546	0.544	0.538	0.531	"	"	"	"	"
20,000	0.549	0.550	0.551	0.552	0.547	0.539	"	"	"	"	"	"
30,000	0.559	0.561	0.560	0.559	0.553	0.544	0.537	0.518	"	"	"	"
50,000	0.542	0.557	0.565	0.568	0.564	0.554	0.545	0.527	0.511	0.495	0.480	"
70,000	0.490	0.534	0.556	0.566	0.568	0.562	0.554	0.536	0.520	0.502	0.487	0.462
100,000	0.440	0.488	0.520	0.541	0.557	0.560	0.558	0.546	0.530	0.513	0.496	0.468
150,000	0.416	0.440	0.460	0.477	0.506	0.528	0.542	0.550	0.540	0.524	0.508	0.480
200,000	0.409	0.419	0.430	0.440	0.462	0.490	0.521	0.544	0.540	0.528	0.515	0.491

[a] Cu.ft./lb.mole

TABLE AI-VII. SPECIFIC HEAT FUNCTIONS FOR NITROGEN AND HYDROGEN

T^{*}[a]	$\frac{\phi}{R}$		$\frac{1}{T^{*}-1}\frac{\psi}{R}$	
	H_2	N_2	H_2	N_2
1.0	2.469	2.503	2.469	2.503
1.5	2.499	2.515	2.497	2.518
2.0	2.508	2.538	2.506	2.548
2.5	2.515	2.571	2.517	2.593
3.0	2.524	2.609	2.531	2.644
3.5	2.535	2.646	2.550	2.697
4.0	2.550	2.681	2.573	2.749
4.5	2.567	2.713	2.601	2.798
5.0	2.585	2.743	2.631	2.844
5.5	2.603	2.769	2.662	2.885
6.0	2.622	2.793	2.694	2.922
6.5	2.640	2.814	2.726	2.956
7.0	2.658	2.834	2.759	2.988
7.5	2.676	2.853	2.791	3.016
8.0	2.693	2.869	2.823	3.043
8.5	2.710	2.884	2.853	3.067
9.0	2.726	2.898	2.882	3.089
9.5	2.741	2.911	2.910	3.110
10.0	2.756	2.923	2.937	3.128
11.0	2.784	2.944	2.990	3.162
12.0	2.809	2.963	3.038	3.192
13.0	2.832	2.980	3.083	3.218
14.0	2.854	2.996	3.122	3.242
15.0	2.874	3.010	3.159	3.263
16.0	2.893	3.023	3.195	3.283
17.0[b]	2.912	3.034	3.228	3.301
18.0	2.929	3.044	3.261	3.318
19.0	2.944	3.054	3.293	3.333
20.0	2.958	3.063	3.324	3.348

[a] Based on reference temperature of 536.7° Rankine

[b] Specific heats extrapolated beyond 9000° R. ($T^{*} = 16.7$)

TABLE AI-VIII. SPECIFIC HEAT FUNCTIONS FOR METHANE AND n-HEXANE

T^{*}[a]	$\frac{\phi}{R}$		$\frac{1}{T^{*}-1}\frac{\psi}{R}$	
	CH_4	$n\text{-}C_6H_{14}$	CH_4	$n\text{-}C_6H_{14}$
1.0	3.298	16.21	3.298	16.21
1.2	3.460	17.50	3.465	17.60
1.4	3.630	18.78	3.651	18.94
1.6	3.806	19.94	3.843	20.24
1.8	3.974	21.04	4.040	21.51
2.0	4.143	22.04	4.245	22.74
2.2	4.312	22.96	4.452	23.88
2.4	4.472	23.80	4.655	24.90
2.6	4.620	24.56	4.859	25.90
2.8	4.758	25.27	5.054	26.87
3.0	4.894	25.93	5.247	27.77
3.2	5.024	26.55	5.432	28.63
3.4	5.151	27.13	5.609	29.45
3.6	5.272	27.68	5.784	30.19
3.8	5.388	28.20	5.952	30.93
4.0	5.500	28.69	6.111	31.66
4.2	5.603	29.14	6.265	32.32
4.4	5.702	29.57	6.412	32.94
4.6	5.797	29.98	6.554	33.54
4.8	5.889	30.38	6.692	34.10
5.0	5.977	30.76	6.825	34.65
5.5[b]	6.178	31.61	7.125	35.88
6.0	6.359	32.36	7.402	37.02
6.5	6.520	33.03	7.656	38.00
7.0	6.667	33.62	7.885	38.92
7.5	6.803	34.18	8.092	39.75
8.0	6.926	34.68	8.279	40.50
8.5	7.038	35.15	8.450	41.18
9.0	7.136	35.57	8.607	41.81
9.5	7.229	35.95	8.754	42.39
10.0	7.320	36.31	8.886	42.92

[a] Based on reference temperature of 536.7° Rankine

[b] Specific heats extrapolated beyond 2700° R. ($T^{*} = 5.0$)

TABLE AI-IX. AVERAGE COVOLUME $\bar{b}^{a,b}$ FOR n-HEXANE

Temp. °R.	1500	1750	2000	2250	2500	2750	3000
Pressure (Lb./Sq.In.)							
0	-2.53	-1.83	-1.10	-0.42	0.00	0.28	0.49
1,000	-2.305	-1.640	-0.920	-0.260	0.135	0.390	0.585
2,000	-1.993	-1.355	-0.688	-0.098	0.268	0.502	0.683
3,000	-1.555	-0.993	-0.497	0.073	0.400	0.617	0.778
4,000	-1.108	-0.645	-0.226	0.241	0.527	0.729	0.873
5,000	-0.737	-0.352	0.000	0.396	0.649	0.832	0.971
7,000	-0.217	0.074	0.346	0.651	0.864	1.030	1.143
10,000	0.240	0.467	0.680	0.919	1.094	1.232	1.324
15,000	0.635	0.800	0.991	1.177	1.316	1.425	1.509
20,000	0.850	0.996	1.163	1.322	1.444	1.539	1.620
30,000	1.079	1.194	1.333	1.463	1.570	1.658	1.731
50,000	1.276	1.356	1.455	1.552	1.640	1.718	1.782
70,000	1.361	1.421	1.496	1.571	1.659	1.710	1.765
100,000	1.418	1.462	1.517	1.573	1.629	1.680	1.723
150,000	1.448	1.479	1.517	1.557	1.595	1.631	1.662

[a] $\bar{b} = \frac{1}{P} \int_0^P b\,dP$

[b] Cu.ft./lb.mole

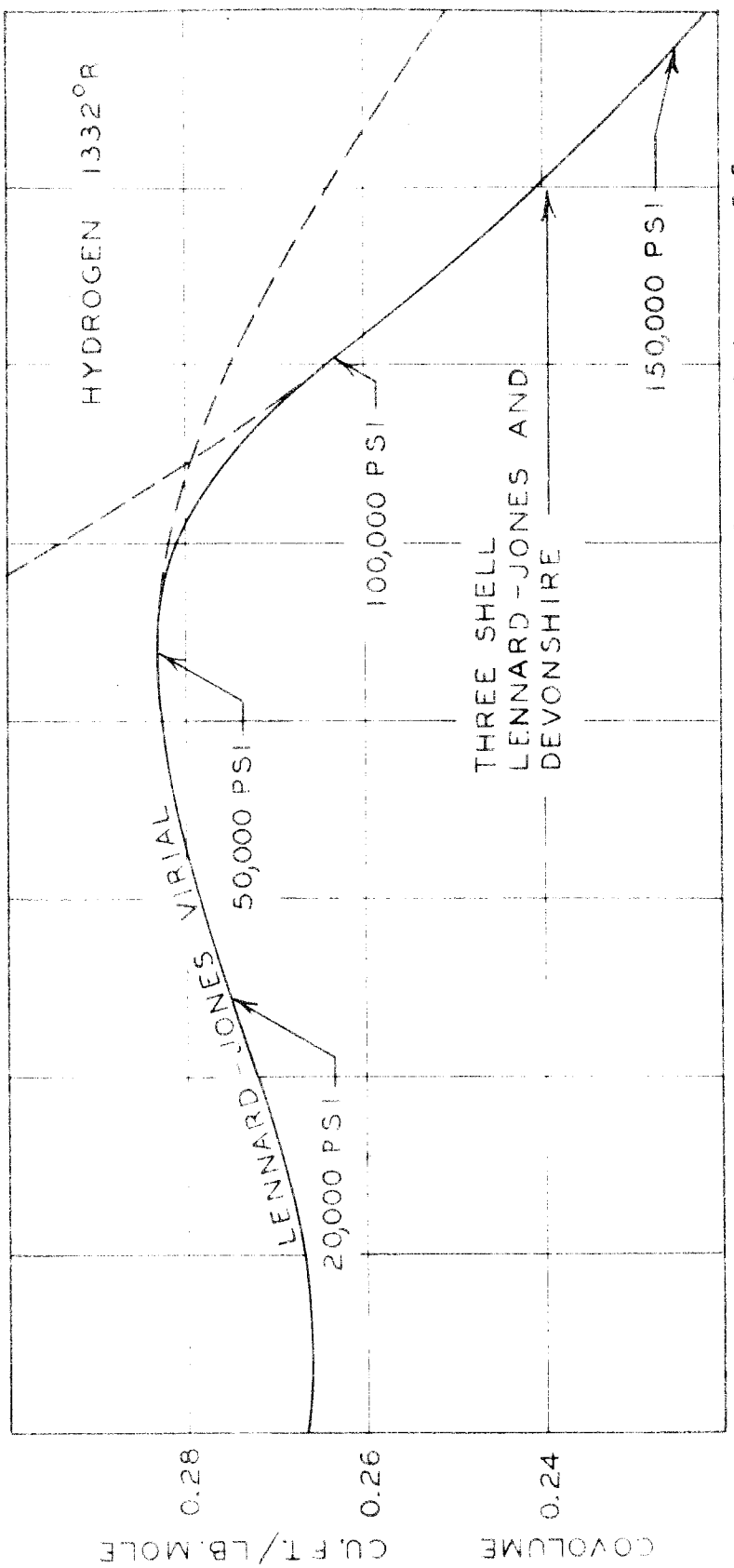

Fig. AI-1. Typical Covolumes from Equations of State

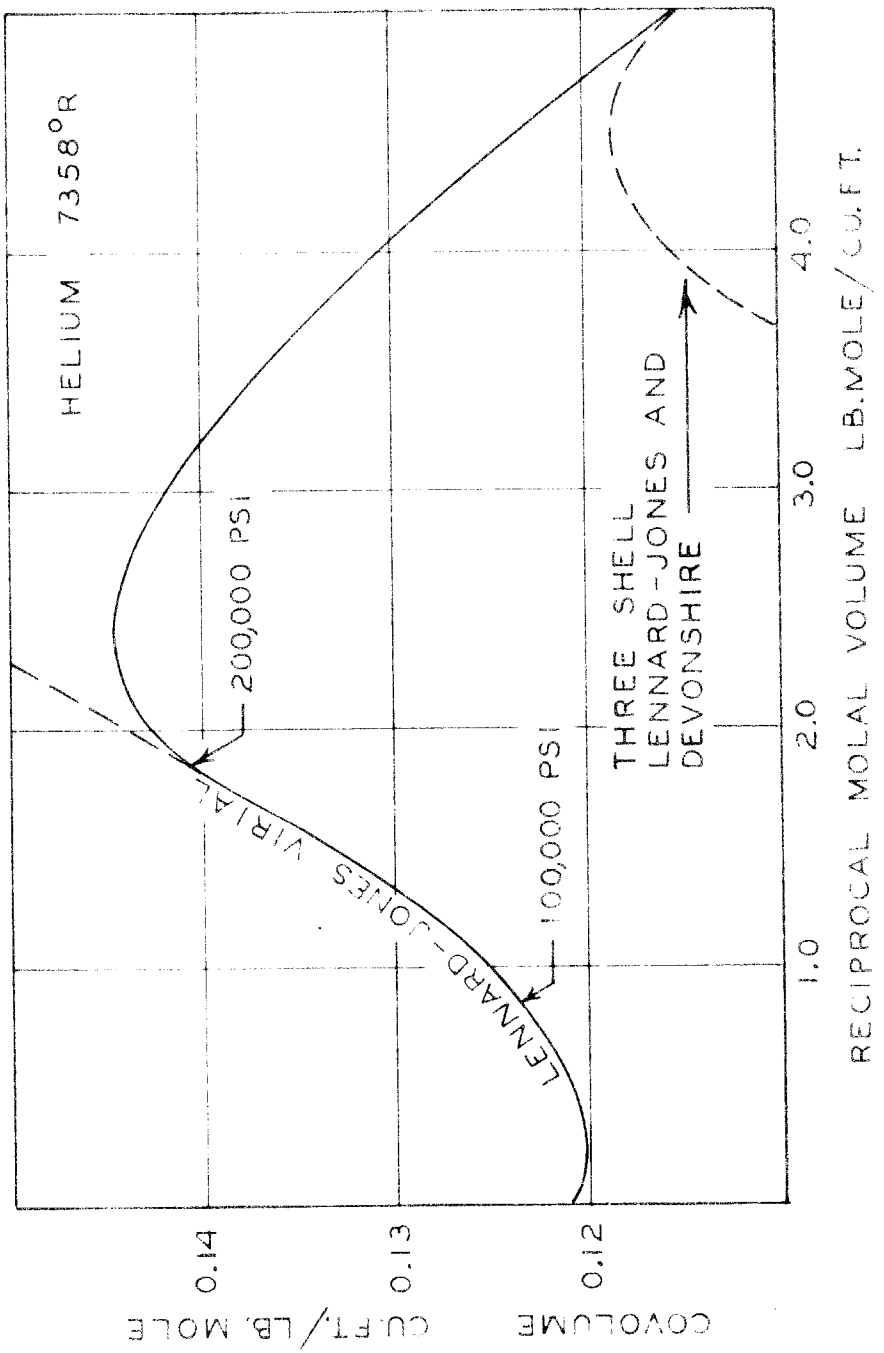

Fig. AI-2. Poor Agreement Between Equations of State

REFERENCES

1. Ryabinin, Yu. N., Zhur. Eksptl. i. Teoret. Fiz. (U.S.S.R.) 23, No. 4, 461 (1952).

2. Ablard, J. E., and Larson, R. L., NOL Memo. 10,526, U. S. Naval Ordnance Laboratory, 9 September 1949.

3. Wack, J. M., and Price, Donna, NAVORD Report 2219, U. S. Naval Ordnance Laboratory, 4 October 1951.

4. Price, D., Thalos, G., Edwards, P. L., and Allgaeir, R. S., NAVORD Report 3990, U. S. Naval Ordnance Laboratory, 10 May 1955.

5. Seigel, A. E., Ph.D. thesis, University of Amsterdam, January, 1952.

6. Seigel, A. E., NAVORD Report 2692, U. S. Naval Ordnance Laboratory, 15 July 1952.

7. Jacobs, S. J., Ph.D. thesis, University of Amsterdam, June, 1953.

8. Seigel, A. E., NAVORD Report 2694, U. S. Naval Ordnance Laboratory, 16 December 1952.

9. Tsiklis, D. S., Doklady Akad. Nauk. (S.S.S.R.) 91, 327 (1953).

10. Ryabinin, Yu. N., Markevich, A. M., and Tamm, I. I., Doklady Acad. Nauk (S.S.S.R.) 95, No. 1, 111 (1954).

11. Furman, M. S., and Tsiklis, D. S., Proc. Acad. Sci. U.S.S.R., 91, No. 3, 597 (1953).

12. Hanson, V. F., E. I. du Pont de Nemours and Co. Engineering Research Laboratory, Private Communication (1956).

13. Kouzmine, E., French Patent 860,410, June 13, 1939.

14. Kouzmine, E., French Patent 884,219, March 11, 1942.

15. Kouzmine, E., French Patent 966, 320, March 1, 1950.

16. Longwell, P. A., and Sage, B. H., Chemical Engineering manuscript 2745, Department of Chemical Engineering, California Institute of Technology, September, 1955.

17. Hirschfelder, J. O., Curtiss, C. F. and Bird, R. B., "Molecular Theory of Gases and Liquids," John Wiley and Sons, Inc., New York, 1954.

18. Kirkwood, John G., and Crawford, Bryce, J. Phys. Chem., 56, 1048 (1952).

19. Davis, R. S., Corcoran, W. H., and Sage, B. H., Chemical Engineering manuscript 2660, Department of Chemical Engineering, California Institute of Technology, May, 1953.

20. Lewis, G. N., J. Am. Chem. Soc., 30, 668 (1908).

21. Jahnke, E., and Emde, F., "Tables of Functions with Formulae and Curves," Dover Publications, New York (1945).

22. Rossini, F. D., et al., "Selected Values of Physical and Thermodynamic Properties of Hydrocarbons and Related Compounds," Carnegie Press, Pittsburgh, Pa., 1953.

23. Noyes, Arthur A., and Sherrill, Miles S., "A Course of Study in Chemical Principles," The MacMillan Company, New York, 1938.

24. Landau, L., and Teller, E., Phys. Zeits. Sowjitunion, 1, 34 (1936).

25. Kantrowitz, A., J. Chem. Phys., 14, 150 (1946).

26. Huber, P. W., and Kantrowitz, A., J. Chem. Phys., 15, 275 (1947).

27. Lambert, J. D., and Rowlinson, J. S., Proc. Roy. Soc. (London) A204, 424 (1950).

28. Sage, B. H., and Lacey, W. N., "Volumetric and Phase Behavior of Hydrocarbons," Stanford University Press, Stanford University, California, 1939.

29. Laidler, K. J., "Chemical Kinetics," McGraw Hill Book Company, New York (1950).

30. Steacie, E. W. R., "Atomic and Free Radical Reactions," Reinhold Publishing Corporation, New York, 1946. (ACS Monograph No. 102).

31. Rice, F. O., and Herzfeld, K. F., J. Am. Chem. Soc., 56, 284 (1934).

32. Jost, Wilhelm, "Explosion and Combustion Processes in Gases," McGraw Hill Book Company, New York (1946).

33. Peard, M. G., Stubbs, F. J., and Hinshelwood, Sir Cyril, Proc. Roy. Soc. (London) A214, 471 (1942).

34. Pearce, J. N., and Newsome, J. W., Ind. Eng. Chem., 30, 588 (1938).

35. Kossiakoff, A., and Rice, F. O., J. Am. Chem. Soc., 65, 590 (1943).

36. Caldirola, P., J. Chem. Phys., 14, 738 (1946).

37. Hirschfelder, J. O., and Roseveare, J. L., J. Phys. Chem., 43, 15 (1939).

38. Corner, J., "Theory of the Interior Ballistics of Guns," John Wiley and Sons, Inc., New York, 1950.

39. Wentorf, R. H., Buehler, R. J., Hirschfelder, J. O., and Curtiss, C. F., J. Chem. Phys., 18, 1484 (1950).

40. Lennard-Jones, J. A., and Devonshire, A. F., Proc. Roy. Soc. (London) A163, 53 (1937).

41. Fickett, W., and Wood, Wm. W., J. Chem. Phys., 20, 1624 (1952).

42. Zwanzig, R. W., J. Chem. Phys., 22, 1420 (1954).

43. Bird, R. B., and Spotz, E. L., University of Wisconsin, CM. 599 (Project NORD 9938) May 10, 1950.

44. Bird, R. B., Spotz, E. L., and Hirschfelder, J. O., J. Chem. Phys., 18, 1395 (1950).

45. Rossini, F. D., "Chemical Thermodynamics," John Wiley and Sons, Inc., New York (1950).

46. Williams, V. C., Trans. A.I.Ch.E., 39, 93 (1943).

PROPOSITIONS

1. It is concluded in this thesis that the decompositions of hydrocarbons under conditions reached in the ballistic piston apparatus are chain reactions which yield many free radicals. It is proposed that these mechanisms be investigated further by determining the effects on reaction rates and on products of small amounts of nitric oxide or of propylene. These materials act as inhibitors (1,2,3) to chain reactions at lower temperatures and pressures.

2. Ethylene oxide is said (4) to decompose thermally to give free radicals which will frequently increase rates of reaction. The effects on reaction rates and on products of the presence of a small amount of ethylene oxide or other sensitizer in hydrocarbon mixtures subjected to ballistic piston conditions should be determined.

3. A heavy piston was used in the tests on n-hexane reported in this thesis. It would be interesting to make similar tests using a light piston, thereby reducing the time at high temperature and pressure by a factor of three or so. The effects on computed reaction rates and on products should be observed.

4. The solution for the temperature in a finite slab of thickness "a", specific heat "c", specific weight "γ", and thermometric conductivity "K", initially at a uniform temperature "T_o", and subjected to an

instantaneous source of "Q" energy/unit area at the plane x = 0 at time $\theta = 0$ is

$$T - T_o = \frac{Q}{\tau C \sqrt{\pi K \theta}} \sum_{n=0}^{\infty} \left\{ \exp\left(-\frac{[2(n+1)a - x]^2}{4K\theta} \right) + \exp\left(-\frac{[2na + x]^2}{4K\theta} \right) \right\}$$

if there is no interchange of energy with the surroundings after the initial instanteous source is applied. The temperature at the plane x = a is

$$T_a - T_o = \frac{2Q}{\tau C \sqrt{\pi K \theta}} \sum_{n=0}^{\infty} \exp\left(-\frac{[2n+1]^2 a^2}{4K\theta} \right)$$

This solution was needed for design of a thermal flux meter and could not be found in the literature.

5. A covolume equation of state, such as

$$P(V_o - b) = RT$$

with the covolume being a function of pressure and temperature, has advantages over compressibility factors for use in the region of high pressures and temperatures.

6. Linear partial differential equations of the type

$$\frac{\partial \phi}{\partial x} = f_1(y) \frac{\partial}{\partial y}\left[f_2(y) \frac{\partial \phi}{\partial y} \right]$$

may oftentimes be solved rather easily by graphical means similar to the "Schmidt Method".

7. The solution of the differential equation

$$\frac{\partial}{\partial y}\left[(\epsilon_c + K) \frac{\partial t}{\partial y} \right] = u_x \frac{\partial t}{\partial x}$$

which was performed on an electrical analog computer by Schlinger et al. (5) may easily be done by graphical means. ϵ_c, K and u_x are functions of y.

8. A graphical method for solution of heat conduction problems involving latent heat as well as specific heat is proposed.

9. A 40 word CUBR entry subroutine for searching and interpolating between tabular data is proposed for use on the Datatron.

10. A method for the solution on an analog computer of a relatively simple case of reversible chemical reaction in the ballistic piston apparatus has been outlined. It requires at least

20 operational amplifiers (summing and integrating)

18 multipliers

6 dividers

5 squarers

10 function generators

plus numerous factor potentiometers.

Scaling has not been attempted but it is obvious that the enormous range of variables encountered during a run would make it necessary to change scale factors several times (probably at least 5 times) during a simulated compression stroke and a similar number of times during the decompression stroke.

It is concluded that digital equipment of reasonable memory, such as the Datatron, is more suitable for use in analyzing the behavior of samples in the ballistic piston apparatus.

(1) Stavely, L. A. K., and Hinshelwood, C. N., Proc. Roy. Soc. (London) A154, 335 (1936).

(2) Stubbs, F. J., and Hinshelwood, Sir Cyril., Proc. Roy. Soc. (London) A200, 458 (1950).

(3) Jach, J., and Hinshelwood, Sir Cyril., Proc. Roy. Soc. (London) A231, 145 (1955).

(4) Laidler, K. J., "Chemical Kinetics," McGraw Hill Book Company, New York (1950).

(5) Schlinger, W. G., Berry, V. J., Mason, J. L. and Sage, B. H., Ind. Eng. Chem., 45, 662 (1953).